

Geology and Hydrology of Groundwater-Fed Springs and Wetlands at La Cienega, Santa Fe County, New Mexico

Peggy S. Johnson, Daniel J. Koning
Stacy S. Timmons, and Brigitte Felix



H Y D R O G E O L O G Y

Bulletin 161 2016

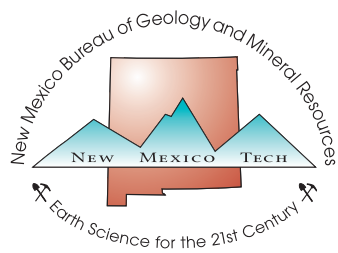
Hydrogeology of New Mexico

This page intentionally left blank to avert any facing-page issues.

Geology and Hydrology of Groundwater-Fed Springs and Wetlands at La Cienega, Santa Fe County, New Mexico

Peggy S. Johnson, Daniel J. Koning,
Stacy S. Timmons, and Brigitte Felix

Bulletin 161
2016



New Mexico Bureau of Geology and Mineral Resources
A division of New Mexico Institute of Mining and Technology

Bulletin 161—Geology and Hydrology of Groundwater-Fed Springs and Wetlands at La Cienega, Santa Fe County, New Mexico

Peggy S. Johnson, Daniel J. Koning, Stacy S. Timmons, and Brigitte Felix

Copyright © 2016

New Mexico Bureau of Geology and Mineral Resources
Matthew J. Rhoades, *State Geologist and Director*

A division of New Mexico Institute of Mining and Technology
Daniel H. López, *President*

Board of Regents

Ex-Officio

Susana Martinez, *Governor of New Mexico*
Dr. Barbara Damron, *Secretary of Higher Education*

Appointed

Deborah Peacock, *President, 2011–2016, Corrales*
Jerry A. Armijo, *Secretary/Treasurer, 2015–2020, Socorro*
David Gonzales, *2015–2020, Farmington*
Donald Monette, *2015–2018, Socorro*
Myissa Weiss, *student member, 2015–2016, Farmington*

Series design, ArcGIS, layout, cartography, graphics, and tables: Brigitte Felix
Production and editorial assistance: Rick Arthur
Cover photo: Leonora Curtin Wetland Preserve by Stacy Timmons

New Mexico Bureau of Geology and Mineral Resources
801 Leroy Place
Socorro, NM 87801
(575) 835-5490
<http://geoinfo.nmt.edu>

ISBN 978-1-883905-33-0
First Edition 2016
Published by authority of the State of New Mexico, NMSA 1953 Sec. 63-1-4

Printed in USA

Project Funding:
New Mexico Bureau of Geology and Mineral Resources, Aquifer Mapping Program
Healy Foundation
New Mexico Environment Department, Surface Water Quality Bureau
U.S. Environmental Protection Agency, Wetlands Program Development Grant

SUGGESTED CITATION: Johnson P.S., Koning, D.J., Timmons, S.S., and Felix, B., 2016, Geology and Hydrology of Groundwater-Fed Springs and Wetlands at La Cienega, Santa Fe County, New Mexico: New Mexico Bureau of Geology and Mineral Resources Bulletin 161, 92p.

Available electronically
<http://geoinfo.nmt.edu/publications/monographs/bulletins/161>



CONTENTS

Executive Summary	1
I. Introduction	7
Background	7
Purpose and scope	7
Previous work	7
Description of the study area	10
II. Methods	13
Geologic mapping and cross sections	13
Precipitation and streamflow	14
Water-level measurements, water-table map, and well hydrographs	14
Geochemical methods.....	19
III. Geology of the La Cienega Area	23
Geologic setting and geologic structure	23
Geologic history	23
Geologic units and their hydrologic significance	28
How large is the Ancha groundwater reservoir?	37
IV. Hydrology of La Cienega Wetlands and the Santa Fe Group Aquifer	39
A wetland water balance	39
Precipitation.....	40
Surface-water hydrology	43
Regional groundwater hydrology	48
Groundwater hydrology in the La Cienega area	51
Summary of hydrologic investigation	65
V. Chemical Characteristics and Age of Groundwater	67
Major ion chemistry and water type	67
Summary of chemical and isotopic investigations.....	77
VI. Summary and Discussion	79
Geology, groundwater, and wetlands	79
Wetland water balance	82
Building hydrologic resilience into the La Cienega wetlands	85
Project Staff & Acknowledgments	87
References	88
Acronyms	92
Figures	
1. Location map and regional setting of the La Cienega study area	8
2. Conceptual illustration of wetlands and their hydrologic features	9
3. Orthophoto of the study area showing streams, drainages, and sites of interest	11
4. Map of wells, springs, and surface-water sites ...	15
5. Generalized geologic map and regional geologic setting	24
6. Geologic map	26
7. Stratigraphy of the La Cienega area	28
8. Conceptual block diagram of the Espanola Basin 21 to 25 million years ago	29
9. Hydrogeologic cross sections	30
10. Subcrop geologic map of strata underlying the Ancha Fm	31
11. Percentile plot of hydraulic conductivity by geologic unit	32
12. Elevation contour map of the base of the Ancha Fm	33
13. Isopach map showing thickness of the Ancha Fm	35
14. Saturated thickness map of the Ancha Fm	36
15. A local hydrologic cycle for groundwater-fed wetlands	39
16. A plot of monthly precipitation for NOAA station SF 2	40

17. Precipitation plots for weather stations near La Cienega	42
18. Map of drainages near La Cienega showing stream gages and weather stations	44
19. Plots of stream discharge for Cienega Creek at the Acequia de la Cienega head gate 1966–2014	47
20. Bar chart of stream discharges for Cienega and Alamo Creeks and precipitation	49
21. Map of regional groundwater flow conditions for 2000 to 2005	50
22. Groundwater map of 2012 water-table conditions	52
23. Conceptual illustration of groundwater-fed wetlands	53
24. Maps of seasonal and short-term (2004–2012) changes in groundwater level	55
25. Groundwater hydrographs from wetland wells and daily precipitation	58
26. Location map and photos for wells with hydrographs	59
27. Groundwater hydrographs near La Cienega	60
28. Groundwater hydrographs and regression analysis for decline rates	60
29. Map of water-level declines between three historic measurement periods	62
30. Groundwater hydrographs and precipitation from wet-dry cycles	64
31. Distribution maps for total dissolved solids and calcium-to-sodium ratios	69
32. Piper diagram of major ions in wells, springs, and surface water	71
33. Distribution maps for chloride and chloride-to-bromide ratios	72
34. Plot of stable isotope data for groundwater from wells and springs	73
35. Distribution maps for carbon-14 ages and tritium content in groundwater	74
36. Age-dating of wetland springs before and after monsoon recharge	76
37. Hydrogeologic cross section through the aquifer near La Cienega	80
38. Perspective block diagram showing hydrogeology of the wetlands	81
39. Groundwater declines in the Ancha aquifer east of the wetlands	84

Tables

1. Well inventory	16 & 17
2. Spring and surface-water inventory	18
3. Geologic unit descriptions	25
4. Lithologic data for geologic cross sections	27
5. Information and statistics for NOAA/NCDC weather stations	41
6. Streamflow data for USGS station 08317150 Cienega Creek at flume	46
7. Streamflow measurements for Cienega and Alamo Creeks	49
8. Water-level data for 2012 conditions and changes over time	56 & 57
9. Water-level-change data for three historic measurement periods	63
10. Monthly precipitation for dry and wet periods at stations SFCMA and SF2	65
11. Chemistry data for well, springs and stream waters	68
12. Isotopic data for well, spring, and stream waters	70

Appendices

<http://geoinfo.nmt.edu/repository/index.cfm?rid=20160001>
(Available in digital format)

1. Groundwater data from continuous recorders
2. Groundwater data and hydrographs from periodic measurements
3. Chemistry data
4. Streamflow data

EXECUTIVE SUMMARY

La Cienega's springs and wetlands are important hydrologic, ecologic and cultural resources, and provide many beneficial water-related functions. The wetlands discharge groundwater from regional and local aquifers that provide the sole water source for the southern Santa Fe region. We investigate the wetland system by examining the hydrologic interactions manifested in the wetland water balance. This investigation addresses all aspects of the wetland system, including:

1. The links between geology, groundwater flow, and wetland location
2. Groundwater conditions surrounding the wetlands
3. Chemical, isotopic and age indicators of water sources for the wetlands
4. The effects of climate variability on streamflow and groundwater levels
5. Wetland evapotranspiration
6. Groundwater depletion and water-level declines

The various data are integrated into a physical, conceptual model of wetland hydrogeology, which can support and enhance wetland conservation plans. To be successful in their objectives, hydrologic models and wetland management plans must incorporate the hydrogeologic features that create and maintain the wetlands.

Geology, Groundwater, and Wetlands

The groundwater that feeds springs and wetlands discharges from the Santa Fe Group (SFG) aquifer, which is a regional system of thick alluvial deposits of the Tesuque Formation, overlain by shallow, thin, coarse deposits of the Ancha Formation. The wetlands are located at the western edge of the southern Española Basin, where the SFG aquifer thins and dissipates over older, low-permeability strata. Thinning of the aquifer forces groundwater to the surface where it emerges from buried valleys in the Ancha Formation to maintain springs and seeps that create the wetlands. Groundwater stored in the Ancha Formation is the primary source of water for the wetlands. The accretion and storage of groundwater in the Ancha Formation depends on local recharge, upflow of deep groundwater, permeability contrasts between the Ancha and underlying formations, and the buried valleys at the base of the formation that direct groundwater flow and control wetland location. We estimate that the Ancha aquifer near La Cienega contained roughly 67,000 acre-feet of groundwater under 2000–2005 conditions.

Buried-valley aquifers in the Ancha Formation

Buried valleys in the Ancha Formation create coarse-grained, highly transmissive aquifers that take the form of long and narrow, ribbon-like channels scoured into less permeable underlying

formations. The boulder-rich channel-bed deposits and adjacent sheet-like lower alluvial slope deposits form the Ancha aquifer. Two prominent buried valleys at the base of the Ancha aquifer behave as drains that gather groundwater from the surrounding aquifer, concentrate flow, and direct discharge to the springs and wetlands. The El Dorado buried valley east of La Cienega directs water flow to wetlands at Las Lagunitas in Guicu Creek, at the Leonora Curtin Wetland Preserve in Cañorita de las Bacas, and in upper Cienega Creek. The ancestral Santa Fe River buried valley forms Sunrise Springs and wetlands along the western slopes of Arroyo Hondo. Buried-valley aquifers are important sources of groundwater, but are subject to a large and unusual drawdown response to pumping. A pumping well in or adjacent to a buried valley will extract most of its water directly from the buried valley and concentrate large water-level drawdowns along the valley's axis. The wetlands in Arroyo Hondo, Guicu Creek and Cienega Creek (Figs. 14 and 9) are vulnerable to the large drawdown response that is characteristic of these aquifers, but they are also linked to sources of enhanced recharge.

Sources of groundwater feeding the wetlands

As groundwater flows across the basin from the Sangre de Cristo Mountains it circulates to various depths, creating an age-stratified system. Chemical, isotopic, and age (^{14}C and ^3H) data verify that wetland waters are a mixture of modern (post-1952) and older waters from shallow and deep aquifer zones, as well as recent storm recharge. These sources intermix at the edge of the basin where the aquifer thins.

Wetland waters have distinctive chemical and age characteristics depending on the buried valley source and its location east or west of Cienega Creek. The east wetland zone in upper Cienega Creek, Guicu Creek and Canorita de las Bacas (connected to the El Dorado buried valley) exhibits relatively young ^{14}C ages (2,480 to 5,720 RCYBP uncorrected), small amounts of tritium (0.1 to 0.9 TU), and high concentrations of calcium relative to sodium. These characteristics indicate a mixture of old groundwater and modern, locally-derived recharge. The west wetland zone at El Rancho de las Golondrinas and the western slopes of Arroyo Hondo and Sunrise Springs (connected to the ancestral Santa Fe River buried valley) are rich in sodium, have older ^{14}C ages (4,860 to 7,240 RCYBP uncorrected) and zero tritium, which indicates a source dominated by old groundwater from the Tesuque Formation to the north. Stable isotope and ion chemistry show similar partitioning between east and west wetland zones.

Age dating of wetland springs following large monsoon storms in September 2013 shows that groundwater ages decreased after the storms relative to samples collected during drought conditions in June-July 2011. A dramatic water-table spike coinciding with the storms, and decreasing spring-water ages following the storms, demonstrated that storm runoff rapidly recharged the shallow Ancha aquifer.

Effluent discharge from the wastewater treatment plant (WWTP) has a unique ion chemistry and chloride-bromide content not observed in well and spring samples in the study area, indicating that wetland waters are not chemically influenced by WWTP discharge.

Wetland Water Balance

The wetland water balance describes water inflows, outflows and changes in groundwater storage in the wetland. Wetland inflow comes directly from groundwater and indirectly from precipitation. Wetland outflows include evapotranspiration (ET), groundwater discharge to surface water, and groundwater withdrawals from wells, which became a significant anthropogenic impact to groundwater storage starting in the mid-20th century.

Groundwater storage and wetlands

Changes in groundwater storage reflect imbalances between recharge to and discharge from an aquifer. Storage changes manifest in fluctuations of the water table and are documented by measuring groundwater levels over time. A long-term negative water balance (where discharge exceeds recharge) can result from prolonged drought, increased evaporation, well withdrawals and/or decreased recharge, and can lead to reductions or disruptions in groundwater discharge to springs, or elimination of springs and wetlands altogether. Drought, recharge, ET, and groundwater depletion from pumping each generates a unique water-level variation, which is observable in groundwater hydrographs with high measurement frequencies. We apply water-table fluctuation methods to examine how changes in climate, seasonal cycles, ET, and groundwater extraction affect groundwater storage at the wetlands.

Climate variability and drought—Highly variable precipitation, punctuated by periods of drought, is characteristic of the upper Rio Grande in New Mexico. The Santa Fe area suffered severe to extreme drought conditions from April 2011 through July 2014, whereas the 2013 summer monsoon was among the wettest on record. Climate research has showed that the 1950s and 2000s droughts were among the most extreme of the past seven centuries and are likely to return with greater frequency as a result of climate change. Extended drought and climate change are projected to decrease groundwater levels by increasing evaporation and groundwater withdrawals, reducing recharge, and escalating groundwater depletion.

The groundwater-level response to climate events near La Cienega was revealed in a time-series comparison of local groundwater levels and monthly precipitation from extreme wet and dry periods. Water-table spikes of about +1.2 ft followed a record monsoon in 1991 and record snowmelt runoff in spring 2005. Small water-table rises of +0.1 to +0.4 inches occurred when monthly precipitation exceeded 4 inches. Annual water-table cycles, with high water levels in fall following the summer monsoon and low levels in the spring, occurred near the study area. Droughts lasting a year or more coincided with drops in the water table of 0.4 to 0.6 ft (well EB-220), but the drought-depressed water table was typically restored by post-drought rainfall.

Streamflow—Periodic measurements of streamflow at the Cienega head gate (USGS station 08317150) in the headwaters of Cienega Creek show a mean and median flow of 0.53 cubic feet per second (cfs, ft^3/s) for the period 1966–2014. Four measurements taken between 1966 and 1975 ranged from 1.55 to 0.55 ft^3/s . Measurements taken at more regular intervals starting in 1986 indicate that post-1986 discharge was generally lower, with most flows being near or below the long-term mean.

Streamflow at the Cienega head gate varies both seasonally and year-to-year. Discharge is lowest during summer months and generally higher the rest of the year, despite a substantial increase in precipitation from the summer monsoon. The seasonal variation in streamflow is driven by high summer ET. Long-term streamflow variability relates to climate cycles and is most affected by multi-year drought. During the dry intervals of 2001–2004 and 2012, the mean streamflow dropped to 0.48 and 0.38 ft³/s, respectively, and most measurements fell considerably below the long-term mean. Wet (1991) and average (1997) years of precipitation produced streamflow near the long-term mean (0.54 ft³/s).

It is difficult to attribute streamflow decline after 1966 solely to drought, given that streamflow in March 1966 (1.55 ft³/s) was exceptionally high for a dry year (March 1966 received 0.03 inches of precipitation). Comparisons of the post-2001 mean dry-season streamflow (0.55 ft³/s) and the March 1966 measurement (1.55 ft³/s) imply that streamflow may have declined at the Cienega head gate by roughly 1 ft³/s (64%) since 1966. The limited data generally indicate that surface water outflow from the wetlands—thus groundwater discharge to the wetlands—has decreased from historic levels.

Evapotranspiration—Seasonal and daily fluctuations of the wetland water table, visible in hydrographs from a wetland well at the Leonora Curtin Wetland Preserve, are caused by groundwater withdrawals by ET. Seasonal water-table fluctuations—low water levels during summer and high levels in winter—are a response to changes in ET between growing and dormant vegetation stages. Wetland groundwater levels rose by +0.04 to +6.60 ft between summer 2011 and winter 2012. Lowering of the water table begins in spring following leaf emergence and coincides with the start of a diurnal (12-hour) fluctuation with a magnitude of about 0.1 to 0.2 ft. Diurnal fluctuations cease after killing frosts and just prior to the winter water-table rise. In 2012, the diurnal signal in a riparian-zone well at the Preserve began in early April, continued through the growing season, and ended in late October. Large summer water-level drops in the wetland aquifer (-4.9 ft in well LC-025) indicate that ET produces a significant, seasonal groundwater outflow from the wetlands.

Groundwater depletion and declining water levels—Groundwater levels in the Ancha aquifer have dropped steadily since at least the early 1970s as a result of long-term groundwater depletion up-gradient (east) of the wetlands. In well EB-220, the water level has declined 7.5 ft since 1973, leaving a remaining saturated thickness of 31 ft. Measurements in 2004 and 2012 show water-table declines of up to 1.9 ft. A comparison of Ancha water levels in the mid-1970s and 1980s with levels measured in the same wells between 2004 and 2012 shows long-term water-table declines up to 8.9 ft. The largest depletions and decline rates have occurred in the Valle Vista area and south of the penitentiary, near the northern and southern edges of the Ancha zone of saturation.

Long-term groundwater depletion is driven largely by overexploitation, whereas shorter-term local trends in depletion are dominated by natural climate variability over months to years. The long-term trends in declining groundwater levels documented near La Cienega cover periods of one to four decades, cross multiple precipitation cycles, and extend beyond the wetland area. The groundwater declines are of a style noted throughout the United States and demonstrate an anthropogenic connection between groundwater depletion and unsustainable

withdrawals from wells. Buried-valley aquifers, like those that maintain the wetlands, focus pumping drawdowns along the buried channels and aggravate groundwater depletion.

Groundwater hydrographs with long records and high measurement frequencies show the cumulative effects of seasonal groundwater fluctuations (winter highs and summer lows) and recharge events from large monsoons (1991) and spring runoff (2005) superimposed on long-term declines associated with groundwater depletion. Dropping water levels in the Ancha aquifer are exacerbated during droughts, but time-series comparisons of groundwater and precipitation hydrographs indicate that drought-depressed water tables are restored by post-drought rainfall. The long-term declining groundwater levels are a key indicator of human-caused groundwater depletions from wells.

Creating Hydrologic Resilience in the La Cienega Wetlands

Findings from this investigation emphasize possible solutions towards hydrologic resilience and successful preservation of the important wetland resources at La Cienega. These solutions focus on reducing groundwater depletions in the Ancha Formation and supporting a positive wetland water balance. Possible remedies include:

- Eliminate groundwater withdrawals from areas near the ancestral Santa Fe River and El Dorado buried valleys
- Manage the timing and location of groundwater withdrawals from the Ancha saturation zone to eliminate or reverse further losses to the Ancha aquifer near the wetlands
- Utilize the natural, recharge capabilities of buried-valley aquifers in the Ancha saturation zone and develop effective aquifer storage projects where opportunities exist
- Manage overgrowth of unwanted invasive vegetation in the wetland riparian zones to minimize summer losses to evapotranspiration



Transition from parched desert slope to spring-fed pond in lower Guicu Creek.

I. INTRODUCTION

Background

The agricultural community of La Cienega, located southwest of Santa Fe (Fig. 1), contains a distinctive wetland environment that includes an exceptional concentration of groundwater-fed seeps and springs, perennial streams, ponds, acequias, ciénegas, and wet meadows (Fig. 2). Wetlands are lands transitional between terrestrial and aquatic systems where the water table is usually at or near the surface, or the land is covered by shallow water at some time during the growing season of each year (Cowardin et al., 1979; Tiner, 1996). New Mexico's wetlands cover about 482,000 acres, mostly in the eastern and northern areas of the state, and include forested wetlands, bottom-land shrublands, marshes, wet and salt meadows, shallow ponds, and playa lakes (Tiner, 1996). About one-third of the State's wetlands have been lost or degraded due to agricultural conversion, diversion of water to irrigation, overgrazing, urbanization, streamflow regulation, and invasion by non-native plants (Tiner, 1996). Groundwater-fed wetlands in semi-arid landscapes, especially those that form large ciénega complexes as at La Cienega (Fig. 2), are among the most diminished and threatened ecosystems in the arid Southwest, and the least studied and documented (Sivinski and Tonne, 2011).

Interest in the health and sustainability of the springs and wetlands stimulated a collaborative project, completed in December 2012, called Comprehensive Wetland Restoration and Protection in Santa Fe County (McGraw and Jansens, 2012). The project was led by the New Mexico Environment Department Surface Water Quality Bureau (NMED SWQB) Wetlands Program and supported by Ecotone (Santa Fe, NM), the U.S. Fish and Wildlife Service (Albuquerque, NM), the NMOSE (Santa Fe, NM), the New Mexico Bureau of Geology and Mineral Resources (NMBGMR, Socorro, NM), and Santa Fe County Public Works Department. The goals of the collaborative study were: 1) to develop and demonstrate an understanding of the surface water and groundwater sustaining wetlands in the La Cienega area; 2) to provide information that is helpful for

future wetland and water management; 3) to identify areas for long-term monitoring; and 4) to inform future actions for wetland restoration and protection.

Purpose and Scope

The hydrogeology of groundwater-fed wetlands in La Cienega was investigated as part of the collaborative project, with the limited purpose of identifying sources of groundwater to the wetlands and assessing vulnerability of the wetlands to potential impacts (Johnson et al., 2012). This scientific investigation report supplements and expands on the collaborative project. Significant issues of concern for the La Cienega area are the dwindling, disrupted or erratic water flows and drying of springs and wetlands. Understanding the wetland system is best achieved through understanding the interactions of its parts. This investigation addresses all aspects of the wetland system, including: 1) the links between geology, groundwater flow, and wetland location; 2) regional and local groundwater conditions; 3) climate variability and the effects on streamflow and groundwater levels; 4) evapotranspiration; 5) water-level declines and groundwater depletion; and 6) chemical, isotopic and age characteristics of spring discharge and wetland groundwater.

Results of the investigation are integrated into a physical conceptual model of spring and wetland hydrogeology. This study presents the first comprehensive assessment of the geology and hydrogeology of wetlands and springs in the La Cienega area and can also serve as a scientific model for the investigation of groundwater-fed wetlands in other settings. We hope this report can help direct the public discussion on conservation and preservation of the unique wetland resources at La Cienega.

Previous Work

Since the 1950s there have been many hydrogeologic studies of the southern Española Basin and the La Cienega area. These range from regional studies of

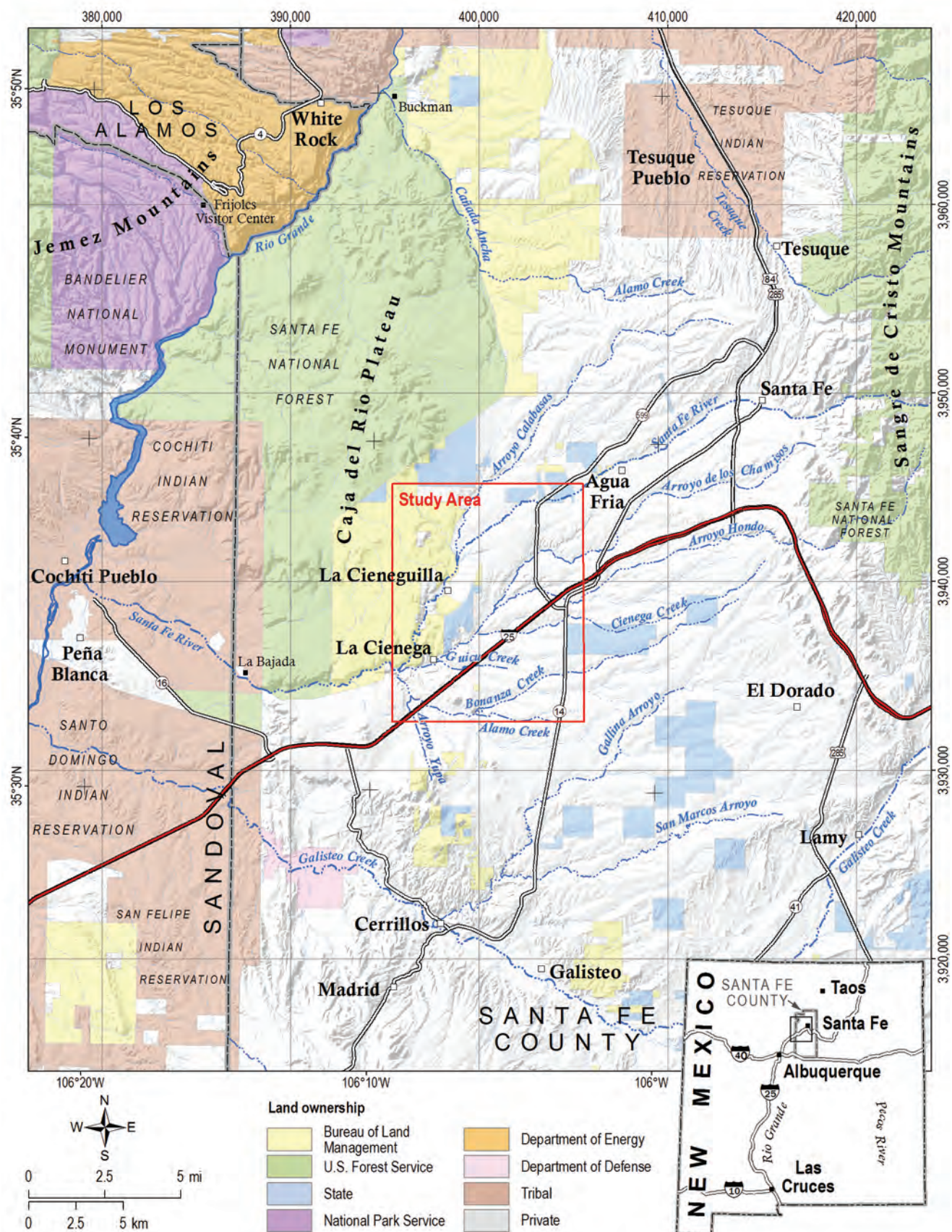


Figure 1. Location map and regional setting of the La Cienega study area.

the basin that include information on local hydrologic or geologic features to focused studies of its geology, surface water, and groundwater. These studies provide a context for the La Cienega study and we build upon them to improve the collective hydrogeologic understanding of this important area.

The comprehensive study of water resources and groundwater conditions in the Santa Fe area by Spiegel and Baldwin (1963) was the first to identify La Cienega as a discharge zone for the Santa Fe Group aquifer south of the Santa Fe River. The study also identified groundwater in the Ancha Formation as the source of water feeding the springs and proposed that “[s]prings emerge where pre-Ancha valleys, cut into the bedrock floor, have been exposed along the sides of post-Ancha valleys. Where these post-Ancha valleys are cut below the water table in the Ancha, springs and seeps emerge into the valley floors and lower side slopes” of the Cienega Creek valley and its tributaries (Spiegel and Baldwin, 1963, p. 137). At that time, insufficient reliable geologic, hydrologic, or geophysical data existed in the area to determine the details of the sub-Ancha topography beyond a general form of the buried surface. Recent studies of the Santa Fe Group aquifer by scientists at the NMBGMR and the U. S. Geological Survey (USGS) have advanced the understanding of groundwater saturation and flow in the Ancha and Tesuque Formations, which together comprise the Santa Fe Group aquifer.

Spiegel and Baldwin (1963) provided important summaries of La Cienega and La Cieneguilla. This work included: 1) some of the earliest known streamflow measurements that were made between 1951 and 1953 along Cienega Creek and the Santa Fe River below La Cieneguilla; 2) the first investigations of the Ancha Formation and its hydrologic significance; and 3) the first delineation of groundwater divides and basins that contribute discharge to the Santa Fe River and wetlands at La Cienega and La Cieneguilla. Spiegel (1963, 1975) was the first to propose that highly permeable deposits in pre-Ancha buried channels conveyed substantial amounts of groundwater across the plains from the mountain front and controlled the locations of springs and wetlands. Spiegel (1975) was also the first to discuss the combined effects of all natural and artificial recharges and withdrawals on the La Cienega springs, and evaluated the effects of pumping wells at the Santa Fe Downs on the Acequia de la Cienega in this context.

Geologic studies over the past 15 years have significantly improved understanding of the geologic framework of the Santa Fe Group aquifer near Santa Fe, including La Cienega and La Cieneguilla. New geologic mapping, coupled with detailed sedimentologic and stratigraphic studies, resulted in subdivisions of the Santa Fe Group (called *lithosomes*) based on texture, composition, and paleodrainage (Koning and Read, 2010; Read et al.,

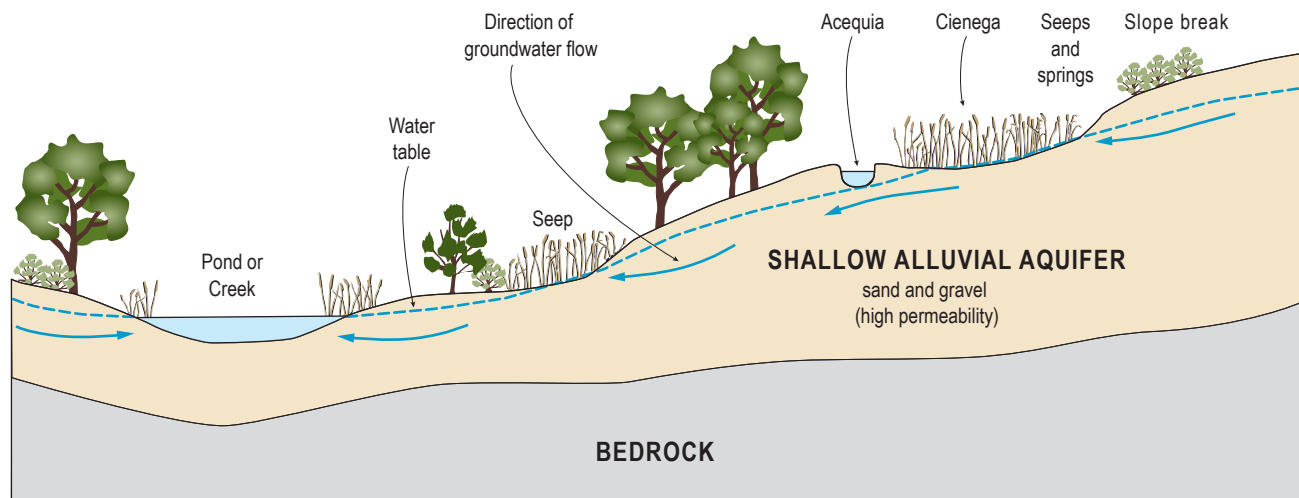


Figure 2. Conceptual illustration of wetlands and their hydrologic features. Wetlands are lands transitional between terrestrial and aquatic systems where the water table intersects the land surface. A ciénaga is a marshy area with standing water and vegetation due to the presence of seeps or springs. A common setting for ciénagas and wetlands is an area of shallow groundwater with topographic depressions or a sloping land surface. Originating from the Spanish *ciénaga*, a “marsh, bog, or miry place”, the term is common in the southwestern U.S. (Wilson and Moore, 1998; Carter, 1996). In La Cienega, groundwater-fed springs and wetlands supply streams and acequias, a Spanish word of Arabic origin for an irrigation ditch or canal.

2004). The USGS documented thickness changes of the basin fill and delineated buried faults and volcanic strata using a geophysical data model (Grauch et al., 2009). Recent studies of the Ancha Formation have produced a series of maps that depict the structural base, thickness, and extent of saturation for the formation (Johnson and Koning, 2012). This collective research has refined depositional and tectonic interpretations and updated the geologic framework of the Española Basin.

Several studies of groundwater conditions in the Santa Fe Group aquifer have been conducted over the past 50 years. These include regional water-table maps and general summaries of groundwater flow that cover the La Cienega area (Spiegel and Baldwin, 1963; Mourant, 1980; Daniel B. Stephens and Associates, 1994; Johnson, 2009). Subsurface recharge from the Sangre de Cristo Mountains and mountain-front stream infiltration were examined by Wasiolek (1995) using water-budget methods. Recharge to the Santa Fe Group aquifer by stream and channel infiltration was examined by Thomas et al., (2000) and Moore (2007), whereas Anderholm (1994) applied chloride balance and isotopic methods to study areal recharge to the basin-fill aquifer. Several recent studies have examined physical, chemical and isotopic data from precipitation, stream, spring and well waters in the Santa Fe Group aquifer to determine many aspects of regional groundwater movement, recharge, discharge, and residence time (Johnson et al., 2008; Manning, 2009; Johnson et al., 2013). Numerical simulations of the Tesuque aquifer system near Santa Fe (McAda and Wasiolek, 1988) incorporated available hydrologic and geologic information to enhance understanding of the basin geohydrology and assess effects of existing and future groundwater withdrawals, but these efforts pre-date recent advancements to the hydrogeologic framework by the USGS and the NMBGMR mentioned above.

A recent hydrogeologic study of the area, completed by HydroScience Associates, Inc. (2004) for the Acequia de La Cienega, reviewed contemporaneous geologic investigations taking place in the southern Española Basin, updated the local hydrogeology, and explored the possible reasons for springflow decline. Important conclusions from this study include:

1. The La Cienega area is an “altitude dependent drain for the southern portion of the Santa Fe Embayment.” Water moving west and southwest through the Ancha and Tesuque aquifers is forced to the surface as the aquifer thins over relatively

impermeable Oligocene volcanic rocks. The general area in which discharge occurs is controlled by the structure of the basin and the presence of the volcanic rocks.

2. The source of water discharging from the springs is likely not limited to just the watershed encompassing the Arroyo de los Chamisos, the Arroyo Hondo, and Cienega Creek, but is determined by groundwater divides, which have probably been affected by human activities in the basin.
3. The ditch measurements made on the Acequia de La Cienega in 2004 indicated an apparent slow decline between 1991 and 2003, but most of the decline occurred prior to 1991.

Data for twelve springs in the vicinity of La Cienega and La Cieneguilla were included in White and Kues (1992), who inventoried springs in New Mexico. Seepage studies have measured streamflow in Cienega Creek, its tributaries, and above and below its confluence with the Santa Fe River in order to assess gains and losses in flow (NM Hydrologic, LLC and the New Mexico Office of the State Engineer, 2012a, b; Petronis et al., 2012; Peery et al., 2007).

Description of the Study Area

The agrarian community of La Cienega is a prehistoric settlement site of several, early Native American and Puebloan cultures and is one of the oldest Hispanic settlements in New Mexico, dating back to the 1700s. Early Spanish settlements were established wherever sufficient perennial water existed for irrigation, including Cienega Creek (1715) and Alamo Creek (1730) (Spiegel, 1963, p. 94 (from Candelario, 1929)). The area's traditional agricultural systems are supported by acequia irrigation supplied by waters from the many springs in the area and small perennial flow in Cienega Creek and its tributaries.

The study area is situated in the lower Santa Fe River watershed upstream of the confluence of the Santa Fe River, Cienega Creek and Alamo Creek (Fig. 3). The study area includes lower Cienega Creek and its tributaries (Arroyo de los Chamisos, Arroyo Hondo, Canorita de las Bacas, and Guicu Creek) and a portion of the Santa Fe River above and below the City of Santa Fe's Paseo Real wastewater treatment plant (WWTP, Fig. 3). Alamo Creek and its tributary Bonanza Creek are also included on most study-area maps.

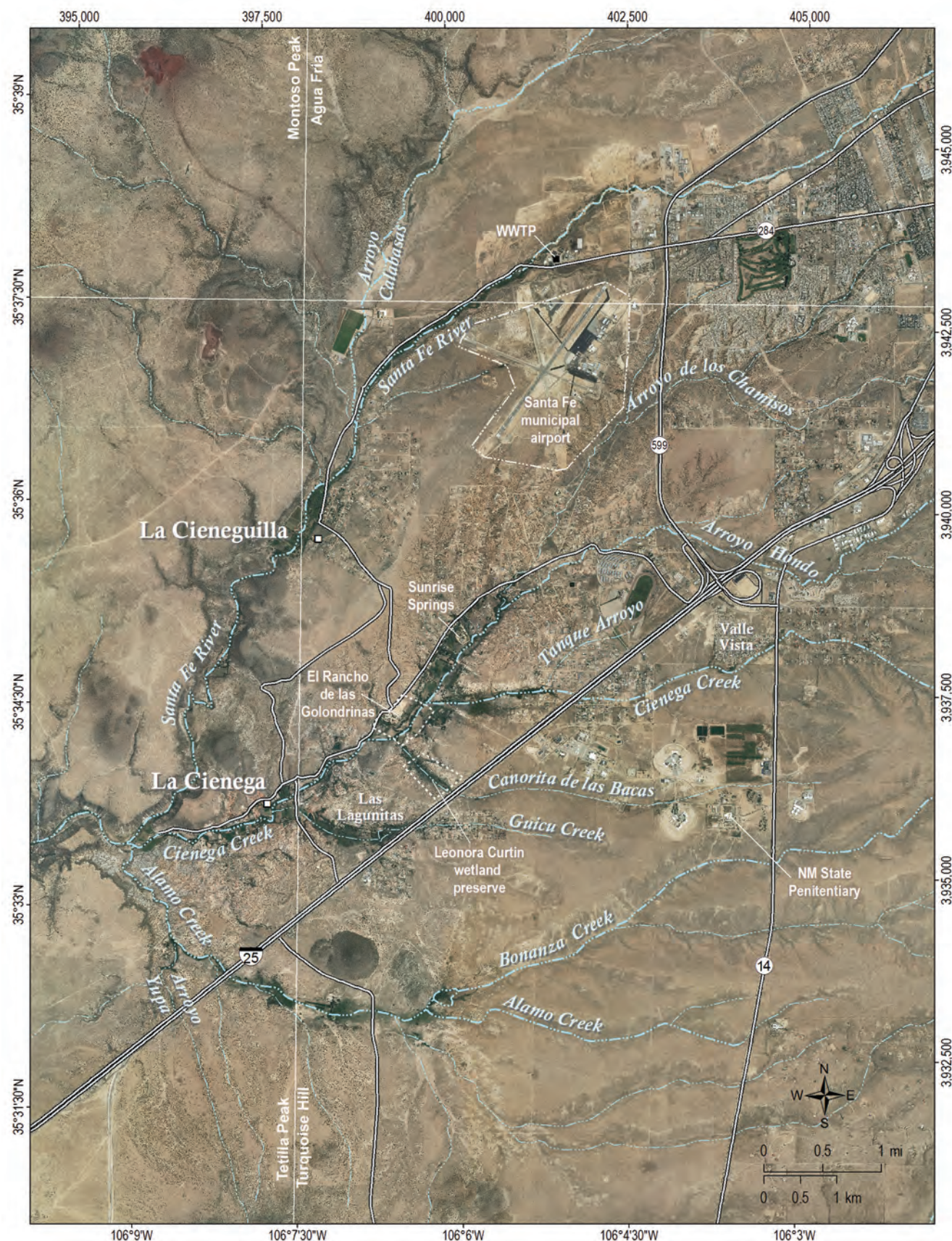


Figure 3. Orthophoto of the study area showing streams, drainages, and sites of interest near La Cienega.

La Cienega lies along the southwest margin of the Española Basin, which is a geologic depression bordered by the Sangre de Cristo Mountains on the east and the Jemez Mountains on the west. The area is characterized by the convergence of multiple drainages emanating from the Sangre de Cristo Mountains. These drainages have carved 30- to 100-ft deep valleys into a broad, west-sloping alluvial surface extending westward from the Sangre de Cristo Mountains (Figs. 1, 3). Groundwater-fed springs and wetlands line the slopes and bottoms

of the valleys. West of Cienega Creek, a 200-ft tall highland separates the Cienega valley from the Santa Fe River and the Caja del Rio volcanic plateau. The Cienega valley is an area of shallow groundwater and surface water that supports a verdant riparian-wetland ecosystem of predominantly native cottonwoods, willows, rushes, sedges, and cattails, as well as exotic invasive species such as Russian olive and tamarisk. In contrast, the surrounding arid uplands are dominated by piñon-juniper shrub and grassland savanna.



Measuring a groundwater level near ponds at El Rancho de las Golondrinas.

II. METHODS

This section describes the methods applied to collection and analysis of the geologic, hydrologic, and geochemical data used in the wetland study. Hydrogeologic field work was conducted by New Mexico Bureau of Geology and Mineral Resources staff between March 2011 and March 2014.

Geologic Mapping and Cross Sections

Understanding the nature, characteristics, relative age and distribution of geologic strata is essential to any groundwater study. The geologic map used in this report integrates detailed 1:12,000 scale mapping, completed for this study in 2011, with previous versions of the 7.5-minute Turquoise Hill quadrangle (1:24,000 scale) (Koning and Hallett, 2002).

Quaternary deposits were delineated using aerial photography combined with local field checks. Pre-Quaternary formation contacts were mapped by: 1) physically walking the contacts and data logging their GPS positions; and 2) visually comparing the position of a contact with topography and drawing it on a topographic base map. Maps from 2002 and 2011 were compiled using ArcGIS.

We created four new geologic cross sections for this study using the following steps. First, the vertical positions, or depths, of stratigraphic contacts were interpreted in wells. The well locations and stratigraphic contacts were compiled into a single database. Second, topographic profiles were generated in ArcGIS from a 10-meter digital elevation model (DEM) from the National Elevation Dataset (ned.usgs.gov/). Third, stratigraphic contacts were drawn on the topographic profile surfaces, and wells with interpreted stratigraphic contacts were projected along strike into the cross sections. Fourth, measurements of bedding attitudes, which give the dip of strata at the surface, were used to draw subsurface stratigraphic contacts on the cross sections. The subsurface location of a monoclinal hinge beneath La Cienega—the western limb of the Rancho Viejo hinge zone of Grauch et al., (2009)—was incorporated into the cross sections. The base of the Santa Fe Group from Grauch et al., (2009) and

the base of the Ancha Formation from Johnson and Koning (2012) were also projected onto the geologic cross sections.

Aeromagnetic maps (Grauch et al., 2009) were useful in delineating certain buried rocks, especially the Cieneguilla basanite. Four different flow packages of this basanite were delineated in the area, using variances of remnant magnetism and magnetic susceptibility. Based on outcrop study, these flows are separated by volcaniclastic strata with lower magnetic susceptibility. The locations of buried flows were interpreted from the aeromagnetic maps and their boundaries or contacts transferred to the geologic map and cross sections.

Ancha Formation maps

The latest lithologic, thickness, and hydrologic observations for the Ancha Formation near Santa Fe were presented by Johnson and Koning (2012) in four maps: 1) an elevation contour map of the base of the Ancha Formation; 2) an isopach map showing thickness of the Ancha Formation; 3) a map of the saturated thickness of the Ancha Formation (2000 to 2005 groundwater conditions); and 4) a subcrop geologic map showing distribution of strata underlying the Ancha Formation. Because local versions of these maps for the La Cienega area are incorporated into this report, the methods for producing them are reiterated here. Site data for depth to base of formation, formation thickness, saturated thickness, and subcrop formation are presented in table form in Johnson and Koning (2012).

The characteristics of the base of the Ancha Formation and its thickness are important to regional groundwater studies. The base of the Ancha Formation and the nature of underlying strata were mapped using lithologic interpretations of drill-hole cuttings (NMBGMR core and cutting archives, Socorro, NM), descriptive lithologies and geophysical logs from exploration and water-well records, field outcrop exposures (Koning and Johnson, 2004), and stratigraphic contacts from geologic maps (Koning and Read, 2010, and maps cited therein; Koning and Hallett, 2002).

Coordinates for site locations were derived from a combination of sources, including (from highest to lowest data quality): handheld GPS devices at the data site, coordinates reported by professional consultants and the NMOSE, map locations reported by consultants, Santa Fe County's ArcGIS plat map coverage and lot locator database, and township-range-section locations reported on well records on file with the NMOSE. Surface elevations of data sites were generated using the 10-meter DEM. Basal elevations of the Ancha Formation were calculated by subtracting the depth of the formation's base from the surface elevation. Therefore, in some cases, small thicknesses of late-Pleistocene to Holocene surficial deposits were incorporated into thickness estimates for the Ancha Formation. Base elevation and thickness contours were interpolated from point data using a kriging function in ArcGIS, and then smoothed by hand. A subcrop map showing distribution of underlying strata was constructed using lithologic interpretations from wells penetrating into strata beneath the Ancha Formation.

Saturated thickness estimates for the Ancha Formation were calculated from a subset of wells used to map the formation base, combined with additional wells having NMOSE well records that met the following data requirements: full or nearly full penetration of the Ancha Formation by the water well, a known location, an interpretable lithologic record, and a measured or otherwise reliable water level. Saturated thickness was calculated at well sites by subtracting the depth to water, measured in Ancha wells, from the formation thickness. Contours were constructed by hand from point data and constrained by the elevation of springs emerging from Ancha Formation sediments.

Precipitation and Streamflow

Because wetland sustainability requires a relatively stable influx of water (Carter, 1996), it is important to understand the temporal variability in precipitation when assessing wetlands. Precipitation records from National Oceanic and Atmospheric Administration, for the National Climatic Data Center (NOAA/NCDC) weather stations for the La Cienega and Santa Fe areas (available at www.ncdc.noaa.gov/cdo-web/datasets) were evaluated for this purpose. Summary statistics of monthly and annual precipitation, including median and other percentile values applicable to skewed data (Helsel

and Hirsch, 1995), were used to: 1) characterize precipitation patterns and variability; and 2) define and identify wet and dry periods, which we correlated to records of streamflow and groundwater level.

Streamflow that is measured during the winter and unaffected by surface runoff reflects the discharge of groundwater through the wetlands to streams. We analyzed existing streamflow data using plots of discharge versus time from two locations—upper Cienega Creek near the Acequia de la Cienega head gate, and the Santa Fe River above and below the confluence with Cienega and Alamo Creeks—to better understand multi-year and seasonal variability in surface-water and groundwater discharge from the wetlands, the short- and long-term trends in streamflow, and possible causes for declining flows over time. Streamflow data at the Cienega head gate (USGS station 08317150 LA CIENEGA CR AT FLUME NR LA CIENEGA, NM), available since 1997 from the NWIS website waterdata.usgs.gov/nwis/measurements/?site_no=08317150 are combined with prior measurements by the USGS (1986–1992) and other sources reported in Hydroscience Associates, Inc. (2004). Recent seepage and flow-measurement data (NM Hydrologic, LLC and the New Mexico Office of the State Engineer, 2012a, b; Petronis et al., 2012; Peery et al. 2007; Spiegel, 1963) are integrated with historic measurements to evaluate changes in discharge over time.

Water-Level Measurements, Water-Table Map, and Well Hydrographs

Water-level measurements from observation wells are the principal source of information about the hydrologic stresses acting on aquifers and how these stresses affect groundwater recharge, storage, and discharge (Taylor and Alley, 2001). A major component of this study was to collect water-level data from a network of wells tapping the shallow aquifer near springs and wetlands (Fig. 4, Tables 1 and 2). Current and historic water-level data were used to: 1) characterize groundwater flow near the wetlands; 2) establish how groundwater levels have changed over time; and 3) evaluate the effects of natural recharge, climatic variability and groundwater development on the water table. Groundwater data and hydrographs are presented in Appendices 1 and 2.

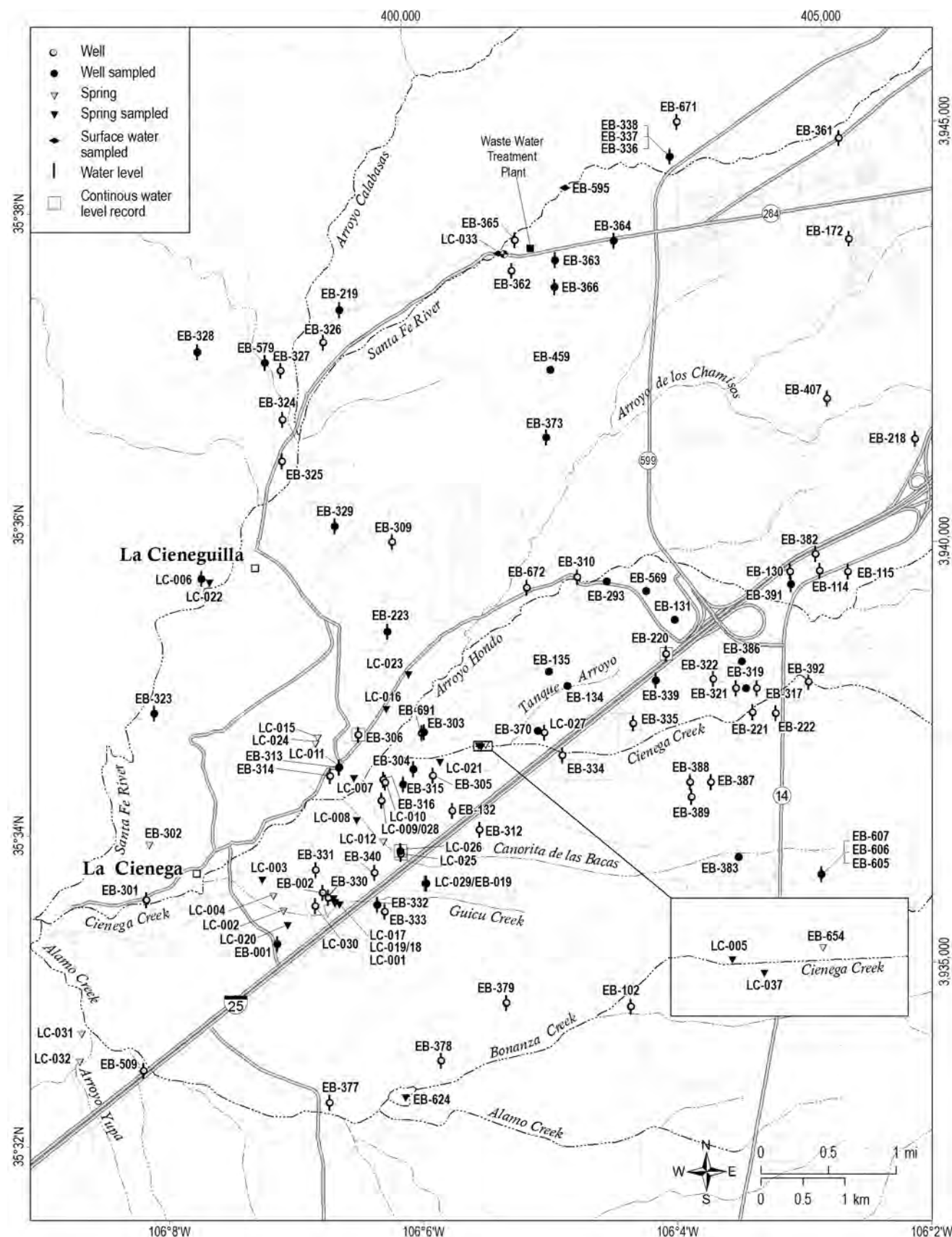


Figure 4. Map of wells, springs, and surface water sites used in the study. Well and spring information is found in Tables 1 and 2.

Table 1. Well inventory with location, site and construction information (sites shown on Fig. 4).—Continued

WELL LOCATION				SITE INFORMATION				WELL CONSTRUCTION						
Site ID	UTM easting NAD83	UTM northing NAD83	Elevation (ft asl)	NMOSIE well record	Water sample	Water level	Site visit	Water bearing formation*	Well depth (ft bsl)	Screen top (ft bsl)	Screen bottom (ft bsl)	Drill date	Driller static water level (ft bsl)	Static water elevation (ft asl)
EB-001	398529	3935208	6065	RG-39419	x	x	x	QTaas/Tg	221	47	221	3/15/83	32	6033
EB-002	399070	3935822	6073	RG-61825		x	x	QTa/Ti	380	90	370	3/3/95		
EB-019	400304	3935932	6144	RG-27637S	x	x	x	QTa	80	50	80	3/1/79	37	6108
EB-102	402734	3934466	6199	Unknown		x	x	QTa						
EB-114	404980	3939648	6340	RG-35281		x		Tts	320	280	320	29573	200	6140
EB-115	405319	3939633	6354	RG-35282		x		Tts	320	280	320	29573	200	6154
EB-130	404633	3939633	6325	Unknown		x	x	Tts	225			1/1/51	180	6146
EB-131	403262	3939063	6276	RG-29416Ex	x			QTa/Tts	222	180	220	10/1/77	142	6134
EB-132	400609	3936794	6180	RG-08223		x	x	QTaas	135	60	90	12/2/62	60	6113
EB-134	401980	3938280	6190	RG-32553	x			QTaas	137	90	134	6/1/79	61	6129
EB-135	401760	3938450	6212	RG-32554Ex	x			QTaas	116	73	112	6/20/79	70	6142
EB-172	405330	3943594	6462	RG-24042		x	x	Tts	493	353	470	10/13/73	307	6156
EB-218	406118	3941215	6412	RG-09982		x		Tts	337	317	332	2/19/64	255	6158
EB-219	399267	3942749	6218	RG-00590	x	x	x	Tts	244	76	237	8/24/56	76	6143
EB-220	403153	3938661	6260	RG-03824T		x	x	QTa	161	125	161	5/10/71	125	6138
EB-221	404187	3937969	6243	RG-22251X7		x	x	QTa/Tts	220	160	220	1/20/74	130	6115
EB-222	404457	3937957	6269	RG-22251X8		x	x	QTa/Tts	220	160	220	1/19/74	130	6141
EB-223	399840	3938918	6165	RG-25952	x	x	x	QTa	100	40	95	5/8/75	42	6123
EB-293	402450	3939520	6199	RG-11826S	x			Tts	340	102	340	9/5/70	60	6139
EB-301	396972	3935730	5889	RG-32228		x	x	Tg	30			6/1/51	24	5867
EB-303	400274	3937732	6123	RG-80582	x	x	x	QTa	62			1/1/42	31	6085
EB-304	400149	3937292	6103	RG-21300	x	x	x	QTa	60	20	40	7/20/78	14	6090
EB-305	400377	3937211	6127	RG-21301		x	x	QTa	75	20	75	7/24/78		
EB-306	399495	3937699	6102	Unknown		x	x	QTa	43					
EB-309	399896	3939990	6231	RG-23683x2		x	x	Tts	300	120	280	5/1/92	107	6125
EB-310	402100	3939571	6180	RG-56355		x	x	QTa/Tts	307	47	267	7/1/98	43	6140
EB-312	400935	3936570	6179	RG-08823		x	x	QTa	135			12/2/62	60	6112
EB-313	399260	3937304	6075	RG-14450	x	x	x	QTa/Tte	100			3/20/67	85	5993
EB-314	399155	3937207	6060	RG-14450X		x	x	QTa	12			1/1/86		
EB-315	400028	3937110	6113	RG-11278	x	x	x	QTa/Tte				1/1/62		
EB-316	399790	3937163	6086	None		x	x	QTa/Tte	8			10/4/07		
EB-317	404232	3938253	6265	RG-22251x6		x		Tts	200	140	200	10/18/73	135	6130
EB-319	404105	3938254	6274	RG-22251x4	x		x	Tts	200	160	200	1/22/74	125	6151
EB-321	403986	3938251	6263	RG-22251x2		x	x	QTa/Tts	180	140	180	1/20/74	130	6134
EB-322	403716	3938365	6265	RG-22251x1		x		Tts	200	140	200	1/24/74	120	6145
EB-323	397066	3937953	6041	RG-58916	x	x	x	Tg	220	160	220	2/1/94	60	5974
EB-324	398590	3941443	6170	RG-65490		x	x	Tts	300	200	280	5/21/97	40	6130
EB-325	398586	3940948	6149	RG-65564		x	x	Tts	300	200	280	5/18/97	35	6114
EB-326	399072	3942360	6201	RG-65488		x	x	Tts	300	200	280	5/18/97	50	6151
EB-327	398568	3942028	6188	RG-65489		x	x	Tts	300	200	280	5/23/97	50	6139
EB-328	397578	3942243	6374	RG-75421	x	x	x	Tts	510	410	510	3/9/01	285	6090
EB-329	399211	3940177	6212	RG-29536	x	x	x	Tts	132	100	132	8/1/78	80	6133
EB-330	399133	3935759	6068	RG-34701S		x	x	QTa	100			5/28/82	10	6061
EB-331	398988	3936088	6104	RG-61494		x	x	QTa/Tt/Tcb	400	70	390	1/25/95	50	6057
EB-332	399720	3935678	6099	RG-74595	x	x	x	QTa	160	80	140	8/30/00	18	6081
EB-333	399807	3935592	6120	RG-55622		x	x	QTa	140	80	120	6/26/92	16	6098
EB-334	401921	3937456	6143	RG-74594		x	x	QTa	140	60	120	9/5/00	58	6086

Table 1. Well inventory with location, site and construction information (sites shown on Fig. 4).—Continued

WELL LOCATION				SITE INFORMATION				WELL CONSTRUCTION						
Site ID	UTM easting NAD83	UTM northing NAD83	Elevation (ft asl)	NMOSSE well record	Water sample	Water level	Site visit	Water bearing* formation	Well depth (ft bsl)	Screen top (ft bsl)	Screen bottom (ft bsl)	Drill date	Driller static water level (ft bsl)	Static water elevation (ft asl)
EB-335	402763	3937837	6212	RG-73995	x	x		QTa	160	100	160	6/28/00	65	6142
EB-336	403199	3944575	6366	Exempt	x	x		Tts	1900	1880	1900	3/29/04	212	6155
EB-337	403199	3944575	6366	Exempt	x	x		Tts	1065	1045	1065	3/29/04	206	6161
EB-338	403199	3944575	6366	Unknown	x	x	x	Tts	600	580	600	3/29/04	190	6177
EB-339	403035	3938347	6259	RG-44219	x	x	x	QTa	200	160	200	8/20/85	135	6126
EB-340	399686	3936057	6126	RG-05530X	x	x		QTa	155			11/17/56		
EB-361	405210	3944796	6446	RG-75063	x	x		Tts	500	460	500	2/2/04	280	6167
EB-362	401318	3943215	6283	RG-45867	x	x		QTa	150	130	150	6/25/86	131	6155
EB-363	401833	3943342	6300	RG-45867	x	x	x	QTa	170	145	160	5/8/90	148	6157
EB-364	402532	3943573	6335	RG-45867	x	x	x	Tts	214	194	214	4/12/90	185	6152
EB-365	401354	3943580	6277	RG-54182	x	x		QTa	125	105	125	11/1/91	119	6160
EB-366	401829	3943023	6348	Exempt	x	x	x	QTa	204	184	204	8/5/95	189	6161
EB-370	401630	3937747	6159	RG-48749	x			QTaaS	90	24	61	12/23/87	27	6132
EB-373	401729	3941231	6273	RG-29860	x	x	x	Tts	300			1/1/40	80	6194
EB-377	399150	3933319	6047	RG-45727	x	x		QTt	65			7/22/86	23	6026
EB-378	400477	3933822	6124	RG-51797	x	x		QTt	110	60	109	1/24/90	18	6107
EB-379	401253	3934512	6206	RG-45723	x	x		QTa/Tte	227	137	227	7/25/86	108	6099
EB-382	404931	3939843	6335	RG-54184	x	x		Tts	252	231	252	8/10/91	180	6155
EB-383	404020	3936245	6289	RG-03824	x	x		Ttse/Tta	715			10/1/54	125	6164
EB-386	404058	3938572	6315	RG-69607	x	x		Tts/Tta	900	460	900	1/30/99	168	6149
EB-387	403690	3937134	6242	Exempt	x	x		QTa	115					
EB-388	403442	3937136	6224	Exempt	x	x		QTa	91					
EB-389	403458	3936959	6241	Exempt	x	x		QTa	121					
EB-391	404639	3939485	6306	RG-75255	x	x	x	Tts	300	200	300	6/14/01	159	6148
EB-392	404853	3938331	6270	RG-73973	x	x		QTa/Tts	220	160	200	5/17/00	152	6119
EB-407	405069	3941697	6365	RG-26718	x	x		Tts	247			1/1/53		
EB-459	401778	3942035	6311	RG-29860S	x	x		Tts	470	360	470	10/29/80	175	6136
EB-509	396936	3933700	5955	RG-24679	x			Tg	272	20	271	9/4/74	12	5945
EB-569	402917	3939407	6246	Unknown	x			Tts						
EB-579	398379	3942119	6197	RG-55884	x	x	x	Tts	240	180	220	8/5/92	35	6162
EB-605	405006	3936039	6337	Exempt	x	x		Te	1320	1300	1310	5/13/05	70	6267
EB-606	405006	3936039	6337	Exempt	x	x		Tta/Tte	640	590	630	5/13/05	143	6194
EB-607	405006	3936039	6341	Exempt	x	x	x	QTa/Tta	340	230	330	5/13/05	198	6143
EB-671	403283	3944985	6393	RG-89039	x			Tts	700	380	680	3/29/07	175	6218
EB-672	401499	3939441	6160	RG-79212	x			Tts	500	460	480	9/10/05	35	6125
EB-691	400249	3937717	6118	RG-92758	x	x		QTa/Tte/Tcb	180			9/23/11	37	6082
LC-006	397628	3939546	6112	RG-90070	x	x	x	QTa/Tcb	86			1/1/88	3	6104
LC-009	399771	3936914	6079	RG-34497CLW	x	x		QTa/Tcb	180			10/1/07		
LC-010	399811	3937131	6105	RG-34500POD2	x	x		QTa/Tcb	180	60	180	10/4/07	22	6084
LC-011	399265	3937311	6075	RG-14450POD3	x	x		Tcb/Tte	340	240	320	2/15/07	61	6016
LC-025	400000	3936280	6084	None	x	x		Qva/QTa	18			1/1/02		
LC-026	399995	3936316	6087	None	x	x	x	QTa	8			1/1/02		
LC-027	401705	3937727	6163	RG-60798	x	x		QTa/Tts	102			11/14/94	37	6118
LC-028	399769	3936918	6079	RG-34497	x	x		QTa/Tcb						
LC-029	400290	3935932	6145	None	x	x		QTa						
LC-030	398982	3935662	6044	None	x	x		QTa	13					

asl—above sea level; bsl—below land surface; *—see Table 3 for formation codes and descriptions

Measurement methods

Periodic water levels were measured using a graduated steel tape for pump-equipped wells and a Solinst™ electronic sounder for unequipped wells. Measurements were made to a repeatable accuracy of 0.02 ft. Continuous monitoring of water levels was accomplished using automatic sensing and recording instruments. The instrumentation combines a pressure sensor to measure total water and atmospheric pressure at a specified frequency and memory for storing data. In this study, measurements were taken at 12-hour (00:00 and 12:00 hours, midnight and noon) or 6-hour intervals (00:00, 06:00, 12:00 and 18:00 hours) and recorded using a Schlumberger Water Services Diver DI242 20-meter and Mini-Diver DI501 10-meter. Changes in total pressure due to atmospheric variations were corrected using an on-site Schlumberger Baro-Diver DI250 and software. Wells and springs were located in the field with a handheld GPS device and assigned site identification numbers. Elevations of measured wells and springs were calculated in ArcGIS using a 10-meter DEM and GPS-derived coordinates.

Water-table map

A water-table map shows lines of equal elevation of the water table for an unconfined aquifer or the potentiometric surface for a confined aquifer. It is used to interpret several important aspects of groundwater flow and conditions. Interpretations that can be made from a water-table map include hydraulic gradient, horizontal flow direction, changes in aquifer transmissivity, discharge zones and approximate locations of groundwater mounds and groundwater divides (Brassington, 2007).

A groundwater map was constructed using water levels measured at 45 sites between March 2011 and May 2012, combined with the elevations of 22 springs emerging at the head of wetlands. Published data from 1997–2007 for 29 wells (Johnson, 2009; NMBGMR, 2008) filled data gaps and provided water-table control at study area boundaries (noted as “control well” in water-level data tables). Site information for wells and springs is presented in Tables 1 and 2; locations are shown on Figure 4. Well locations and water-level elevations were plotted in ArcGIS. Groundwater elevation contours were drawn by hand and digitized. The placement of water-table elevation contours was checked against land-surface elevation to ensure accuracy in lowland and wetland areas. Flow lines showing horizontal flow direction

Table 2. Spring and surface-water inventory (sites shown on Fig. 4).

Site ID	SITE INFORMATION					
	UTM easting NAD83	UTM northing NAD83	Elevation (ft asl)	Site type	Water bearing formation*	Water sample
EB-302	397006	3936374	6002	Spring	Tg	x
EB-595	401950	3944200	6301	Stream	NA	x x
EB-624	400057	3933375	6099	Spring	Ti	x
EB-654	401005	3937572	6120	Spring	Qva/QTa	x
LC-001	399265	3935671	6036	Spring	Qva/QTa	x x
LC-002	398603	3935594	6004	Spring	Qva/QTa	x
LC-003	398346	3935963	6020	Spring	QTa/Tg	x x
LC-004	398481	3935768	6027	Spring	QTa/Tg	x
LC-005	400922	3937561	6119	Spring	Qva/QTa	x x
LC-007	399439	3937177	6039	Spring	QTasr/Tcb	x x
LC-008	399472	3936672	6050	Spring	QTaa/Te	x x
LC-012	399793	3936418	6076	Spring	Qva/QTa/Tte	x
LC-015	399009	3937651	6115	Spring	QTasr/Tcb	x
LC-016	399824	3937994	6095	Spring	QTa	x x
LC-017	399197	3935742	6052	Spring	QTa	x x
LC-018	399212	3935682	6036	Spring	QTa	x x
LC-019	399212	3935699	6036	Spring	QTa	x x
LC-020	398652	3935424	6034	Spring	QTa	x x
LC-021	400462	3937369	6088	Spring	QTaa/Tcb	x x
LC-022	397721	3939493	6088	Spring	Qva/QTa/Tcb	x x
LC-023	400085	3938409	6105	Spring	QTa	x x
LC-024	398982	3937584	6101	Spring	QTasr/Tte	x
LC-031	396201	3934130	5917	Spring	Not examined	
LC-032	396176	3933800	5922	Spring	Not examined	
LC-033	401185	3943424	6260	Effluent	Not examined	x x
LC-037	400951	3937549	6119	Spring	Qva/QTa	x x

asl—above sea level; *—see Table 3 for formation codes and descriptions

were constructed normal to water-table elevation contours (assuming the aquifer is horizontally isotropic). Converging flow lines were used to identify zones of groundwater discharge to surface waters.

Groundwater-level fluctuations

Monitoring groundwater-level fluctuations, seasonally and over long periods of time, is an important aspect of studying wetland hydrology and sustainability (Carter, 1996; Taylor and Alley, 2001). Repeat groundwater-level measurements were taken in 37 wells near the wetlands to evaluate seasonal (summer-to-winter) variations throughout the study area. Seasonal, diurnal, and episodic fluctuations of groundwater level were monitored in four wells, including

2 wetland wells, using the automated technology described above. Changes in groundwater level were evaluated over an 8-year period in wells measured in 2004 (Johnson, 2009) and remeasured in 2012 (this study). Multi-decadal changes were evaluated by comparing results between three historic measurement periods: 2004–2012 (Johnson, 2009 and this study), the mid-1970s (Mourant, 1980) and the 1950s (Spiegel and Baldwin, 1963). The combined effects of climate variability and groundwater pumping on the water table are evaluated using high-frequency groundwater-level measurements correlated with extreme monthly precipitation greater than 90th percentile values (wet months) and less than 10th percentile values (dry months) from local NOAA weather stations.

Geochemical Methods

Over the last several decades a variety of chemical, isotopic, and dating methods have been developed to trace groundwater movement through the hydrologic cycle. For summaries of data collection, application and interpretation see Hounslow (1995), Clark and Fritz (1997), Mazor (2004), and Timmons et al., (2013). Previous studies of the Santa Fe Group aquifer in the southern Española Basin (Anderholm, 1994; Moore, 2007, Johnson et al., 2008; Manning, 2009; Johnson et al., 2013) have examined a variety of chemical, isotopic and thermal data from precipitation, soil water, streams, springs, and groundwater to determine many aspects of groundwater recharge, movement, discharge and residence time. Results of these studies advanced understanding of the regional groundwater and surface water systems in the basin, and provide a context for our studies of local wetland hydrology at La Cienega.

Between March and October 2011, groundwater samples were collected by NMBGMR from 9 wells and 13 springs in the area, and from the discharge outflow of the Santa Fe WWTP (Fig. 4, Tables 1 and 2). The primary objective of geochemical characterization was to determine the source or sources of groundwater for the springs. Samples were collected from domestic wells using dedicated submersible pumps. Spring waters were sampled using a peristaltic pump and Viton® tubing inserted into a discharge vent or a stand pipe driven through saturated surface materials. WWTP discharge outflow was collected as a grab sample. Waters were field tested for specific conductance (SC), dissolved oxygen (DO), pH and temperature and were analyzed for

ion and trace element chemistry, and oxygen and hydrogen isotopes ($^{18}\text{O}/^{16}\text{O}$ and $^2\text{H}/\text{H}$ ratios). Thirteen samples were also analyzed for carbon isotopes (^{14}C and $^{13}\text{C}/^{12}\text{C}$ ratio) and tritium (^3H). Seven samples were analyzed for chlorofluorocarbon (CFC) and sulfur hexafluoride (SF6) recharge ages. Historical geochemical data from an existing database (NMBGMR, 2008, unpublished data) and previous studies (Johnson et al., 2008; Manning, 2009) were also incorporated.

Chemical and isotopic data from springs and wells near wetlands were examined for relationships and spatial patterns useful in identifying groundwater sources, mixing, and residence time. We focused on parameters that distinguish between shallow groundwater in the Ancha Formation and deep groundwater circulating through the Tesuque Formation. Parameters evaluated include total dissolved solids (TDS), calcium (Ca^{2+}), sodium (Na^+), magnesium (Mg^{2+}), sulfate (SO_4^{2-}), chloride (Cl^-), deuterium ($\delta^2\text{H}$), and oxygen-18 ($\delta^{18}\text{O}$). Chemical attributes are presented in contoured plots constructed by kriging concentration values followed by manual smoothing of contours. Surface-water sites were not used to control concentration contours, but appear on figures for comparison. Ion and isotopic compositional differences among wetland and groundwater zones are illustrated using a trilinear Piper diagram (Piper, 1944) and a linear plot of stable isotope compositions relative to a local meteoric water line (LMWL) developed by Anderholm (1994). Chemical data from water sampling are presented in Appendix 3.

Groundwater residence time was evaluated using multiple methods, including radiocarbon (^{14}C) dating of dissolved inorganic carbon (DIC), tritium (^3H) content, $\delta^2\text{H}$ and $\delta^{18}\text{O}$, and chlorofluorocarbons (CFCs). Radioisotopes of ^{14}C and ^3H are produced in the atmosphere by natural and anthropogenic processes, become entrained in the hydrologic cycle, enter the groundwater system with recharge, and slowly decay as groundwater flows through the aquifer. Large volumes of anthropogenic ^3H and ^{14}C produced between 1951 and 1962 by atmospheric testing of thermonuclear weapons created a “bomb” spike of these radioisotopes in groundwater that has been used as a tracer of groundwater movement. Carbon-14 has a relatively long half-life (5,730 years) and is used to detect groundwater with residence times of several 100s to many 1,000s of years. Results are reported as radiocarbon years before present, RCYBP, where “before present” means prior to 1950. Tritium has a relatively short half-life (12.43 years)

and its presence in groundwater provides evidence of post-1952 recharge. The average tritium content in mountain front streams of the Sangre de Cristo Mountains in northern New Mexico is 7 tritium units (TU) (Johnson and Bauer, 2012) and is about 6 TU in precipitation in the Sacramento Mountains of southern New Mexico (Newton et al., 2012). By measuring both the ^3H content and ^{14}C activity in groundwater, and comparing to modern levels, we can estimate how long groundwater has resided in the aquifer and detect whether the water represents a mixture of sources with different ages. In some geologic settings, chemical interactions between dissolved carbonate and carbonate-rich sediments or rocks in the aquifer can dilute the amount of ^{14}C measured in a water sample, and provide an anomalously old age. No corrections for geochemical effects have been completed on data collected in this study. The ^{14}C activity and apparent ^{14}C age are used as a relational tool to interpret hydrologic differences between wells and identify groundwater mixing.

CFCs and SF6 are atmospheric contaminants that are resistant to degradation and soluble in water, making them a useful marker for modern groundwater recharge. Because CFC concentrations have been measured in the atmosphere since the 1940s, and have increased until recently, their input to the aquifer is known and can, under the right conditions, provide a precise age for young groundwater. In this study, point-source contamination derived from discarded automobiles, refrigerators and the like rendered the method useless for groundwater dating. Results of CFC sampling and analysis are presented in Appendix 3.3 but are not discussed further.

Field parameters

Groundwater discharge temperature, specific conductance (SC), pH and dissolved oxygen (DO) were measured in the field prior to sampling using a YSI 556 multi-probe system. The probe has a rated accuracy of 0.15°C for temperature, 0.5% for SC, 0.2 units for pH, and 2% for DO. The DO probe was calibrated onsite before measurement. The pH electrode was calibrated weekly against pH 7 and 10 buffers. For springs, field parameters were measured in the spring pool. For wells, field parameters were monitored continuously during the well purge using an in-line flow cell. Sample collection was initiated following parameter stabilization. Between one and three bore-hole volumes of water were extracted during purge and sample collection.

Major ions and trace metals

Water samples were collected in new, certified clean 125-mL (for trace metals) or 250-mL (for ions) polypropylene containers that were triple rinsed with sample water prior to filling. Trace metal samples were filtered on site (where possible) through an in-line 0.45 micron filter and acidified to pH less than 2 using ultra-pure nitric acid. If a sample could not be field filtered, it was filtered and acidified immediately in the laboratory. All water samples were stored on ice or refrigerated until analysis at the NMBGMR laboratory within one week. Laboratory measurements of pH were performed with an Orion 420A meter, and conductivity was measured using a YSI 3200 meter. Alkalinity was determined by titration. Major anions (Cl , SO_4 , and NO_3) were analyzed using a Dionex DX-600 ion chromatograph (IC). Major cations (Ca , Mg , Na , and K) were analyzed using a Perkin Elmer OPTIMA 5300 DV inductively coupled plasma optical emission spectrometer (ICP-OES). Trace metals were analyzed by inductively coupled plasma mass spectrometry (ICPMS) using an Agilent 7500 IS. The quality of chemical analyses was inspected by analyzing blanks, standards, duplicate samples, and checking ion balances. Analytical error for detectable concentrations of major ions and trace metals is generally less than 10% using IC, ICP-OES, and ICP-MS. Ion balance errors for analyses conducted by NMBGMR are within $\pm 5\%$.

Hydrogen and oxygen isotopes

Samples for hydrogen ($^2\text{H}/\text{H}$, $\delta^2\text{H}$) and oxygen ($^{18}\text{O}/^{16}\text{O}$, $\delta^{18}\text{O}$) isotope ratios were collected in 25-mL amber glass bottles that were triple rinsed with sample water prior to filling. Sample bottles were clear of air bubbles, kept from direct sunlight, and stored at room temperature in sealed bottles until analysis at the New Mexico Institute of Mining and Technology, Department of Earth and Environmental Sciences stable isotope laboratory using a cavity ring down spectrometer, Picarro L1102-I isotopic water liquid sampler. Analytical uncertainties for $\delta^2\text{H}$ and $\delta^{18}\text{O}$ are typically less than 1 per mil (‰, parts per thousand) and 0.15‰, respectively.

Carbon isotopes

Select spring and well samples were analyzed for carbon-14 (^{14}C) activity and $^{13}\text{C}/^{12}\text{C}$ ratios ($\delta^{13}\text{C}$) to evaluate groundwater age. Water samples were

collected in a 1-L polypropylene bottle that was tripled rinsed with sample water. Sampling followed protocols described at www.radiocarbon.com/ground-water.htm. Samples were chilled and stored in a dark environment until shipment to Beta Analytic, Miami, Florida, for analysis. The ^{14}C activity and $^{13}\text{C}/^{12}\text{C}$ ratios ($\delta^{13}\text{C}$) of the water sample were derived from the dissolved inorganic carbon (DIC) by accelerator mass spectrometry. Measured $\delta^{13}\text{C}$ values were calculated relative to the PDB-1 standard. Result verification and isotopic fractionation correction using $\delta^{13}\text{C}$ were completed by Beta Analytic. Results are reported as ^{14}C activity (in percent of modern carbon (pmC)) and as the apparent radiocarbon age (in radiocarbon years before present (RCYBP), where “present” is 1950 AD), with an uncertainty of one standard deviation.

Tritium (^{3}H)

Tritium samples were collected in two 500-mL polypropylene bottles that were tripled rinsed with sample water. Sampling followed protocols described at www.rsmas.miami.edu/groups/tritium/analytical-services/advice-on-sampling/tritium/. Samples were shipped to the University of Miami Tritium Laboratory where they were analyzed by internal gas proportional counting with electrolytic enrichment. The enrichment step increases tritium concentrations in the sample about 60-fold through volume reduction, yielding lower detection limits. Accuracy of this low-level measurement is 0.10 tritium unit (TU) (0.3 pCi/L of water), or 3.0%, whichever is greater. The stated errors, typically 0.09 TU, are one standard deviation. Results reported as less than 0.10 TU are shown on figures as <0.1 TU or below detection, but actual reported values are shown in data tables.

Chlorofluorocarbons (CFCs) and sulfur hexafluoride (SF6)

CFC and SF6 samples were collected from well and spring waters into three 250-mL glass bottles with foil-lined caps. The bottles and caps were thoroughly rinsed with sample water and filled and capped underwater in a plastic bucket with no atmospheric exposure. Sampling followed stringent protocols described at www.rsmas.miami.edu/groups/tritium/analytical-services/advice-on-sampling/cfc-and-sf6/. Samples were shipped to the University of Miami Tritium Laboratory where they were analyzed using a purge-and-trap gas chromatograph with an electron capture detector. Precision values for CFCs are 2% or less. SF6 precision is 5% or less. The accuracy of CFC- and SF6-derived recharge ages is 3 years or less. Calculations of CFC and SF6 recharge ages assumed a recharge elevation of 2,100 meters and a recharge temperature of 11°C, which are the estimated average elevation and mean annual temperature at the base of the Sangre de Cristo Mountains east of Santa Fe.

Data compilation and data quality

General chemistry data compiled from the NMBGMR database were reviewed and filtered for data quality based on several criteria including an accurate map location or geographical coordinates for the sample site and ion balance. Ion chemistry data originating from external laboratories do not always meet the NMBGMR ion balance criteria ($\pm 5\%$). The compiled data used in this study have an ion balance of $\pm 13\%$ or less.



Ancha Formation gravels (right foreground) cover a hillslope near the confluence of Cienega Creek and Guicu Creek.
Galisteo Formation and Cieneguilla basanite are visible in the center photo.

III. GEOLOGY OF THE LA CIENEGA AREA

Geologic Setting and Geologic Structure

The study area lies along the southwest margin of the Española Basin (Fig. 5), one of a series of structural basins in the Rio Grande rift. The Española Basin is bordered by the Sangre de Cristo Mountains on the east and the Jemez Mountains on the west. The sediments that fill the basin, collectively called the Santa Fe Group (SFG), were derived from erosion of surrounding highlands as the basin tectonically subsided. This basin fill consists of sand, silt, clay, and gravel, which are locally interbedded with minor volcanic flows and ashes. In the Santa Fe area and near La Cienega, SFG sediments form the primary aquifers (Spiegel and Baldwin, 1963). Rift tectonics and regional faulting control the geometry and shape of the basin, as well as the thickness and distribution of SFG sediments and aquifers.

The southern boundary of the Española Basin is roughly defined by the Rancho Viejo hinge zone of Grauch et al., (2009, p. 53, 62) (Fig. 5). The mapped trace of the Rancho Viejo hinge zone is curved, facing north, and transects the study area from northwest to southeast. A north-plunging syncline has been mapped north of the hinge zone (Fig. 5) (Koning et al., 2003; Read et al., 2003 and 2004). Miocene-age Santa Fe Group strata dip northeastward on the west side of the syncline axis and northwestward on the east side of the syncline axis. The Ancha Formation is minimally affected by the hinge zone, but the syncline may account for thickening of Ancha sediments in the center of the basin south of Santa Fe (Koning and Hallett, 2002; Johnson and Koning, 2012, Plate 2). The hinge zone separates two dominant structural domains—an extensive platform structure called the Santa Fe platform to the south and the deep west-tilted half graben of the Española Basin to the north. South of the hinge zone, over the Santa Fe platform, the Santa Fe Group is relatively thin (averaging 250 feet in thickness). North of the hinge zone the SFG sediments thicken abruptly as the bottom of the unit plunges north into the basin. Basin fill thickens northward at a rate of about 700–800 ft/mi, reaching thicknesses of about 4,000 ft near the northern

border of the study area (Koning and Hallett, 2002; Grauch et al., 2009; Koning and Read, 2010).

The basin boundary on the east consists of a system of discontinuous, small-displacement faults and monoclines along the base of the Sangre de Cristo Mountains. The few faults that have been mapped in the study area are small, with low displacements, but a more prominent fault may exist west of the WWTP (Figs. 5, 6). The Cerrillos uplift lies southwest of the study area (Fig. 5). This north-plunging, structural high is covered by relatively thin SFG strata and lavas of the 2 to 3 million-year-old Cerros del Rio volcanic field (Thompson et al., 2006). Santa Fe Group sediments thicken to the northeast of this feature (Grauch and others, 2009).

Geologic History

For the last 26–27 million years, tectonic forces have slowly torn the North American continent apart along the Rio Grande rift. The Earth's crust has been uplifted, stretched, broken, and invaded by magma, and the rift's subsiding basins have filled with sediments and volcanic rocks. The geologic features found within the rift-related Española Basin shape the region's aquifers, control how and where groundwater moves, and influence the locations of springs and wetlands. The genesis of the various rock formations that influence local hydrogeology is briefly described below (Figs. 7, 8).

Pre-rift volcanic activity between 36 and 28 million years ago created volcanic edifices between La Cienega and Madrid to the south and emplaced igneous intrusions beneath and near the volcanoes. Erosion of these volcanic highlands produced the grayish, volcanic sediment deposits of the Espinaso Formation in adjacent lowlands to the north, including in and around La Cienega.

Initiation of rifting around 27 million years ago was accompanied by basaltic volcanism, tectonic subsidence, and progressive deposition of sediment in the Española Basin, which produced the thick sequences of sediment and minor volcanic flows now referred

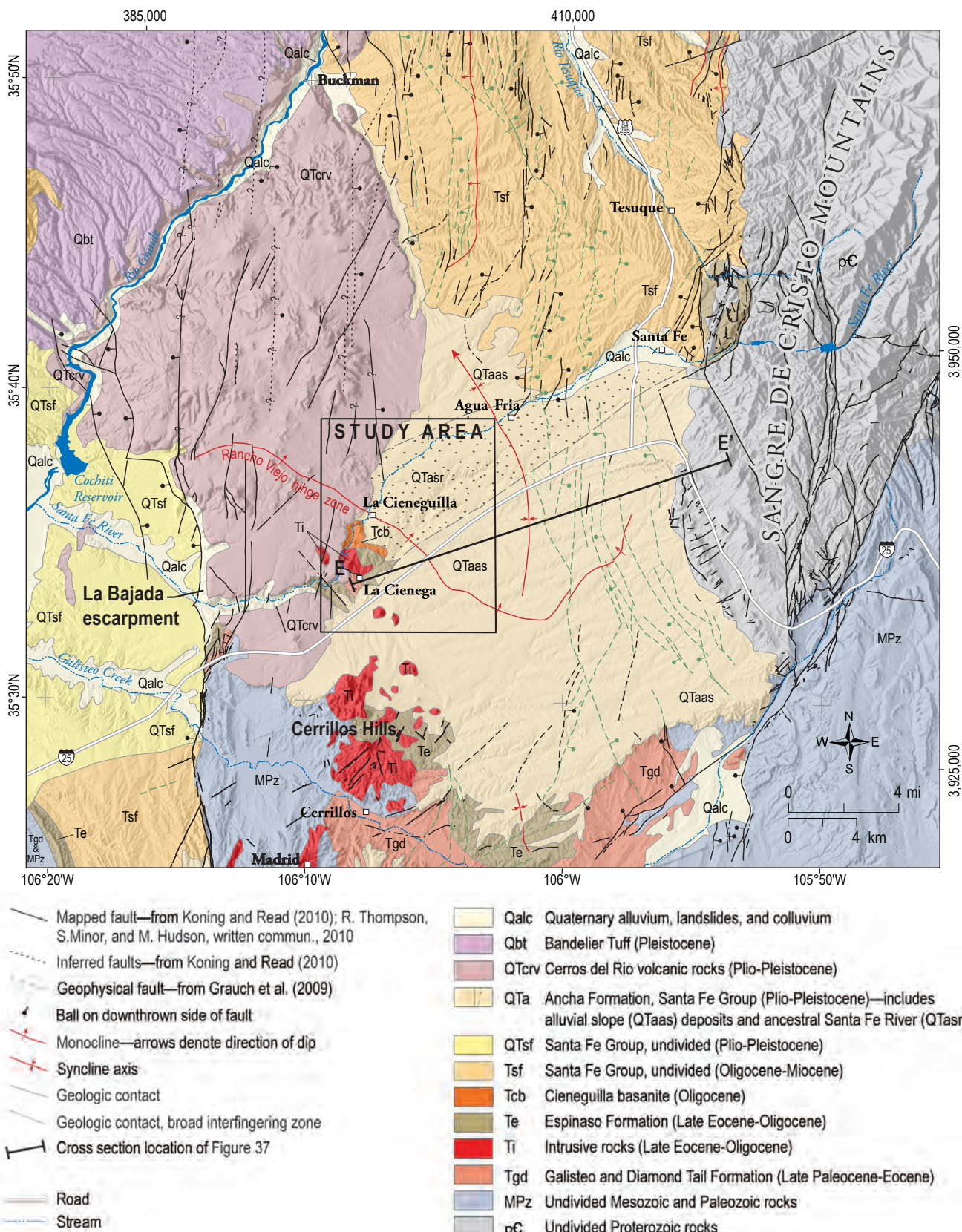


Figure 5. Generalized geologic map and regional geologic setting of La Cienega and Cieneguilla, southern Española Basin. Geologic contacts are generalized from Koning & Read (2010), R. Thompson, S. Minor and M. Hudson, written communication (2010), Minor (2006), and New Mexico Bureau of Geology and Mineral Resources (2003). Geologic unit descriptions are given in Table 3.

to as the Santa Fe Group. Near La Cienega, volcanism was dominated by low-silica, basaltic magmas called the Cieneguilla basanite. Between basanite eruptions, tectonic tilting and uplift to the west caused erosion of the Espinaso Formation from the Cerrillos uplift. Northeast-flowing streams transported sediment derived from the Espinaso Formation and Cieneguilla basanites and deposited it on alluvial fans near La Cienega (Fig. 8) (Koning and Johnson, 2006; Koning and Read, 2010). This sediment, called lithosome E of the Tesuque Formation, underlies and

interingers with lithosome S of the Tesuque Formation beneath La Cienega (Figs. 7–9) (Koning and Read, 2010). Lithosome S was deposited on a west-sloping fluvial fan by an ancestral version of the Santa Fe River (Koning et al., 2004). Lithosome A was deposited on piedmonts to the north and south by smaller mountain front drainages. Deposition of the Tesuque Formation continued until about 8 million years ago, after which erosion began. In the study area, this erosion removed Tesuque Formation strata younger than about 13 million years, and created a topographic surface with hills and valleys.

Table 3. Geologic unit descriptions.

UNIT	DESCRIPTION
Quaternary alluvial and colluvial deposits (Qalc)	
Qva	Valley floor alluvium—Interbedded sand, clayey-silty sand, and subordinate gravel that underlies valley floors. Includes gravelly terraces alongside the Santa Fe River. Weakly consolidated and inset against older strata.
Qctl	Colluvium, talus, and landslides—Poorly sorted gravel in a matrix of sand or clayey-silty sand; deposited chiefly by gravitational processes on slopes. Locally includes minor landslides.
Pliocene-Quaternary volcanic rocks	
Qbt	Bandelier Tuff—Rhyolitic ash flow tuffs erupted from the Valles Caldera in the early Pleistocene.
QTcrv	Cerro del Rio volcanic rocks—Basalt, basaltic andesite, and andesite flows that commonly overlie phreatomagmatic deposits.
Pliocene-Quaternary sedimentary deposits of the Santa Fe Group	
QTa	Ancha Formation, Santa Fe Group—Arkosic sand, silty-clayey sand, and gravel unconformably overlying tilted basin-fill. Divided into two interfinger units associated with two paleostream systems.
QTaas	Ancha Formation, alluvial slope deposits—Ribbon-like, sand and gravel channel-fills interbedded in clayey-silty sand. Lower strata generally consist of sand and gravel.
QTasr	Ancha Formation, ancestral Santa Fe River deposits—Laterally extensive, thick, sandy pebble-cobble channel-fills interspersed with floodplain sediments of clayey-silty sand.
QTt	Tuerto Formation, Santa Fe Group—Silty-clayey sand interbedded with coarse channel fills of sandy gravel and gravelly sand derived from intrusive igneous rocks of the northern Cerrillos Hills. <20% granite gravel.
QTsf	Santa Fe Group, undivided—Sand, gravel, silt, and clay deposited by piedmont and axial drainages in the Santo Domingo Basin.
Late Oligocene-Miocene basin-fill deposits of the Santa Fe Group	
Tsf	Santa Fe Group, undivided—Sandstone, conglomerate, and mudstone that are variably cemented and moderately to well consolidated. Tends to coarsen towards pre-Miocene bedrock uplifts.
Tt	Tesuque Formation—Sand with minor gravel, silt, and clay. Subdivided into three lithosomes described below (lithosomes S, E, and A).
Tts	Lithosome S—Reddish sand and pebbly sand channel-fills. Interbedded with clay, silt, and very fine- to fine-grained floodplain deposits (Ttsf). Deposited on fluvial fan by an ancestral Santa Fe River.
Tte	Lithosome E—Gray to brown, volcaniclastic, clayey-silty sandstone, sandstone, and gravel eroded from Cieneguilla basanite (Tcb) and the Espinaso Fm (Te). Trace amounts of green hornfels occur in sand fraction SE of La Cienega (Tteg).
Ttse	Lithosomes S and E that are mixed and interfinger.
Tta	Lithosome A—Fine, arkosic sand and clayey-silty sand interspersed with sparse, coarse-grained channel fills. Deposited on alluvial slope north and south of ancestral Santa Fe River.
Late Eocene-Oligocene igneous rocks	
Tcb	Cieneguilla basanite—Dark gray, mafic lava. On cross sections, it is subdivided into four separate flows (tongues) labeled Tcb1, Tcbm, Tcbu, and Tcbvu (lower, middle, upper, and very upper).
Ti	Intrusive rocks—Igneous rocks that crystallized underground; generally felsic and medium to coarse-grained.
Cretaceous and Eocene-Oligocene sedimentary strata	
Te	Espinaso Formation (Oligocene)—Well-cemented, alluvial fan deposits of volcanic-derived conglomerates and sandstones, and minor lava flows. Light gray color.
Tg	Galisteo Formation (Eocene)—Reddish, fluvial sandstone, pebbly sandstone, and mudstone.
Td	Diamond Tail Formation (middle Paleocene)—Package of sandstone, pebbly sandstone, and mudstone that unconformably underlies the Galisteo Formation in the vicinity of Galisteo.
Tgd	Galisteo and Diamond Tail Formations, undivided
K	Cretaceous strata, undivided—Generally mudstones and cemented sandstones.

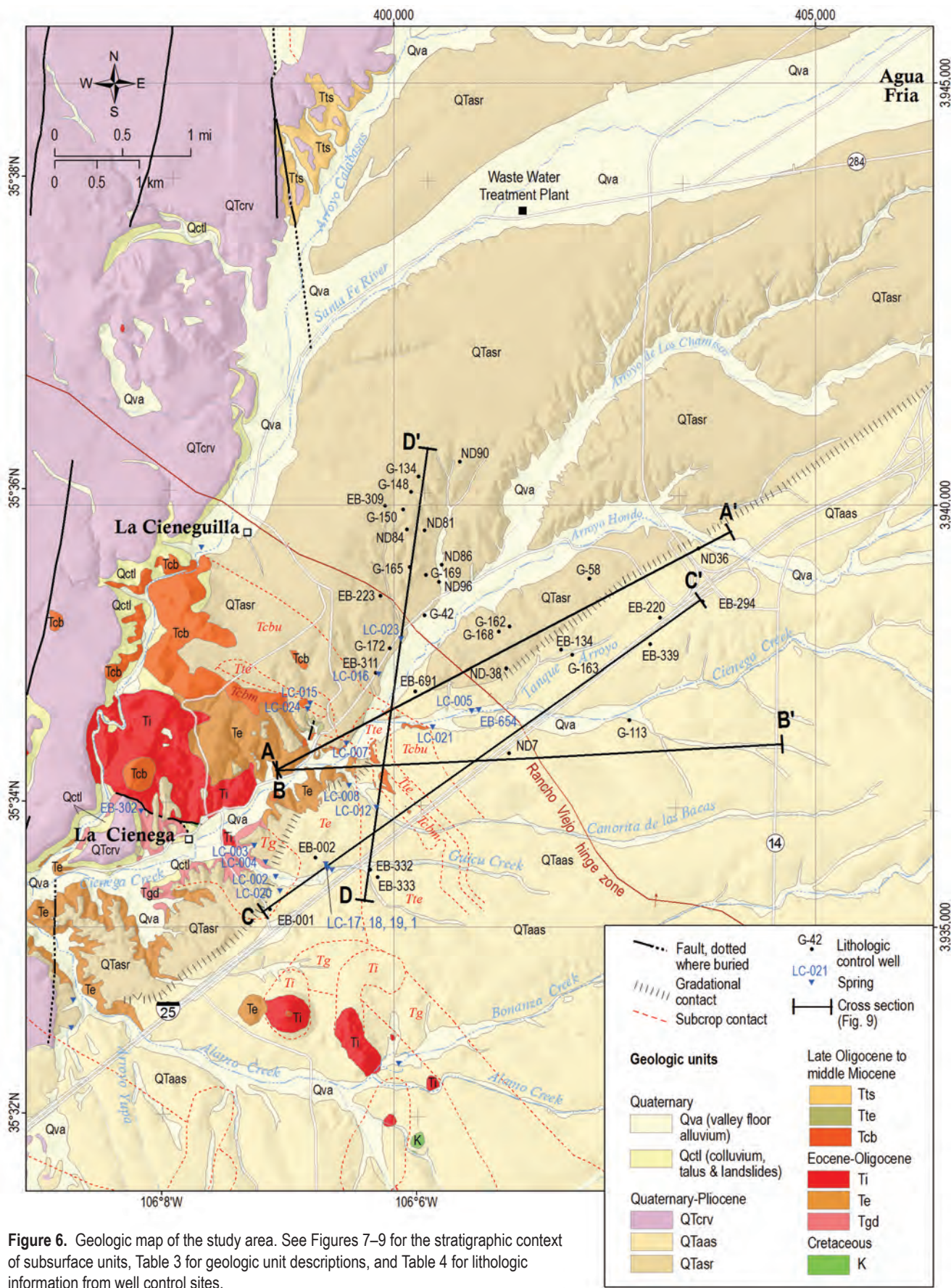


Figure 6. Geologic map of the study area. See Figures 7–9 for the stratigraphic context of subsurface units, Table 3 for geologic unit descriptions, and Table 4 for lithologic information from well control sites.

Table 4. Lithologic data for geologic cross sections (Figs. 6 and 9) (extracted from Johnson and Koning, 2012).

		NUCLEAR DYNAMICS URANIUM EXPLORATION DRILL HOLES						NMBGMR ESPAÑOLA BASIN WATER WELL DATABASE						NMOSE WATER WELL RECORDS								
Data quality		Lithologic and geophysical notes (depths in feet)			Depth to base of Ancha Fm (ft bsl)			Well depth			Data type			Subcrop formation			Base elevation (ft asl)			Surface elevation (ft asl)		
ND7	401411	3936858	6172	16N.08E.34.311	LLe, Cu	695	155	6017	Tis	Red sandstone over red-brown siltstone, Tis 155–187 ft, Tle 187–695 ft	E	G										
ND36	403661	3939279	6246	16N.08E.26.122	LLe, Cu	1400	140	6106	Tis	Grainsize and color changes at QTa/Tls	E	G										
ND38	401379	3937859	6181	16N.08E.27.333	LLe	1145	160	6021	Tis	Red sand-gravel over red-brown gravel, Tls 160–478 ft, Tcbu 480–485 ft, Tlse 485–525 ft, Tts 300–617 ft, Tise 617–TD	E	E										
ND81	400412	3939492	6205	16N.08E.21.344	LLe, Gl	800	110	6095	Tis	Granitic wash over light brown mudstone; hi gamma and green sediment Tls 300–617 ft, Tise 617–TD	E	E										
ND84	400202	3939506	6243	16N.08E.21.343	LLe, Gl	775	80	6163	Tis	Arkose conglomerate over brown claystone-sandstone; high gamma/low resistivity at 425–720 ft, gray-green mudstone at 550 ft Tts-Tle	E	E										
ND86	400617	3939083	6146	16N.08E.28.213	LLe, GL	810	80	6066	Tis	Arkose sandstone QTas over brown mudstone, Tls 80–185 ft, Ttsf 185–500 and 544–726 ft, Tse 500–544 ft, Tle 726–810 ft	E	E										
ND90	400830	3940309	6262	16N.08E.21.234	LLe, GL	1000	155	6107	Tis	QTa/Tls contact at base of last coarse unit, Tls interbedded mudstones/sandstone 155–656 ft, Tsf 656 ft-ID	E	G										
ND96	400565	3938884	6133	16N.08E.28.231	LLe, GL	705	60	6073	Tis	QTa contact at top of brown claystone, Tls 60–120 ft, Ttsf 120–390 ft, Tlse 390–601, Ttsf 601–658 ft, Tse 658–686 ft, Tle 686–705 ft	E	G										
EB-001	398579	3935004	6063	15N.08E.5.323	LLw	221	72	5991	Tg	QTaas: 0–72 ft; Tg: 72–221 ft	E	G										
EB-002	399120	3935618	6073	15N.08E.4.111	LLw	380	120	5953	Te	Log may lump QTaa and Tls. Sand and gravel to 120 ft	E	G										
EB-134	402030	3938076	6180	16N.08E.27.342	LLw	137	125	6055	Tis	QTa to base of last brown sand-gravel	E	G										
EB-220	403203	3938457	6258	16N.08E.26.32112	LLw	272	162	6096	Tis	QTa contact at top of red clay 162–272 ft	E	G										
EB-223	399890	3938714	6186	16N.08E.28.134	LLw	100	93	6073	Tis	QTas interbedded tan sands over Tls brown clay	E	G										
EB-294	403710	3938648	6302	16N.08E.26.322	LLw	740	164	6138	Tis	Coarse brown sand and gravel QTa over red sand and gravel Tls; no red clay	E	F										
EB-309	399946	3939786	6231	16N.08E.21.3321	LLw	300	48	6183	Tis	Gravel over brown clay	E	F										
EB-311	399834	3937807	6109	16N.08E.28.3343	LLw	180	100	6009	Tis-Tle	Fire brown sand-clay over Tls gray gravel 100–120 ft, Tts red clay 120–170 ft, black volcanics Tcbu 170–180 ft	E	G										
EB-332	399770	3935477	6089	15N.08E.4.13324	LLw	160	134	5955	Tle	QTa brown clay-sand over Tls brown-grey clay and cobbles 134–160 ft	E	G										
EB-333	399857	3935388	6119	15N.08E.4.13344	LLw	140	120	5999	Tle	QTa sand-gravel over red clay included in Tle 120–140 ft	E	G										
EB-339	403085	3938143	6258	16N.08E.26.313	LLw	200	200	6058	Tts	Anhistic sand-gravel over red clay at bottom of hole; geologist descriptions	E	E										
EB-691	400304	3937589	6119	16N.08E.28.344	LLw, Cu	180	90	6029	Tcb-Tte	Sand-gravel QTaa over basalt Tcbu 90–100 ft, gray clay Tle 100–140 ft, basalt Tcbu 150–180 ft	E	E										
G-42	400412	3938483	6105	16N.08E.28.233	LLw	65	50	6055	Tis	Tan sand-gravel QTas over red clay-gravel and gray clay Tls	E	E										
G-58	402365	3938919	6218	16N.08E.27.2321	LLw	248	100	6118	Tis	Brown sand-gravel QTa over red clay and sand Tls; gray clay at 190–220 ft	E	E										
G-113	402842	3937246	6181	16N.08E.34.242	LLw	200	140	6041	Tis	Red sand-gravel QTa over clay-sand Tls	E	F										
G-134	400340	3940133	6245	16N.08E.21.3221	LLw	200	30	6215	Tis	Red sand-gravel QTas over brown sand-clay and red, tan sands Tls	E	F										
G-148	400250	3939951	6251	16N.08E.21.3232	LLw	253	35	6216	Tis	Gravel and brown clay QTas over interbedded clay and sand Tls	E	F										
G-150	400161	3939741	6244	16N.08E.21.423	LLw	220	35	6209	Tis	Red sand-gravel QTas over interbedded brown clay and red sand Tls	E	F										
G-162	401421	3938355	6203	16N.08E.27.3131	LLw	200	150	6053	Tis	Red sand-gravel QTa over yellow and brown clay Tls	E	F										
G-163	402160	3938016	6182	16N.08E.27.4313	LLw	140	100	6082	Tis	Sand-gravel QTa over brown-gray clays Tls	E	F										
G-165	400234	3939059	6197	16N.08E.28.1234	LLw	200	140	6057	Tis	Red to brown sand-gravel QTa over interbedded red clay and sand Tls	E	F										
G-168	401293	3938295	6208	16N.08E.28.42424	LLw	270	150	6058	Tis	Red sand-gravel QTa over interbedded brown clay and sand Tls	E	F										
G-169	400429	3938965	6161	16N.08E.28.1422	LLw	100	90	6071	Tis	Red sand-gravel QTa over red clay Tls	E	F										
G-172	399999	3938097	6111	16N.08E.28.332	LLw	160	100	6011	Tse	Brown clay-sand (QTas) over red to brown sand, gravel, and clay (Tls)	E	F										

ash=above sea level; bsl=below land surface

Data type: LLe= lithologic log from exploration drill hole; Cu=cuttings; GL=geophysical log; LLw=geophysical log from water well.

Subcrop formation and Lithologic notes, Quaternary: QTaa—Ancha Formation; QTas—Santa Fe River deposits of the Ancha Formation.

Subcrop formation and Lithologic notes, Tertiary: Ts—Tesuque Fm lithosome S; Tse—Tesuque Fm; gradation and interfingering of lithosomes S and E; Tsf—Tesuque Fm fine-grained floodplain deposits of lithosome S;

Tta—Tesuque Fm lithosome A; Tte—Tesuque Fm lithosome E; Tcb—Cieneguilla basaltic; Te—Espinosa Fm; Tg—Galisteo Fm.

Data quality: E=excellent; G=good; F=fair; Fl=fair; location approximate

Sedimentation and volcanism resumed in the basin about 3 million years ago, beginning with deposition of the Ancha Formation (Koning et al., 2002). These coarse sediments, which comprise the uppermost Santa Fe Group, were derived from the Sangre de Cristo Mountains and deposited on top of the Tesuque Formation by west-flowing piedmont streams and the ancestral Santa Fe River (QTaas and QTasr, respectively, on Figs. 5–7, 9). Because of tectonic tilting and erosion during the preceding 5 million years, an angular unconformity separates the Ancha Formation from the older Tesuque Formation (Spiegel and Baldwin, 1963; Koning et al., 2002). Cerros del Rio volcanism occurred on the north end of the Cerrillos uplift from 2.7 to 1 million years ago, with most rocks being 2.7–2.2 million years old (Thompson et al., 2006). Deposition of the Ancha Formation ceased between 1.5 and 1.2 million years ago (Koning et al., 2002). Erosion has dominated the last 1.2 million years, episodically interrupted by brief periods of aggradation within river valleys. The last period of aggradation resulted in sand, clayey sand, and gravel filling the bottoms of modern valleys.

Geologic Units and their Hydrologic Significance

The rocks and deposits exposed in the study area consist of (from oldest to youngest): 1) bedrock strata that includes Galisteo Formation (Eocene), Espinaso Formation (early to late Oligocene), and Cieneguilla basanite (late Oligocene); 2) Tesuque Formation of the Santa Fe Group and its lithologic subdivisions (late Oligocene to middle Miocene); 3) volcanic rocks of the Cerros del Rio volcanic field and the Ancha Formation of the Santa Fe Group (late Pliocene to early Pleistocene); and 4) surficial deposits of Quaternary age. These units are shown on the geologic map (Fig. 6), a stratigraphic column (Fig. 7), a series of hydrogeologic cross sections (Fig. 9), and a subcrop map showing the distribution of units underlying the Ancha Formation (Fig. 10). Table 3 describes the geologic units and their subdivisions that are cited in the report and shown on maps. The variability in hydraulic conductivity of the different geologic units is shown in Figure 11. The geologic units and their hydrologic significance are summarized below.

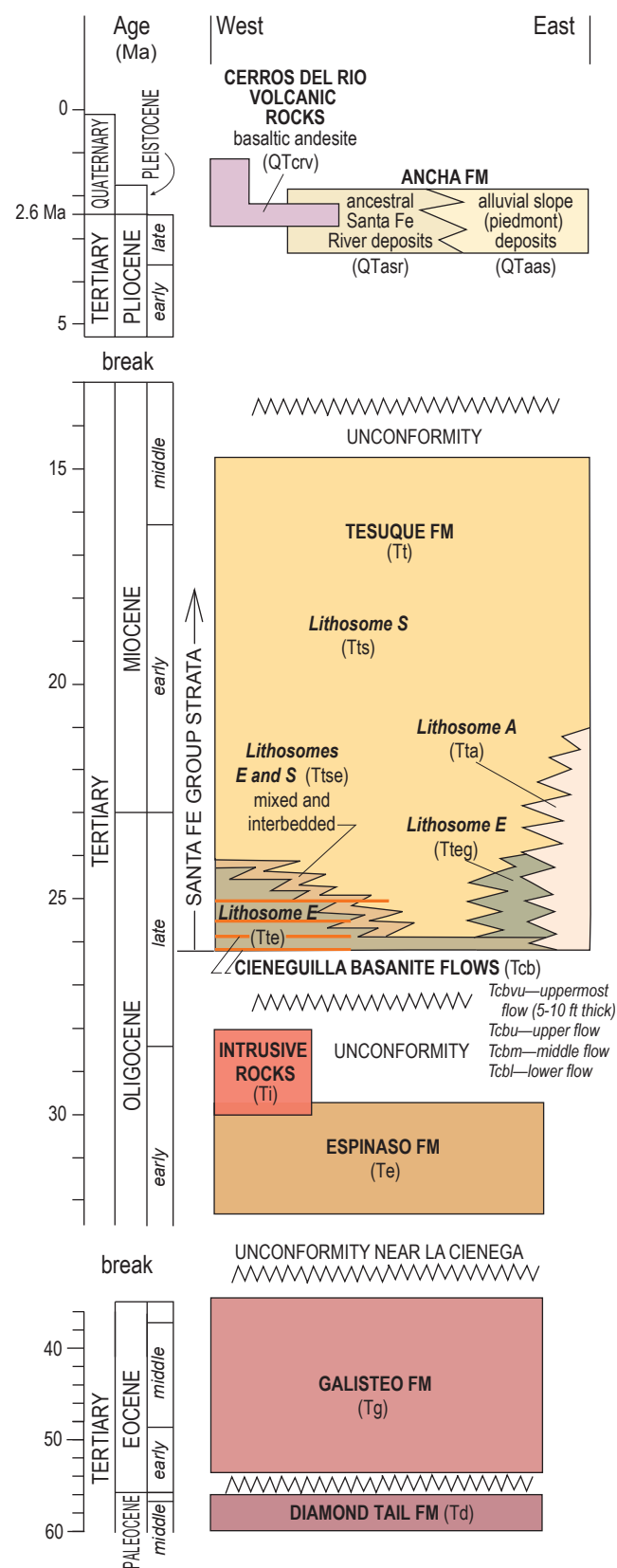


Figure 7. Stratigraphy of the La Cienega area with age on the vertical axis (in millions of years (Ma)). See Table 3 for geologic unit descriptions.

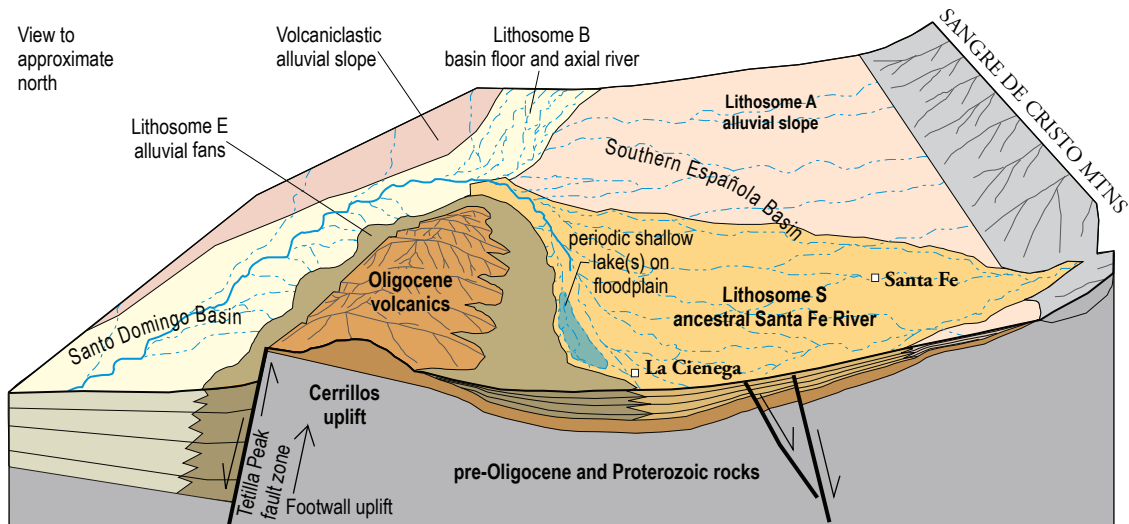


Figure 8. Conceptual block illustration showing the stratigraphy, Tesuque Formation lithosomes (Fig. 7), paleogeography, and depositional setting of the Española Basin 21 to 25 million years ago.

Bedrock strata: Galisteo Formation, Espinaso Formation and Cieneguilla basanite

Aside from a small exposure of Mancos Shale (Cretaceous) in the community of La Cienega, the oldest exposed strata are fluvial sediments of the Galisteo Formation (Eocene), composed of sandstone and pebbly sandstone channel fills interbedded with mudstone-rich floodplain deposits (Sun and Baldwin, 1958; Spiegel and Baldwin, 1963; Koning and Hallett, 2002). Near La Cienega, the overlying, light gray Espinaso Formation (Oligocene) mostly consists of well-cemented, alluvial fan deposits of volcanic-derived conglomerates and sandstones (Sun and Baldwin, 1958; Sawyer et al., 2002; Koning and Hallett, 2002). The Cieneguilla basanite (previously called the Cieneguilla limburgite by Stearns, 1953) disconformably overlies the Espinaso Formation and is a dark gray, mafic lava similar to a basalt. Paleotopography likely influenced the extent of its laterally discontinuous flows. Near the confluence of Arroyo Hondo and Cienega Creek, four Cieneguilla basanite flows were identified within sediments near the base of the Tesuque Formation (Fig. 9). Only two of these flows appear to extend more than 0.5 miles to the south. Buttress style contacts of the lowest Cieneguilla basanite flow (Tcbl) against the older Espinaso Formation near El Rancho de las Golondrinas indicate that the flow filled an east-trending buried valley. Higher flows (Tcbm, Tcbu, and Tcbvu in Fig. 9) are more laterally extensive. Radioisotopic analyses of the Tcbm flow returned an age of 26.08 ± 0.62 million years before present (Koning and Hallett, 2002). As a whole,

bedrock strata are much less permeable than most basin-fill deposits of the Santa Fe Group (Fig. 11), largely due to their strong cementation and high degree of consolidation.

Tesuque Formation

In the Santa Fe area, the Tesuque Formation (upper Oligocene to upper Miocene) forms the bulk of the Santa Fe Group basin fill. The formation consists of silty-clayey sand and sand, with minor gravel, silt, and clay (Spiegel and Baldwin, 1963; Koning and Read, 2010). Its lower strata interfinger with the Cieneguilla basanites and are therefore ~26 million years old. Near the Buckman well field, the Tesuque Formation is as young as 8 million years (Koning and Maldonado, 2002). But in the study area, at the tilted margin of the basin, the oldest Tesuque strata preserved are probably 20–26 million years. Although consolidated, the Tesuque Formation is most often weakly to moderately cemented. The formation has been subdivided into interfingering map units called lithosomes (Cavazza, 1986; Koning and Read, 2010) that correspond to deposits of different regional paleodrainage systems.

In the La Cienega area, there are three significant lithosomes (Figs. 6–10, Table 3). Lithosome E (Tte), the lowest Santa Fe Group unit in the study area, consists of clayey-silty sand and gravel derived from volcanic rocks of the Cieneguilla basanite and Espinaso Formation (Koning and Johnson, 2006; Koning and Read, 2010). Interlayered in this unit are at least four tongues of Cieneguilla basanite. Lithosome E (and the interbedded basanites)

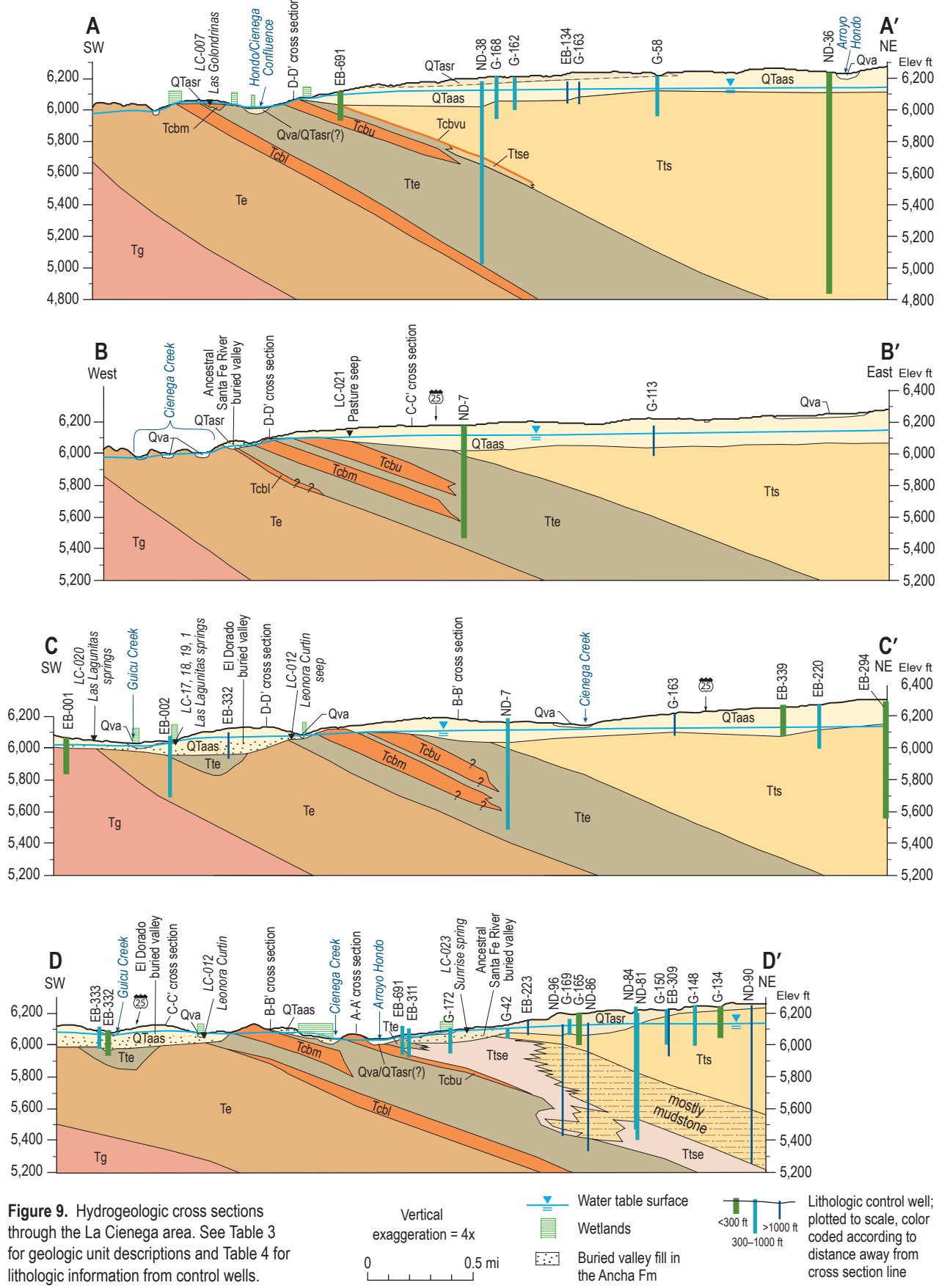


Figure 9. Hydrogeologic cross sections through the La Cienega area. See Table 3 for geologic unit descriptions and Table 4 for lithologic information from control wells.

Vertical
exaggeration = 4x

-  Water table surface
-  Wetlands
-  Buried valley fill in the Ancha Fm

Lithologic control well; plotted to scale, color coded according to distance away from cross section line

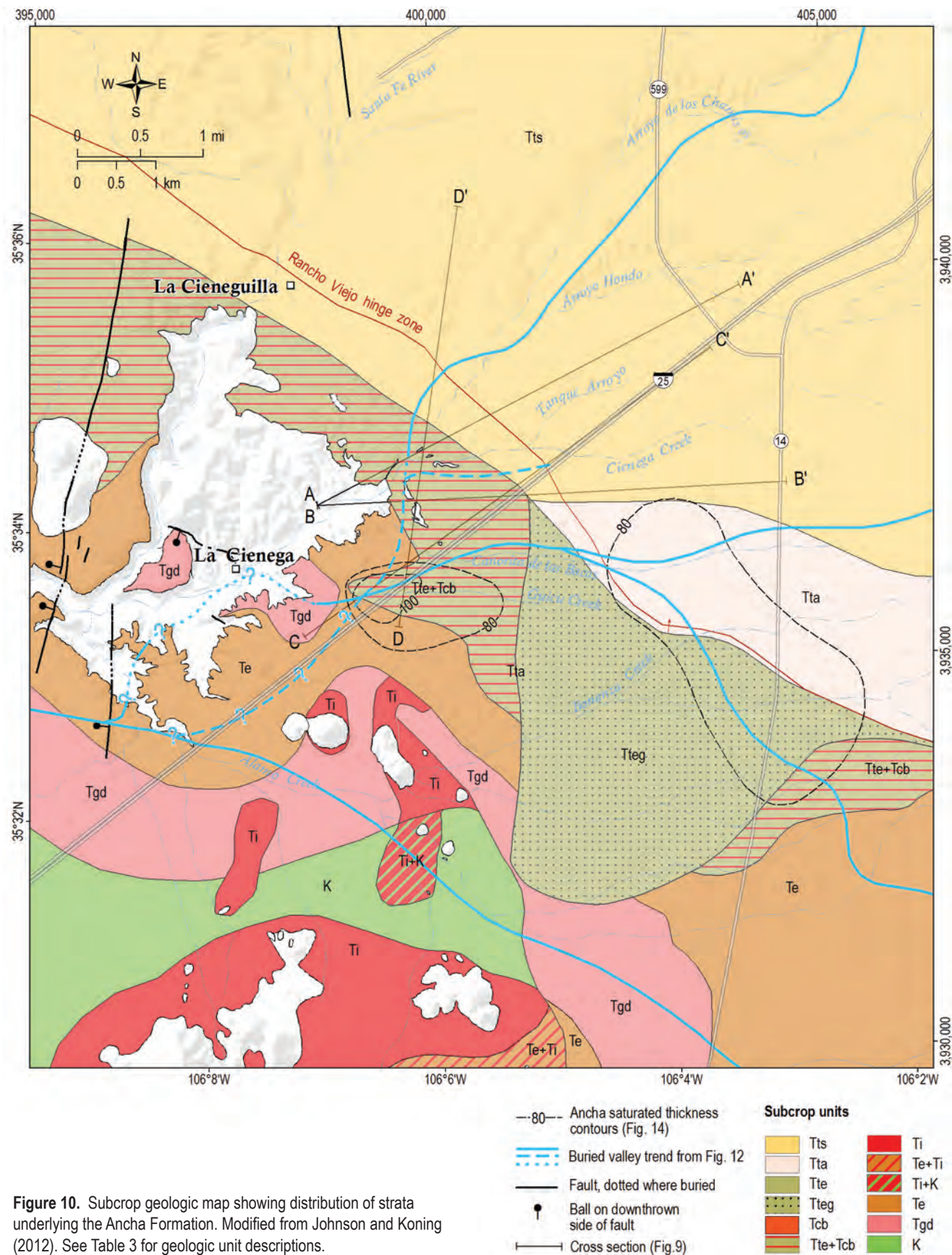


Figure 10. Subcrop geologic map showing distribution of strata underlying the Ancha Formation. Modified from Johnson and Koning (2012). See Table 3 for geologic unit descriptions.

disconformably overlies the Espinaso Formation and paleovalleys are present at its basal contact. Lithosome S (Tts), deposited on a fluvial fan by a west-flowing, ancestral Santa Fe River (Koning et al., 2004; Koning and Read, 2010), is a coarse, pebbly sand that becomes increasingly finer grained away from the mountain front and fan axis. In the study area, it is composed of reddish sand and pebbly sand channel-fills that are interbedded with clay, silt-clay, and very fine to fine-grained floodplain deposits. The floodplain deposits increase to the west and can act as aquitards, locally creating confined or semi-confined aquifers. Lithosome A (Tta) is alluvial slope sediment originating from the Sangre de Cristo Mountains (Cavazza, 1986; Kuhle and Smith, 2001). It is composed of arkosic, fine sand and clayey-silty sand interspersed with sparse, coarse-grained channel fills. The deposit is present beneath the Ancha Formation in the southeast corner of the study area and grades laterally into lithosome S to the north (Fig. 10).

Aquifer test data indicate that lithosomes A and E have significantly lower hydraulic conductivities than the overlying Ancha Formation (Fig. 11). The coarse river deposits of lithosome S (Tts) have hydraulic conductivities comparable to the lower ranges of the Ancha Formation, but the fine sediments in the distal part of the fluvial fan (Ttsf) are significantly less permeable.

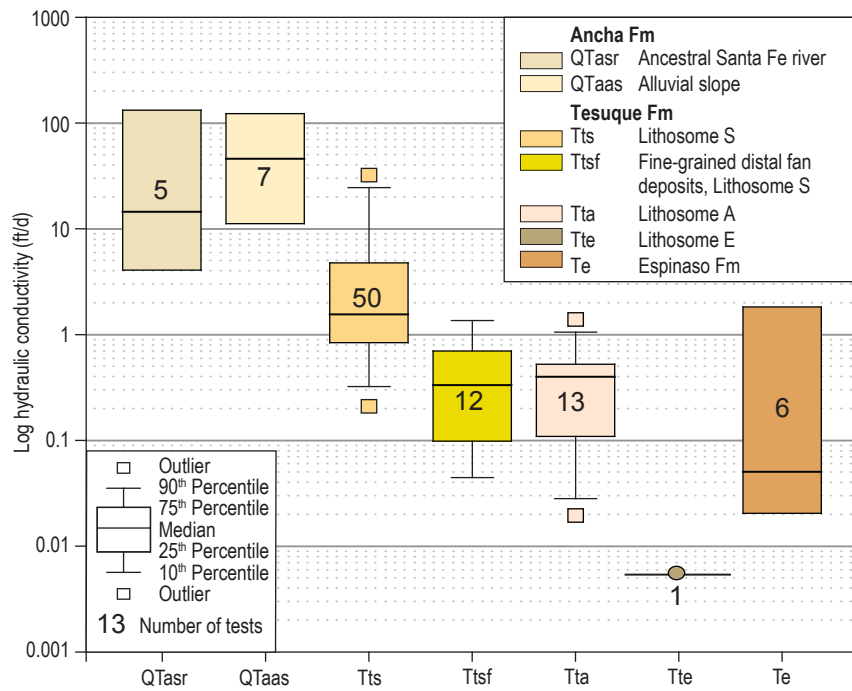


Figure 11. Percentile plot of hydraulic conductivity (feet/day) by geologic unit. Values of hydraulic conductivity are estimated from aquifer tests compiled by Johnson and Koning (2012).

Ancha Formation

The Ancha Formation (Pliocene to lower Pleistocene) occupies the upper portion of the Santa Fe Group basin fill and is comprised of sand, silty-clayey sand, and gravel. It forms a locally important, shallow aquifer for the Santa Fe area. The Ancha Formation consists of two alluvial deposits: 1) sediment associated with the ancestral Santa Fe River (QTasr); and 2) alluvial slope deposits originating from the southwestern Sangre de Cristo Mountains (QTaas) (Figs. 5–7). The ancestral Santa Fe River deposits contain abundant, laterally extensive, thick, sandy pebble-cobble channel-fills interspersed with fine-grained floodplain sediments of clayey-silty sand. In contrast, the upper alluvial slope deposits typically contain narrow, ribbon-like channel-fills interbedded in clayey-silty sand. Lower alluvial slope deposits are coarse grained, commonly containing pebbles and cobbles (and local boulders) and in places are quite thick (up to 120 ft). In general, Ancha sediments are coarser, less consolidated, and more permeable than underlying strata, including the Tesuque Formation (Fig. 11). The base of the Ancha Formation coincides with a late Miocene to early Pliocene erosion surface that has truncated tilted and faulted beds in the underlying Tesuque, Espinaso, and Galisteo Formations (Fig. 9).

Previous work has proposed that accumulation and storage of groundwater in the Ancha aquifer is controlled by three factors: 1) permeability contrasts between the Ancha and underlying formations; 2) the topography of the erosion surface at the base of the formation; and 3) groundwater recharge or inflow to the formation (Spiegel and Baldwin, 1963; McAda and Wasiolek, 1988; Johnson et al., 2008). The existence of buried valleys at the base of the Ancha Formation and their influence over locations of springs and wetlands was originally proposed by Spiegel (1963), noted by McAda and Wasiolek (1988), and studied more intensively by HydroScience Associates, Inc. (2004). However, data limitations prevented extensive mapping or characterization of these features.

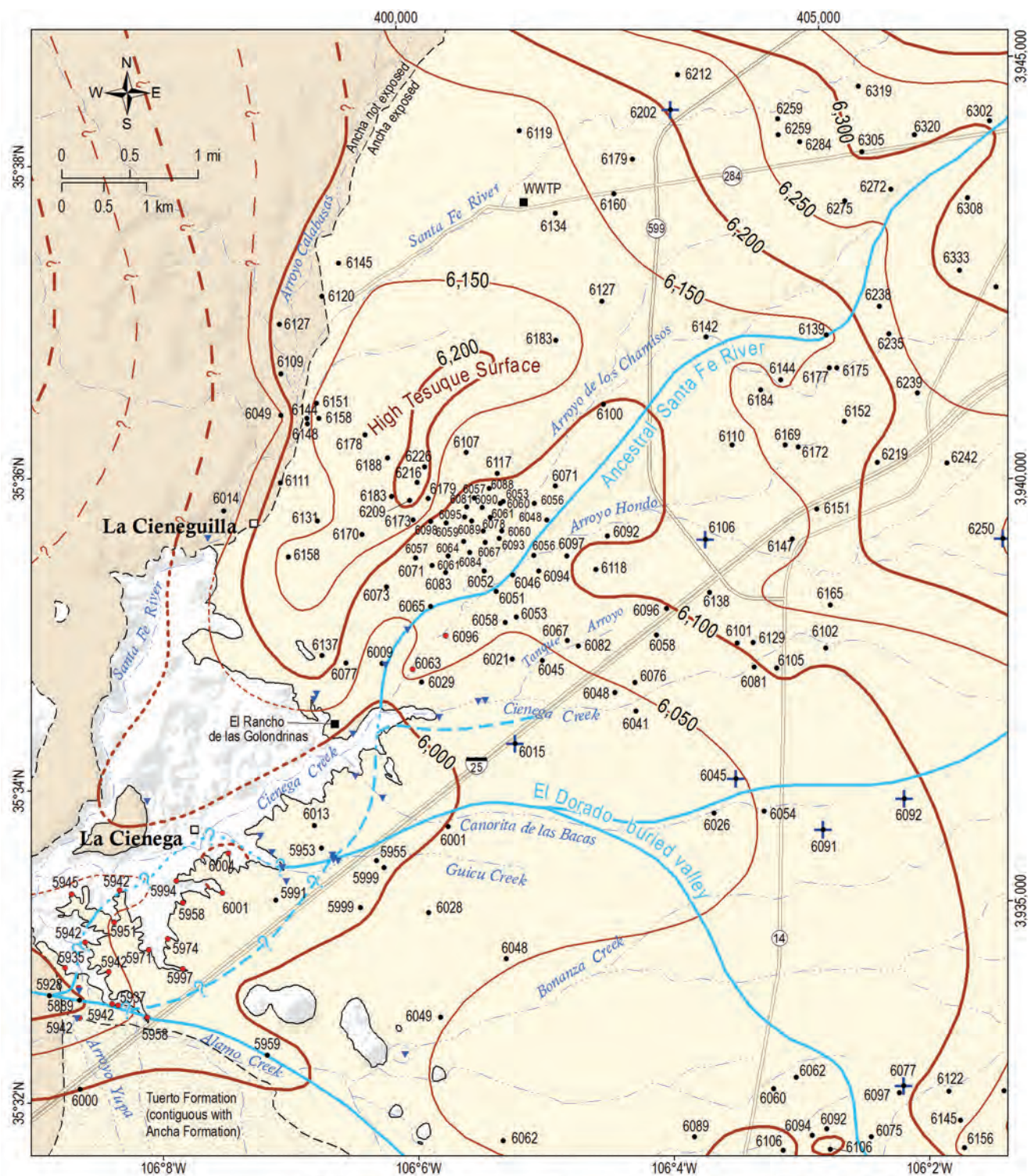


Figure 12. Elevation contour map of the base of the Ancha Formation near La Cienega, showing paleotopography of the pre-Ancha erosion surface and the locations of buried valleys scoured into the underlying Tesuque Formation. These buried valleys control the locations of wetlands and groundwater flow to wetlands (modified from Johnson and Koning, 2012).

Control wells

- + Observed core or cuttings
- Lithologic log from exploration holes and water wells
- Outcrop exposure of contact
- Elevation of base (ft)
- ▼ Spring

Mapped extent of Ancha Fm Extent of Ancha Fm buried

Elevation contours, base of Ancha Fm, interval 50 feet

- 100-ft contour
- 50-ft contour
- ?— Uncertain due to lack of data

Buried valley trend

- From subsurface data
- - - From outcrop mapping
- - - Deposits eroded
- ? Uncertain due to lack of data

The characteristics of the formation's base, thickness, grain size, and permeability are important for understanding how groundwater accumulates in and flows through the formation, and accordingly for our understanding of groundwater sources feeding the springs and wetlands. Because of its importance as a shallow aquifer, Johnson and Koning (2012) developed a series of regional maps for the Ancha Formation that depict the underlying strata (subcrop), the elevation of its structural base, the general location of buried valleys, the thickness, and the extent of saturation. Local versions of those maps are presented here for the La Cienega area (Figs. 10, 12–14).

Structure, thickness and saturation of the Ancha Formation—A significant finding derived from mapping the base of the Ancha Formation is the delineation of buried valleys on the pre-Ancha erosion surface. The elevation contour map of the base of the formation developed by Johnson and Koning (2012)—essentially a topographic map of the pre-Ancha landscape at the time Ancha deposition began—illustrates the general locations of valleys, ridges, and hills in the ancient, pre-Ancha land surface (Fig. 12). Based on paleotopography at the base of the formation, we defined two regional buried valleys. The El Dorado buried valley starts in the southern Sangre de Cristo Mountains near El Dorado and trends west to La Cienega. East of La Cienega, Ancha sediments filling the El Dorado buried valley (QTaas) overlie and are inset into older strata of (from east to west) the Tesuque (lithosomes A and E), Espinaso and Galisteo Formations (Fig. 9 cross sections CC' and D-D' and Fig. 10). A second buried valley, probably associated with the ancestral Santa Fe River, trends southwest from the Santa Fe River Canyon at the mountain front toward La Cienega and generally aligns with the present-day course of Arroyo Hondo and Arroyo de los Chamisos (Fig. 12). In the Santa Fe River buried valley, ancestral Santa Fe River deposits of the Ancha Formation (QTasr) unconformably overlie Lithosomes S and E of the Tesuque Formation (Tts, Tte) as well as the Espinaso Formation (Fig. 9 cross section DD', Fig. 10).

Based on field geologic mapping, we interpret that the ancestral Santa Fe River crossed present-day Cienega Creek—as demonstrated by Santa Fe River sediment (QTasr) buttressed between late Oligocene basalts in an outcrop on the east side of Cienega Creek, 0.2 mi northeast of the mouth of Canorita de las Bacas (Fig. 6)—and converged with the El Dorado buried valley 1.2 mi east of the village of La Cienega (Fig. 12). After merging, the two ancestral

river systems appear to have flowed either: 1) west through the present-day location of Guicu Creek, then south at La Cienega; or 2) southwest between La Cienega and Cerro de la Cruz (Fig. 12). A small Ancha-filled buried valley located east of El Rancho de las Golondrinas and 0.12 mi south of and parallel to Cienega Creek (Fig. 12) was also noted during geologic mapping (Fig. 9 cross section DD', Fig. 10). Additional buried valleys likely exist in the study area, but would probably be of limited extent and are beyond the resolution of the current subsurface dataset.

The pre-Ancha surface (Fig. 12) also defines a northeast-trending paleotopographic high on the top of the Tesuque Formation, situated between La Cieneguilla and Arroyo de los Chamisos. At this location the elevated Tesuque Formation consists of floodplain deposits of clay to fine sand interbedded with sandy fluvial fan deposits associated with the ancestral Santa Fe River. At the start of Ancha aggradation in the Pliocene, this high Tesuque surface was elevated about 150 ft above the ancestral Santa Fe River near the present confluence of Arroyo Hondo and Arroyo de los Chamisos. In the modern subscape, this high-standing remnant of low-permeability Tesuque sediments interrupts zones of saturation in the Ancha Formation.

The lower part of the Ancha Formation generally contains coarse sand and gravel, particularly in alluvial slope deposits in the eastern half of the study area. Lithologic logs from wells completed in the El Dorado buried valley east of La Cienega indicate the presence of cobble- and boulder-sized materials, suggesting that buried-valley deposits may be generally coarser than adjacent and overlying alluvial slope deposits. The buried valleys also coincide with thicker deposits (Fig. 13). In the study area, Ancha deposits vary in thickness from about 250 ft in the El Dorado buried valley to less than 50 ft over the high Tesuque surface east of La Cieneguilla. Geologic mapping at the edge of the formation near El Rancho de las Golondrinas discovered buried-valley fill thicker than 50 ft.

The extent and thickness of saturated zones within the Ancha Formation during the period 2000–2005 and their spatial relation to springs, wetlands, and mapped buried valleys are shown in Figure 14. Saturated thickness contours considered groundwater-fed springs (Table 2) and wetlands mapped by Dick (2012). The saturated thickness of the Ancha aquifer above the wetlands varied from about 30 to 120 ft. Historic water-levels (see regional maps in Johnson and Koning, 2012) suggest that zones of

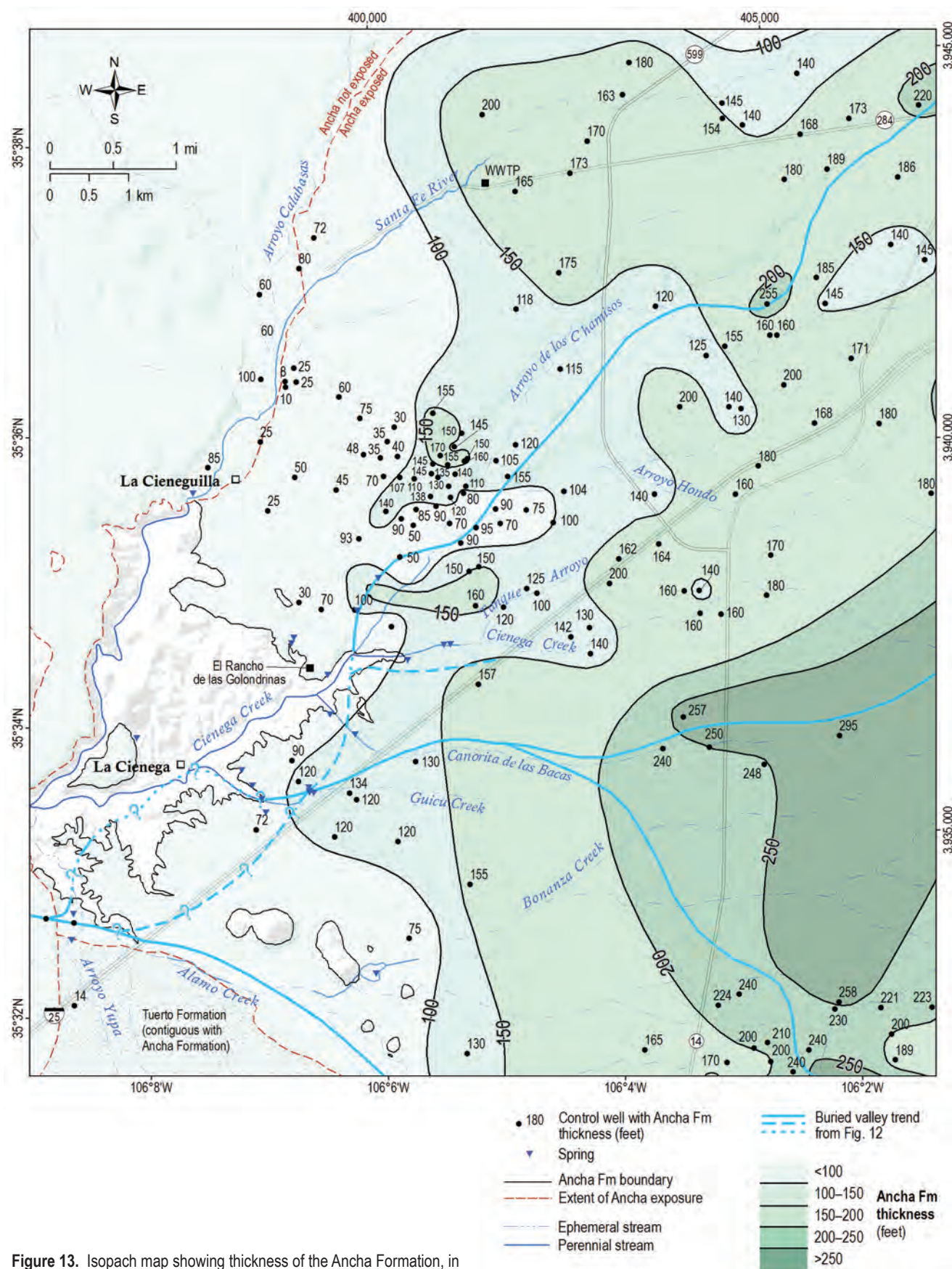


Figure 13. Isopach map showing thickness of the Ancha Formation, in feet (modified from Johnson and Koning, 2012).

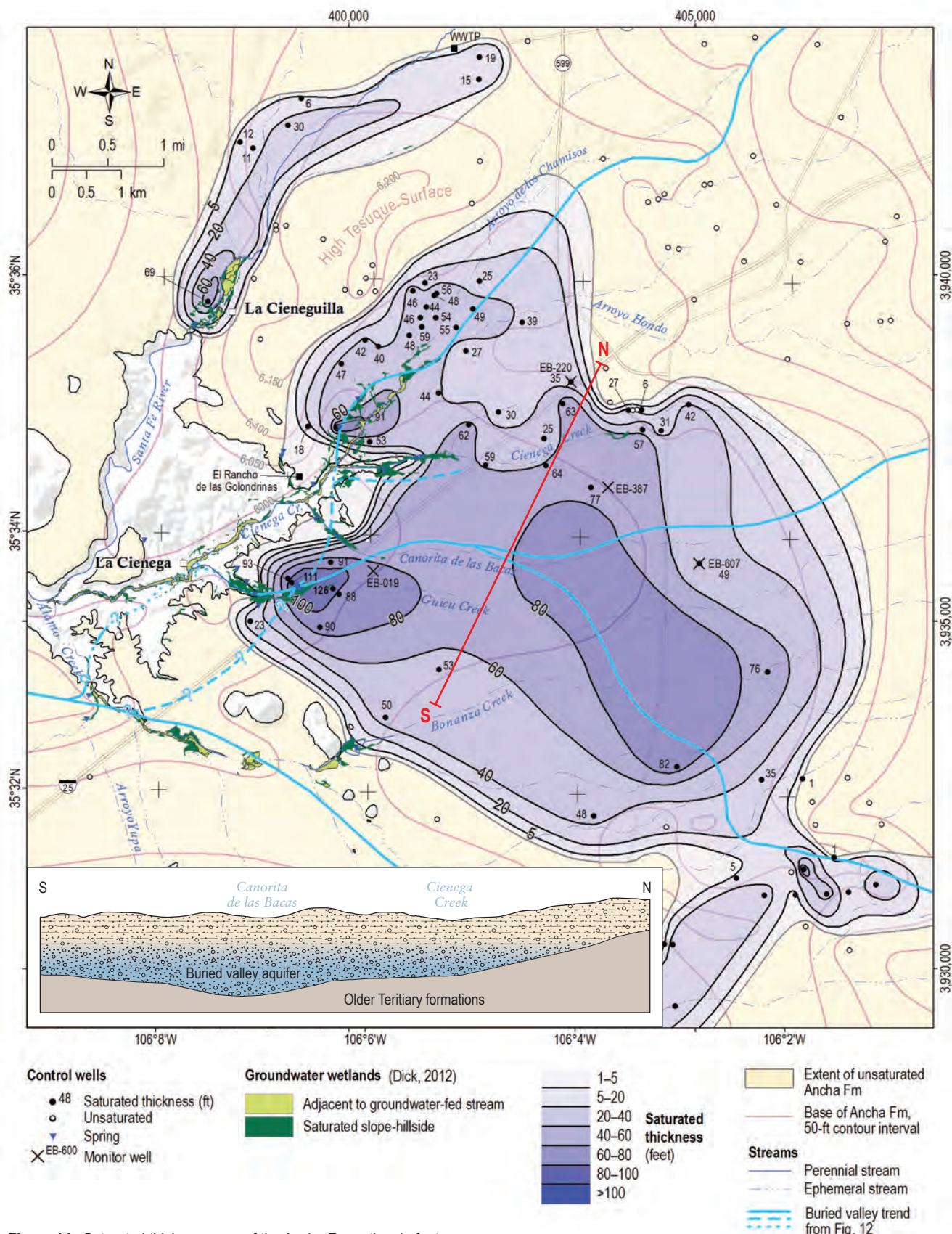


Figure 14. Saturated thickness map of the Ancha Formation, in feet, for 2000–2005 groundwater conditions (modified from Johnson and Koning, 2012) and conceptual cross section of a buried-valley aquifer.

saturation were generally thicker and more extensive in past decades than in the 2000–2005 time period.

Hydraulic conductivity values estimated from aquifer tests show that ancestral Santa Fe River and alluvial slope deposits have hydraulic conductivities that range from 2 to 252 ft/d with a mean of 59ft/d (Fig. 11). These deposits are more permeable than underlying strata in the Tesuque and Espinaso Formations by one to four orders of magnitude. Thick zones of saturation in the Ancha overlie geologic units with lower hydraulic conductivities (Tesuque lithosomes A and E, Cieneguilla basanite, and Espinaso

Formation). This illustrates how high permeability contrasts between the Ancha and underlying formations affect the accumulation and storage of groundwater in the Ancha aquifer. Figure 10 shows the distribution of pre-Ancha geologic formations with an overlay of the 80- and 100-foot Ancha saturation contours from Figure 14.

The hydrologic significance of buried valley aquifers in the Ancha Formation—Buried valleys in the Ancha Formation create coarse-grained, highly transmissive aquifers similar to those found in the

HOW LARGE IS THE ANCHA GROUNDWATER RESERVOIR?

The extent of the zone of groundwater saturation in the Ancha Formation and its thickness (Fig. 14) were mapped using data from well records, geologic logs, and water-level measurements. From these information sources we could identify the base of the formation and the top of the water table for each well point, and thus where or whether the formation was saturated. The largest, continuous saturated zone in the Ancha Formation extends eastward from the wetlands along Cienega Creek to just past NM-14 and northward to where NM-599 intersects Arroyo de los Chamisos. During the time period of about 2000 to 2005, this zone covered an area of about 14,000 acres or 22 square miles.

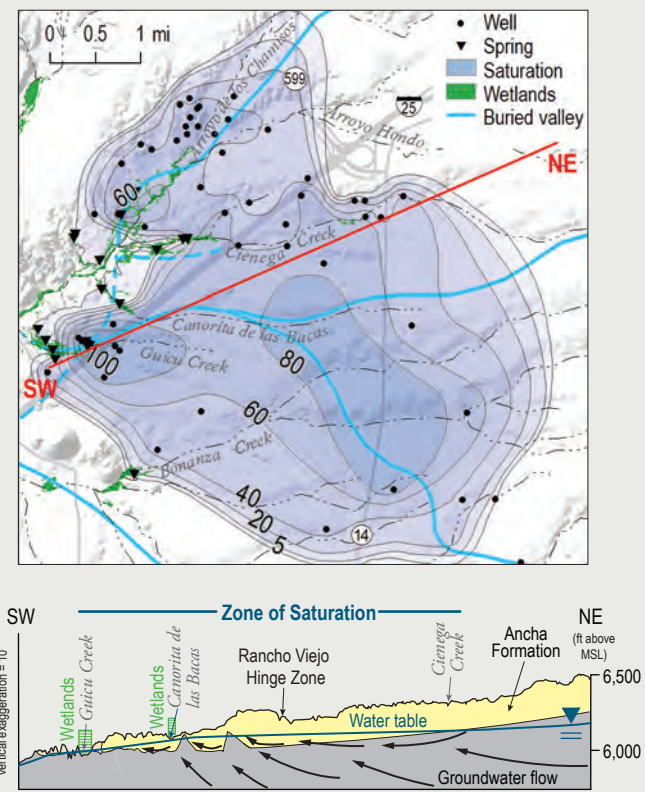
How much groundwater resides in the Ancha aquifer that feeds the wetlands?

Because the saturated portion of the Ancha Formation has identifiable boundaries, we can use ArcGIS software tools to compute how much groundwater resides within the underground reservoir. We first computed the volume of aquifer that was saturated, and then assumed that 10% of that volume consisted of water and the remaining 90% was rock. From this we estimate that about 67,000 acre-feet of groundwater (21,830,543,000 gallons) resides in the portion of the Ancha aquifer that feeds the La Cienega wetlands. This volume is equivalent to 1.3 times the amount of water in Cochiti Reservoir (Cochiti is maintained with a permanent recreation pool of 50,000 acre-feet) or the amount of water held in 69 Houston Astrodomes.

How long will the Ancha reservoir last?

A definitive estimate of how long the water supply in the Ancha Formation can continue to sustain the La Cienega wetlands is not possible. The answer depends on future population growth and water demand, new technologies for recharging groundwater, the effects of a warmer, drier climate on local aquifer recharge, and how groundwater pumping is managed in the basin in the future. Currently, water is being withdrawn from the aquifer faster than it is being replaced; thus groundwater levels are declining (see Fig. 27 and associated text). Such groundwater use will eventually deplete the aquifer because it has limited groundwater storage and fixed or declining recharge. But imagine, if a small creek with a flow of 100 cubic feet per second were draining the Ancha aquifer, it would dry the aquifer in about 338 days.

Peggy Johnson and Brigitte Felix



incised valleys of glaciated terrains (Kehew and Boettger, 1986; Shaver and Pusc, 1992; Seifert et al., 2008; van der Kamp and Maathuis, 2012) and in stream-dominated alluvial fans (Weissmann et al., 2004). Buried-valley aquifers occur as long and narrow, highly transmissive, gravel-sand deposits incised into lower permeability deposits or formations (van der Kamp and Maathuis, 2012; Weissmann et al., 2004). The high degree of gravel-sand body connectivity within the incised-valley fill results in rapid groundwater flow relative to the surrounding, generally finer-grained deposits (Weissmann et al., 2004). In the Ancha Formation, buried-valley aquifers contain gravel-sand deposits with locally abundant cobble- and boulder-sized material and take the form of long, narrow, ribbon-like channels scoured into the less permeable Tesuque, Espinaso and Galisteo Formations (Figs. 10 and 12). The ultra-coarse channel-bed deposits and adjacent coarse sheet-like alluvial slope deposits combine to form the Ancha aquifer (Fig. 14 conceptual cross section).

Buried-valley aquifers are known as important sources of groundwater, but the coarse nature and relatively high hydraulic conductivity of the deposits increase the vulnerability of the aquifers to excessive drawdowns and contamination. Modeling studies show that pumping from or adjacent to a buried valley leads to greater drawdown and more distant drawdown effects along the axis of the valley than in the adjacent finer-grained deposits (van der Kamp and Maathuis, 2012; Seifert et al., 2008; Weissmann et al., 2004). The coarse, highly transmissive sediments also enhance vertical flow and recharge (Seifert et al., 2008; Weissmann et al., 2004). Modeling studies involving buried-valley aquifers also conclude that numerical models must capture the salient hydrostratigraphic features of buried-valley deposits in order to produce reliable predictions (Seifert et al., 2008; Weissman et al., 2004; Harrar et al., 2003; Springer and Bair, 1992).

By combining maps of the Ancha Formation (Johnson and Koning, 2012; Koning and Hallett, 2002; Koning and Read, 2010) and the La Cienega wetlands (Dick, 2012) we show that large wetland

complexes are maintained by groundwater that discharges from buried-valley aquifers. The wetlands in Arroyo Hondo, Guicu Creek and Cienega Creek (Figs. 14 and 9) are vulnerable to the large drawdown response that is characteristic of these aquifers, but they are also linked to sources of enhanced recharge. Wetland aquifer impact assessments, conservation plans and restoration measures should both account for and exploit the hydrologic characteristics of buried-valley aquifers.

Cerros del Rio volcanic rocks

The high plateau west of La Cieneguilla and La Cienega is formed by Pliocene to lower Pleistocene basalt, basaltic andesite, and andesite of the Cerros del Rio volcanic field (QTcrv on Figs. 5–7, Table 3). These volcanic rocks erupted on the surface as fluid lavas and flowed across the landscape, filling valleys and flowing around obstructions. The extrusive lavas formed thin, near-horizontal layers that thickened and thinned over pre-eruption topography. These volcanic rocks cover both Santa Fe Group sediments and pre-rift sedimentary units, generally lie above the water table, and are unsaturated. Where the basalts are fractured by columnar joints, they may be highly permeable in the vertical direction, allowing infiltrating water to recharge underlying aquifers

Surficial deposits

Surficial sedimentary deposits (Qva, and Qal on Fig. 6, Table 3) occur throughout the study area, but most are too thin to show on the geologic map and cross sections or to form significant aquifers. The principal drainages commonly contain 15 to 50 ft of Holocene to latest Pleistocene alluvium (Qva) consisting of sand, gravel and silt. Gravelly terrace deposits flank the Santa Fe River. These young fluvial deposits are important as they form a hydraulic link between shallow groundwater and surface flow, particularly along the perennial reaches of lower Arroyo Hondo and Cienega Creek.

IV. HYDROLOGY OF LA CIENEGA WETLANDS AND THE SANTA FE GROUP AQUIFER

Wetlands continually receive and lose water through exchange with the atmosphere, streams, and aquifers in accordance with the hydrologic cycle. The major components of inflow and outflow (Fig. 15) include precipitation (P), surface-water flow (Q), groundwater flow (G), evaporation (E), and transpiration by plants (T). Evapotranspiration (ET) refers to the combined loss of water by evaporation from open water, wet soils, and shallow groundwater, and by plant transpiration from both surface water and shallow groundwater. A water balance or water budget is a measured accounting of the inflows, outflows and storage of water in a hydrologic system for any time interval and any size area (Todd and Mays, 2005). Considering a water balance for a wetland can improve understanding of the wetland's hydrologic processes and functions, and help predict the effects of natural and human-induced hydrologic alterations (Carter, 1996). We apply a water-balance approach to better understand the hydrology of the La Cienega wetlands and how changes in the water balance may affect their long-term sustainability.

A Wetland Water Balance

In groundwater-fed wetlands such as those at La Cienega, groundwater (G) and surface water (Q) are interconnected. The wetland water budget is a natural mass balance in which the change in storage of groundwater over time equals the sum of the inputs to, minus the outputs from, the groundwater system that feeds the wetlands. Water inputs to the wetland include groundwater inflow (G_{in}), surface-water inflow (Q_{in}), and precipitation that infiltrates to groundwater

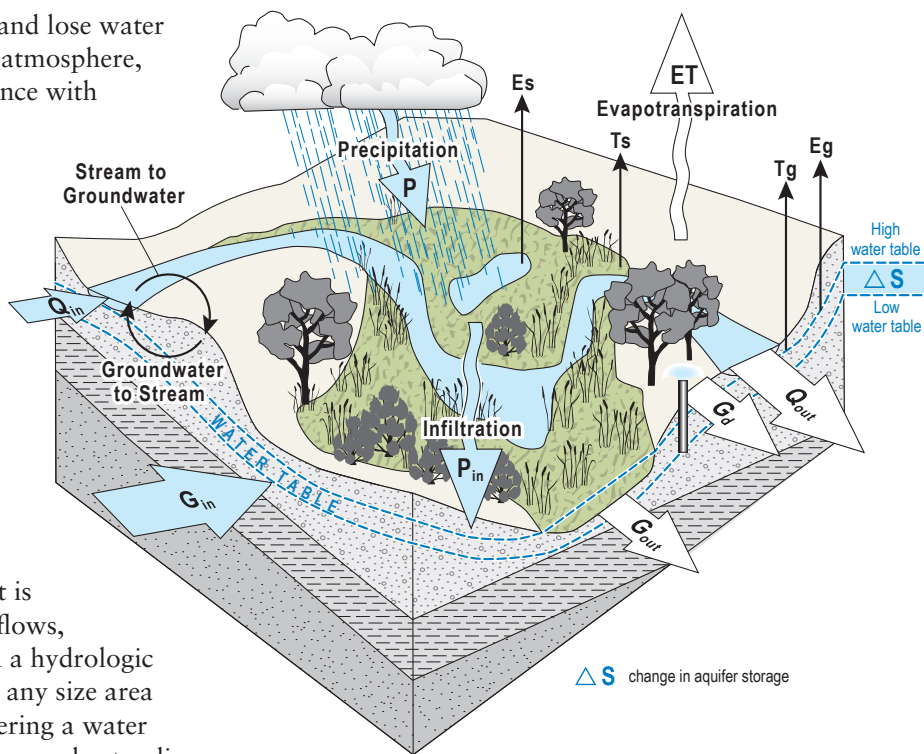


Figure 15. A local hydrologic cycle for the groundwater-fed wetlands at La Cienega, showing the major inflows and outflows of water. Major inflows include groundwater (G_{in}), surface water (Q_{in}), and precipitation that infiltrates to groundwater (P_{in}). Major outflows include surface water (Q_{out}), evaporation (E) and transpiration (T), groundwater (G_{out}), and groundwater depletion from wells (G_d).

(P_{in}). Surface-water inflow to groundwater is a transient event limited to bank storage during storms. It is short-lived inflow that does not contribute significantly to the long-term preservation of the wetlands, and we consider it to be negligible in the water balance. Water outputs are surface-water outflow (Q_{out}) and evapotranspiration (ET), with an undetermined, but probably small, amount of groundwater outflow (G_{out}). Groundwater depletion (G_d) from local and regional groundwater pumping is an additional groundwater outflow that affects the wetland water balance. A wetland water balance describing

the primary inflows and outflows (Fig. 15) can be expressed by an equation as follows:

$$(G_{in} + Q_{in} + P_{in}) - (Q_{out} + ET + G_{out} + G_d) = \pm \Delta S$$

where ΔS is a change in groundwater storage near the wetland. If the change in groundwater storage is positive (+), then the inflows to the system exceed the outflows. Conversely, if the change in storage is negative (-), then the outflows exceed the inflows.

Components of a wetland water budget, illustrated for La Cienega in Figure 15, can be measured or calculated using various methods. However, determining a wetland water budget is imprecise as the climate and the water budget vary from year to year, and the measurement of individual components often has large uncertainties. In this report, we use a water balance to evaluate connections between the major hydrologic elements—precipitation, surface-water outflow, evapotranspiration, and changes in groundwater storage—using available data on climate, stream discharge and groundwater fluctuations. In this section we: 1) provide a hydrologic framework for the wetlands; 2) examine components of wetland inflow and outflow (precipitation, surface-water discharge and ET); and 3) use water-table fluctuations to correlate changes in groundwater storage with hydrologic stresses, including precipitation, drought, ET, and groundwater depletion. Quantifying groundwater flow and ET is beyond the scope of this study and best done using groundwater simulation models.

Precipitation

Highly variable precipitation and streamflow, punctuated with periods of high runoff and drought, are characteristic of the upper Rio Grande basin. Streamflow reconstructions for the upper Santa Fe River indicate that some of the most extreme single-year, 3-year, and 7-year average low flow events of the past seven centuries occurred within the last 60 years (1950s and 2000s drought, for example), but more extreme events have occurred in the past (Margolis et al., 2011). Gutzler and Robbins (2011) indicate that the droughts of the mid-20th century are likely to return with greater frequency through the coming century as a result of climate change.

Precipitation provides water for wetlands, directly through surface runoff and indirectly through recharge to groundwater. Because wetland sustainability requires a relatively stable influx of water (Carter, 1996), it is important to understand the local

and regional climate and the temporal variability of precipitation. Precipitation records from local NOAA weather stations are examined for this purpose.

Data from three NOAA weather stations near the study area are evaluated for general trends in monthly and annual precipitation (Figs. 16, 17). Station Santa Fe 2 (SF 2), located in Arroyo Hondo 9.3 miles east-northeast of the Village of La Cienega, provides a continuous 41-year precipitation record from 1972 through the present (2013) (Fig. 17A). Stations SFCMA at the Santa Fe County Municipal Airport (Fig. 17B) and Turquoise Bonanza Creek (TBC) south of the state penitentiary (Fig. 17C) provide records closer to the study area. Site information and summary statistics (mean, median, maximum, and minimum precipitation and the 10th, 25th, 75th, and 90th percentiles) are shown in Table 5.

Monthly rainfall in New Mexico follows a strong seasonal pattern associated with the North American Monsoon (en.wikipedia.org/wiki/North_American_Monsoon), which produces summer rains from early July through mid-September. An average of 5.75 inches of monsoon precipitation falls at SF-2 during the three-month period and accounts for half of the annual precipitation (Figs. 16, 17A). More than two-thirds (68%) of annual precipitation generally

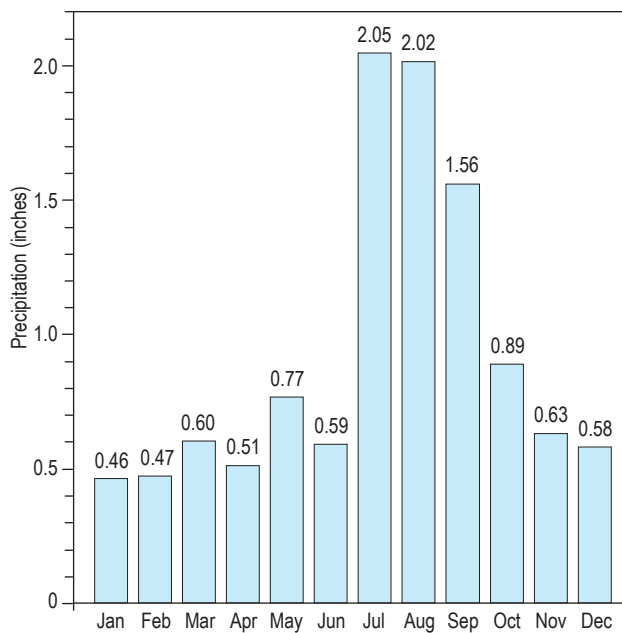


Figure 16. Median monthly precipitation (inches) from the 41-year record (1973–2013) for NOAA station SF 2. Total rainfall during the months of July through September, associated with the North American Monsoon, is typically 5.75 inches and accounts for half (50%) of the annual precipitation. See Figure 18 for station location and Table 5 for monthly statistics.

Table 5. Site information and summary statistics for NOAA NCDC weather stations. See Figure 18 for station locations. Precipitation data are from www.ncdc.noaa.gov/cdo-web/datasets.

STATION		LOCATION			RECORD		ANNUAL PRECIPITATION STATISTICS (inches)							
Name	Number	UTM easting NAD83	UTM northing NAD83	Elevation (ft asl)	Period	Years*	Mean \bar{x}	Median P_{50}	Max (year)	Min (year)	10 th percentile P_{10}	25 th percentile P_{25}	75 th percentile P_{75}	90 th percentile P_{90}
Santa Fe 2 (SF 2) – 9.3 mi ENE of Village of La Cienega	298085	411677	3942174	6755	4/1/1972 to 12/1/2013	41	13.18	13.27	19.48 (1994)	6.43 (2012)	9.66	10.67	15.05	17.75
Turquoise Bonanza Creek (TBC) – 3.2 mi ESE of Village of La Cienega	291236	403017	3934565	6241	6/1/1953 to 2/1/1996	42	12.69	12.76	29.59 (1991)	4.54 (1956)	7.88	9.09	14.98	17.12
Santa Fe County Municipal Airport (SFCMA) – 4.4 mi NE of Village of La Cienega	23049	401387	3942009	6308	1/1/1942 to 12/1/1957	16	9.64	9.30	14.80 (1949)	3.14 (1956)	7.00	8.49	11.53	12.94
Santa Fe County Municipal Airport (SFCMA) – 4.4 mi NE of Village of La Cienega	23049	401387	3942009	6308	4/1/1998 to 12/1/2013	15	10.13	10.47	14.17 (2006)	6.67 (2012)	6.98	8.61	12.08	12.68
STATION		LOCATION			RECORD		MONTHLY PRECIPITATION STATISTICS (inches)							
Name	Number				Period	Months	Mean \bar{x}	Median P_{50}	Max (mly)	Min	10 th percentile P_{10}	25 th percentile P_{25}	75 th percentile P_{75}	90 th percentile P_{90}
SF 2	298085				4/1/1972 to 12/1/2013	499	1.11	0.85	4.81 (7/97)	0	0.09	0.35	1.61	2.51
TBC	291236				6/1/1953 to 2/1/1996	507	1.06	0.71	9.59 (12/91)	0	0.06	0.31	1.49	2.45
SFCMA – 1942–1957	23049				1/1/1942 to 12/1/1957	192	0.80	0.47	4.61 (7/49)	0	0.05	0.22	1.00	2.00
SFCMA – 1998–2013	23049				4/1/1998 to 12/1/2013	189	0.86	0.57	4.76 (7/98)	0	0.04	0.2	1.22	2.06

NOAA NCDC – National Oceanic and Atmospheric Administration, National Climatic Data Center, * – full years in record

falls during the months of May through October. November through April is generally the driest period, with January and February being the driest months. This annual cycle of wet summers and dry winters, and its year-to-year variability over the last several decades, is visible in the monthly precipitation curves in Figure 17.

Annual precipitation at SF 2 (Fig. 17A) varies around a 41-year mean of 13.18 inches (Table 5), but wet and dry years are common. Using the upper and lower quartiles of annual precipitation (P_{75} and P_{25} values, Table 5) to define “wet” and “dry” years (Helsel and Hirsch, 1995), the record shows that the recent 16 years (1998–2013) were notably arid. This period had far fewer wet years (annual precipitation ≥ 15.05 inches) than dry years (annual precipitation ≤ 10.67 inches) and showed a significant decline in the annual mean relative to the preceding period

(1973–1997), which included a balance of wet and dry years. During 2012, when field data were collected for this study, a 41-year low of 6.4 inches in total precipitation fell at SF 2 (Fig. 17A), and the SFCMA station recorded its second driest year in the last fifteen (Fig. 17B).

Precipitation deficits and prolonged drought impact the various parts of the hydrologic system differently over time. Effects of drought on streams can happen fairly quickly—within days or weeks for streams controlled by surface runoff. Groundwater levels in wells, groundwater discharge to springs and wetlands, and the flow in streams and springs fed by groundwater may not reflect a rainfall shortage for months to a year or more after a drought begins (Moreland, 1993; Alley et al., 1999). The sequence of multi-year droughts from 2001 to 2004 and 2011 to present (Figs. 17A and B) may be sufficient to

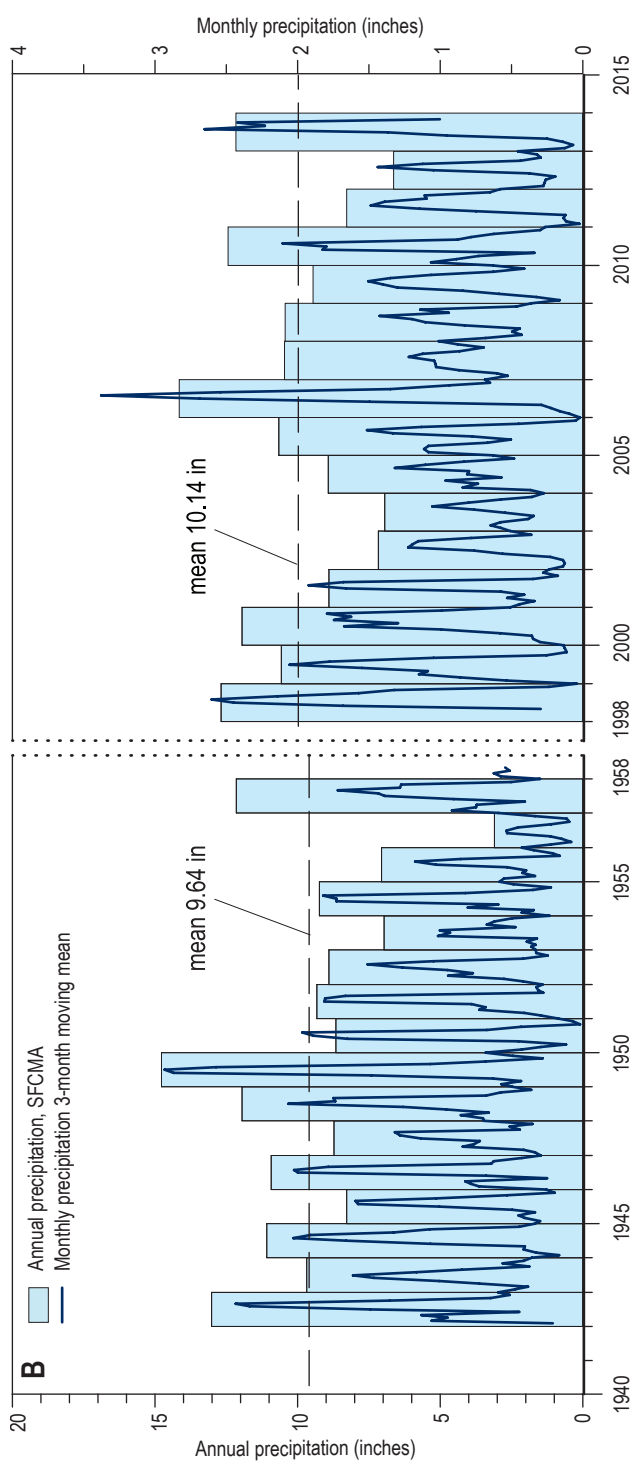
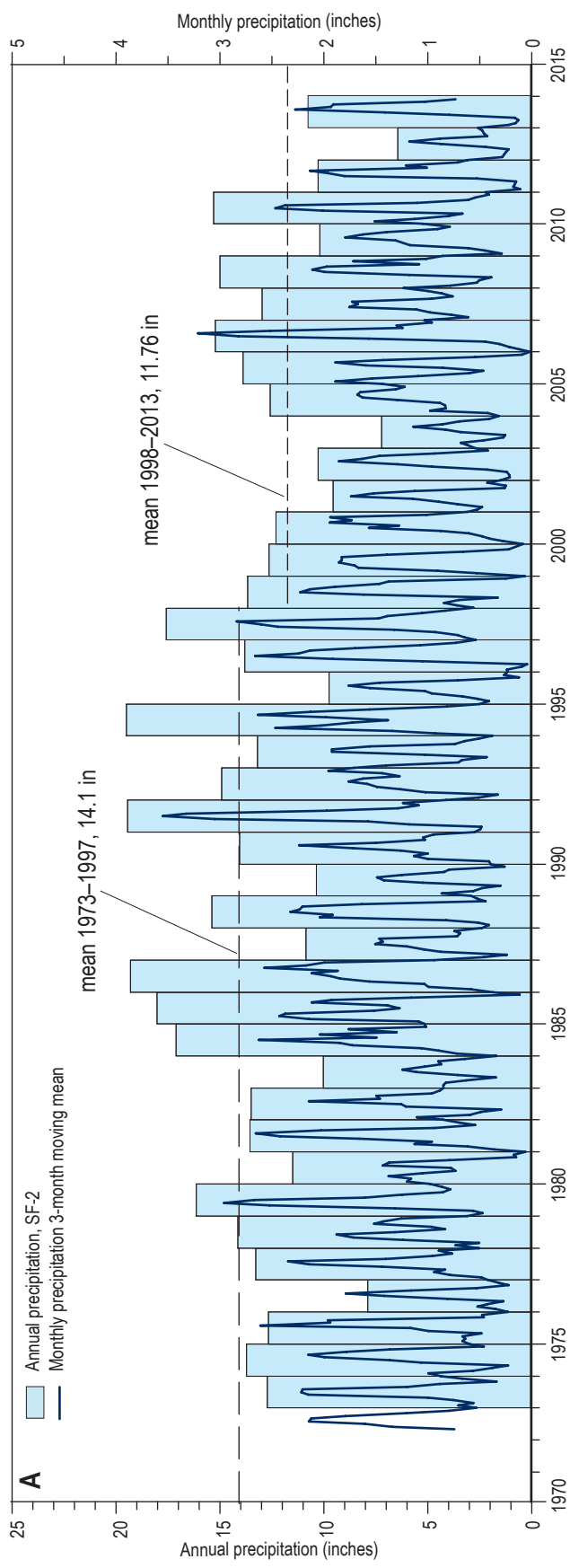


Figure 17. Annual and monthly precipitation (inches) for NOAA stations.

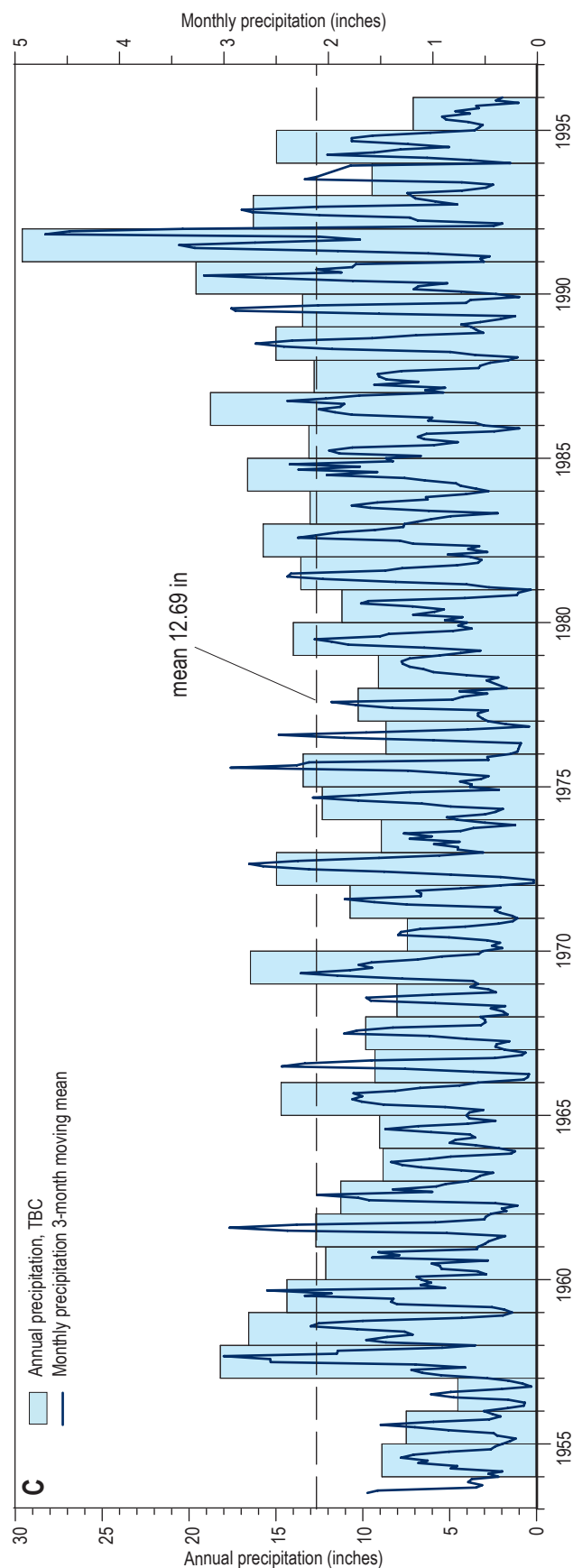
A—Santa Fe 2 (SF 2), 1972–2013.

B—Santa Fe County Municipal Airport (SFCMA), 1942–1958 and 1998–2013.

C—Turquoise Bonanza Creek (TBC), 1954–1995.

Annual precipitation is shown as a bar chart. Monthly precipitation is expressed as a 3-month moving mean.

Station information and summary statistics are shown in Table 5, and station locations are on Figure 18.



negatively affect streamflow, groundwater levels, springs and wetlands. This question is examined in following sections on surface water hydrology and long-term water-level changes.

Extremely wet seasons and extreme storm events increase annual precipitation and can improve streamflow and raise shallow groundwater levels. Wet years result from either high monsoonal precipitation or wet winters or both. For example, at SF 2 (Fig. 17A) 1991 was an extremely wet year (19.44 inches), primarily due to having the strongest three-month monsoon on record (9.96 inches, July–September), and the third highest monthly precipitation (July 1991, 4.43 inches). At the nearby Bonanza Creek station (Fig. 17C), 1991 was by far the wettest year on record (29.59 in) due not only to the strong monsoon (8.1 in) but also to high moisture during the normally dry months of November and December. December 1991 produced the highest monthly precipitation (9.59 in) on record for the Santa Fe area. Late winter storms in January–March 2005 contributed to above average annual precipitation at SF 2 (Fig. 17A) and SFCMA (Fig. 17B) and also resulted in uncommonly high snowmelt and spring runoff observed in the lower Santa Fe River above the WWTP. The effects of extreme wet and dry conditions on streamflow, shallow groundwater levels, and discharge to springs and wetlands are explored further in following sections.

Surface-Water Hydrology

The La Cienega area is characterized by the convergence of multiple drainages emanating from the Sangre de Cristo Mountains that have carved 30 to 100-ft deep valleys into a broad west-sloping alluvial surface. These drainages primarily contain dry sandy channels with ephemeral streams that flow sporadically in response to precipitation and snowmelt. Several studies in the Española Basin and elsewhere in the Rio Grande rift have shown that infiltration events in ephemeral channels that lie above the water table—the Santa Fe River, Arroyo Hondo, Cañada Ancha, and Abo Arroyo particularly—produce focused recharge to the underlying basin-fill aquifers (Johnson et al., 2013; Manning, 2009; Moore, 2007; Stewart-Deaker et al., 2007; Thomas et al., 2000). Near La Cienega where the SFG aquifer thins and the water table rises to land surface, the incised drainages contain perennial streams that flow continuously throughout the year. The base of

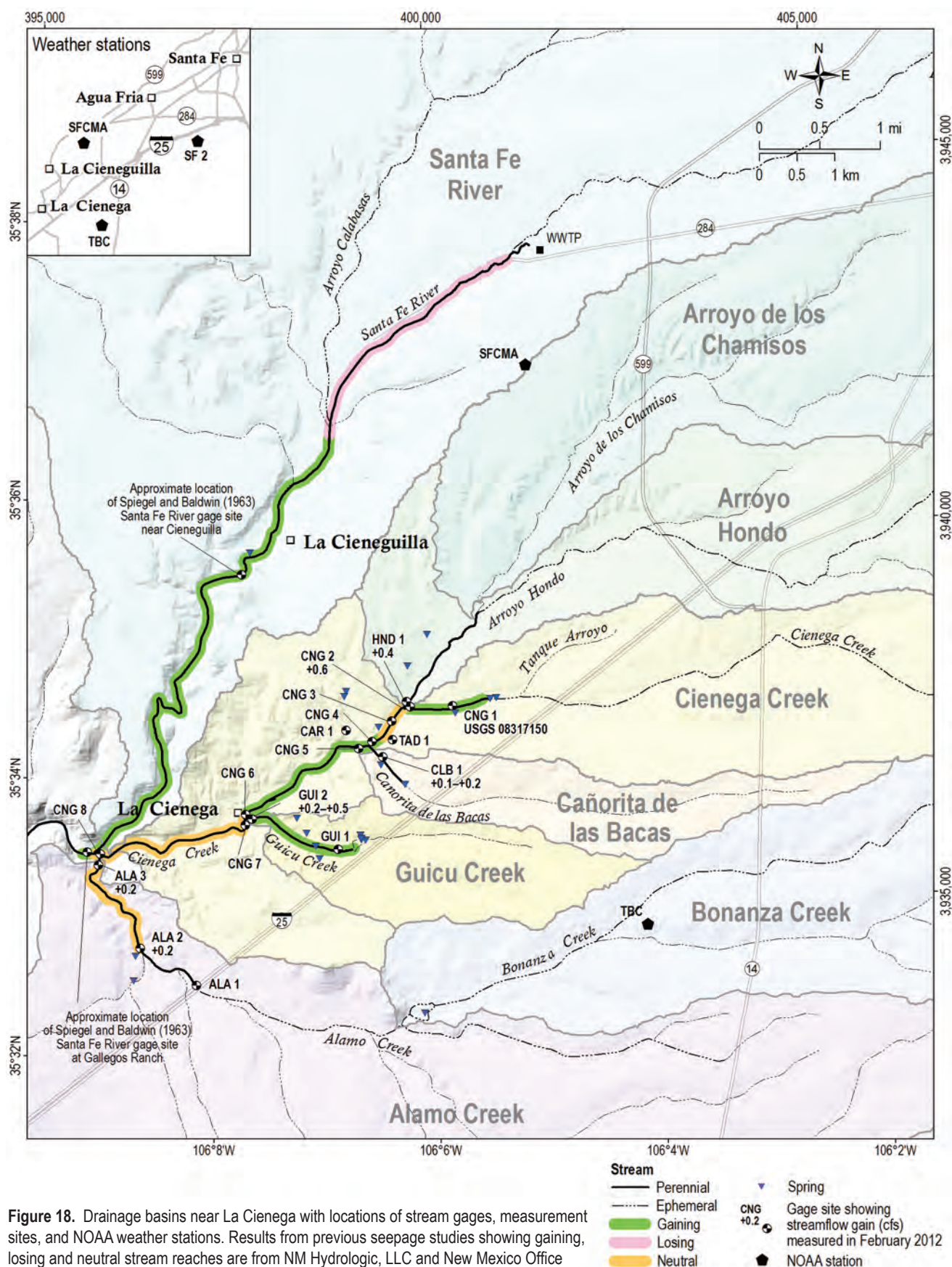


Figure 18. Drainage basins near La Cienega with locations of stream gages, measurement sites, and NOAA weather stations. Results from previous seepage studies showing gaining, losing and neutral stream reaches are from NM Hydrologic, LLC and New Mexico Office of the State Engineer (2012a, b) (Table 7).

these wet channels generally stands lower than the local water table. Perennial stream-flow in Cienega Creek and its tributaries Arroyo Hondo, Cañorita de las Bacas, Guicu Creek, and Alamo Creek (Fig. 18) is sustained by groundwater emerging as springs along the valley slopes and channel bottoms.

The springs, wetlands and streams at La Cienega are a significant hydrologic and cultural resource. Acequia irrigation draws water from small perennial flows in Cienega Creek and its tributaries during irrigation season (April through October) and from ponds and sums that continually collect groundwater along the valleys of Cienega Creek and the Santa Fe River (Petronis et al., 2012). The ephemeral tributaries of Arroyo de los Chamisos and Tanque Arroyo convey surface runoff and locally recharge the aquifer. Cienega and Alamo Creeks convey stream-flow and groundwater discharge from the SFG aquifer to the lower Santa Fe River.

Characterizing streamflow is an important part of understanding the wetland water balance. Streamflow measurements taken during winter months (when transpiration is zero, evaporation is minimal and there is no surface runoff) represent groundwater discharge to the wetland. Streamflow measurements have been made at several locations in the La Cienega area during the past 60 years (Fig. 18). Two locations have historic streamflow data relevant to this study: 1) upper Cienega Creek near the Acequia de la Cienega head gate (also known as “Cienega head gate,” “Cienega Creek at flume,” and CNG-1); and 2) the Santa Fe River above and below the confluence with Cienega and Alamo Creeks (Fig. 18). Groundwater discharge through springs and seeps has not been measured directly, but its contributions to streamflow have been accounted for by stream reach. Seepage studies have measured streamflow in Cienega Creek, its tributaries, and above and below its confluence with the Santa Fe River in order to assess gains and losses in flow (NM Hydrologic, LLC and the New Mexico Office of the State Engineer, 2012a, b; Petronis et al., 2012; Peery et al., 2007).

In the following sections we summarize results of previous efforts to quantify streamflow on Cienega Creek and its tributaries, introduce new streamflow analyses, and discuss streamflow variability in the context of drought, groundwater outflow, and seasonal changes in precipitation and evapotranspiration.

Acequia de la Cienega head gate

The USGS measurement site at the Cienega head gate (station 08317150 LA CIENEGA CR AT FLUME NR LA CIENEGA, NM) is located in the headwater of Cienega Creek approximately 0.3 mi downstream from the first emergence of groundwater-fed springs in the stream channel (Fig. 18). Periodic measurements of streamflow at the Cienega head gate have been taken since 1997 by the USGS and are reported on the NWIS website: waterdata.usgs.gov/nwis/measurements/?site_no=08317150. Prior measurements by the USGS (1986–1992), the U.S. Department of Agriculture Natural Resources Conservation Service (formerly the Soil Conservation Service (SCS)) and others were reported by HydroScience Associates, Inc. (2004). The known record of streamflow measurements at the Cienega head gate (1966–2014) is presented in Table 6 and plotted on Figure 19. Time gaps of months to years between measurements are characteristic of the record. In most years, measurements were taken in multiple seasons. Most measurements taken by the USGS and reported on the NWIS website have a quality rating (good, fair, poor), which is noted in Table 6. Some period and annual means of streamflow data are used as points of reference, but may be biased to some degree as more measurements were generally taken in the months of April through September than during the rest of the year. Stream discharge data and its variability are discussed below.

Long-term variability in historic streamflow data—The streamflow data from the Cienega head gate (Fig. 19A) vary about a mean and median value of 0.53 ft³/s. Measurements are sporadic, particularly prior to 1986 when only four measurements were taken over 20 years. These early measurements range from 1.55 ft³/s in March 1966 to 0.55 ft³/s in June 1975. Measurements between 1986 and 2014 were taken in all seasons across many years. Post-1986 discharge is generally lower than the pre-1986 measurements, and most values are near and below the long-term mean of 0.53 ft³/s. Variability of the post-1986 data is small, with a standard deviation 0.09.

In Figure 19 we address a question posed by previous studies (Peery et al., 2007; Petronis et al., 2012). Does streamflow variability occur not only month-to-month (seasonally) but also year-to-year,

depending on whether it was a wet or dry year? In Figure 19A, we evaluate temporal correlations between stream discharge and wet and dry years identified in the historic precipitation records (Fig. 17, Table 5 and previous discussion). Only four periods occur when multiple streamflow measurements at the Cienega head gate coincide with extremely wet (1991), average (1997) and extremely dry (2001–2004 and 2012) years. During both 1991, a year of record high precipitation, and 1997, a year of average precipitation, the mean measured streamflow was 0.54 ft³/s. During the dry intervals of 2001–2004 and 2012, mean streamflow dropped to 0.48 and 0.38 ft³/s, respectively, and most measurements fell considerably below the long-term mean. Long-term variability in streamflow does relate to climate variability, primarily multi-year drought.

It is difficult, however, to attribute streamflow decline since 1966 solely to drought. Limited measurements at the Cienega head gate prior to 1990 (Fig. 19A) indicate that streamflow was generally higher during and before the early to mid-1970s than

it has been since the 1990s. Studies by HydroScience Associates, Inc. (2004) noted an apparent slow decline on the Acequia de La Cienega between 1991 and 2003, but concluded that most of the decline occurred prior to 1991. Streamflow statistics agree: the pre-1991 mean streamflow is 0.73 cfs and the mean streamflow for the period 1991–2014 is 0.49 cfs. Streamflow in March 1966 (1.55 ft³/s) was exceptionally high for a dry year, compared to measurements taken during the post-2001 droughts. This suggests that increases in other water-budget outflows—particularly ET and groundwater depletions—contribute to declining streamflow, groundwater levels and spring discharge. Comparing the mean of non-summer streamflow measurements taken since 2001 (0.55 ft³/s)—as an estimate for the modern average groundwater-fed streamflow—with the March 1966 streamflow measurement (1.55 ft³/s) suggests that streamflow may have declined at the Cienega head gate by as much as 1 ft³/s (64%) since 1966. Suggestions that stream incision, associated with changes in land use and recharge patterns, has affected flow in Cienega

Table 6. Streamflow data reported for USGS station 08317150, Cienega Creek at flume (same as NMOSE site CNG 1, Table 7), by the sources as noted (Petronis and others, 2012). Data are plotted on Figure 19.

Date	Measured flow (ft ³ /s)	Measurement rating	Source	Date	Measured flow (ft ³ /s)	Measurement rating	Source
3/17/66	1.55		HAI-SCS ¹	7/19/04	0.48	FAIR	USGS NWIS
5/13/71	0.76		HAI-SCS ²	3/30/05	0.53	FAIR	USGS NWIS
6/24/75	0.55		NMOSE files	7/11/05	0.53	FAIR	USGS NWIS
12/18/75	0.78		NMOSE ³	7/15/05	0.34	FAIR	USGS NWIS
6/19/86	0.55		HAI-USGS	3/27/07	0.55	UNSP	USGS NWIS
5/19/89	0.62		HAI-USGS	5/1/07	0.62	UNSP	USGS NWIS
7/17/90	0.48		HAI-USGS	9/4/07	0.50	UNSP	USGS NWIS
10/18/90	0.58		HAI-USGS	6/30/08	0.37	UNSP	USGS NWIS
3/25/91	0.64		HAI-USGS	7/8/08	0.43	FAIR	USGS NWIS
6/17/91	0.56		HAI-USGS	3/25/09	0.50	UNSP	USGS NWIS
8/28/91	0.32		HAI-USGS	4/1/09	0.54	UNSP	USGS NWIS
11/26/91	0.66		HAI-USGS	7/6/09	0.49	POOR	USGS NWIS
7/8/92	0.37		HAI-USGS	7/7/09	0.49	POOR	USGS NWIS
11/19/92	0.61		HAI-USGS	9/10/09	0.37	FAIR	USGS NWIS
2/21/97	0.56	UNSP	USGS NWIS	5/6/10	0.55	FAIR	USGS NWIS
5/20/97	0.56	FAIR	USGS NWIS	8/12/10	0.47	POOR	USGS NWIS
6/23/97	0.57	UNSP	USGS NWIS	9/22/10	0.47	POOR	USGS NWIS
8/22/97	0.46	GOOD	USGS NWIS	4/5/11	0.63	POOR	USGS NWIS
6/14/01	0.36	UNSP	USGS NWIS	5/13/11	0.60	FAIR	USGS NWIS
3/26/02	0.53	FAIR	USGS NWIS	5/17/11	0.66	FAIR	USGS NWIS
7/19/02	0.38	FAIR	USGS NWIS	8/17/11	0.45	FAIR	USGS NWIS
3/26/03	0.54	FAIR	USGS NWIS	2/17/12	0.41	GOOD	NMOSE ⁴
7/11/03	0.50	FAIR	USGS NWIS	5/22/12	0.42	FAIR	USGS NWIS
12/23/03	0.56		HAI-HAI	8/31/12	0.32	POOR	USGS NWIS
4/8/04	0.64	UNSP	USGS NWIS	4/30/14	0.52	POOR	USGS NWIS
7/2/04	0.39	FAIR	USGS NWIS	7/9/14	0.39	POOR	USGS NWIS

¹ Average of two best measurements by R.C.Smith Hydraulics for the Soil Conservation Service (SCS), reported by HydroScience Associates, Inc. (HAI, 2004)

² Measured by B. Kidman and C. Mantelli for SCS using a Sparling flow meter at exit of flume and pipe, reported by HAI (2004)

³ Earl C. Cooper NMOSE memo dated 12/18/75

⁴ Petronis and others (2012); NM Hydrologic LLC and NMOSE (2012b)
USGS—U.S. Geological Survey
NWIS—National Water Information System, waterdata.usgs.gov/nm/nwis/current/?type=flow
UNSP—Unspecified

Creek, has not been supported with scientific data on incision and water levels.

Seasonal variability of streamflow—In Figure 19B, we evaluate how seasonal changes may influence streamflow by plotting stream discharge at the Cienega head gate against the month and day of measurement. The figure shows that streamflow has a consistent seasonal variation wherein discharge is

lowest during summer months and generally higher the rest of the year. Nearly all streamflow measurements taken during the summer months of July, August, and September fall below the 49-year mean of $0.53 \text{ ft}^3/\text{s}$. Four measurements between February and June also fall below the mean value, but were taken during dry years (2001, 2009, 2012). Streamflow between October and June (the dry non-monsoon months) of any year generally falls above the mean.

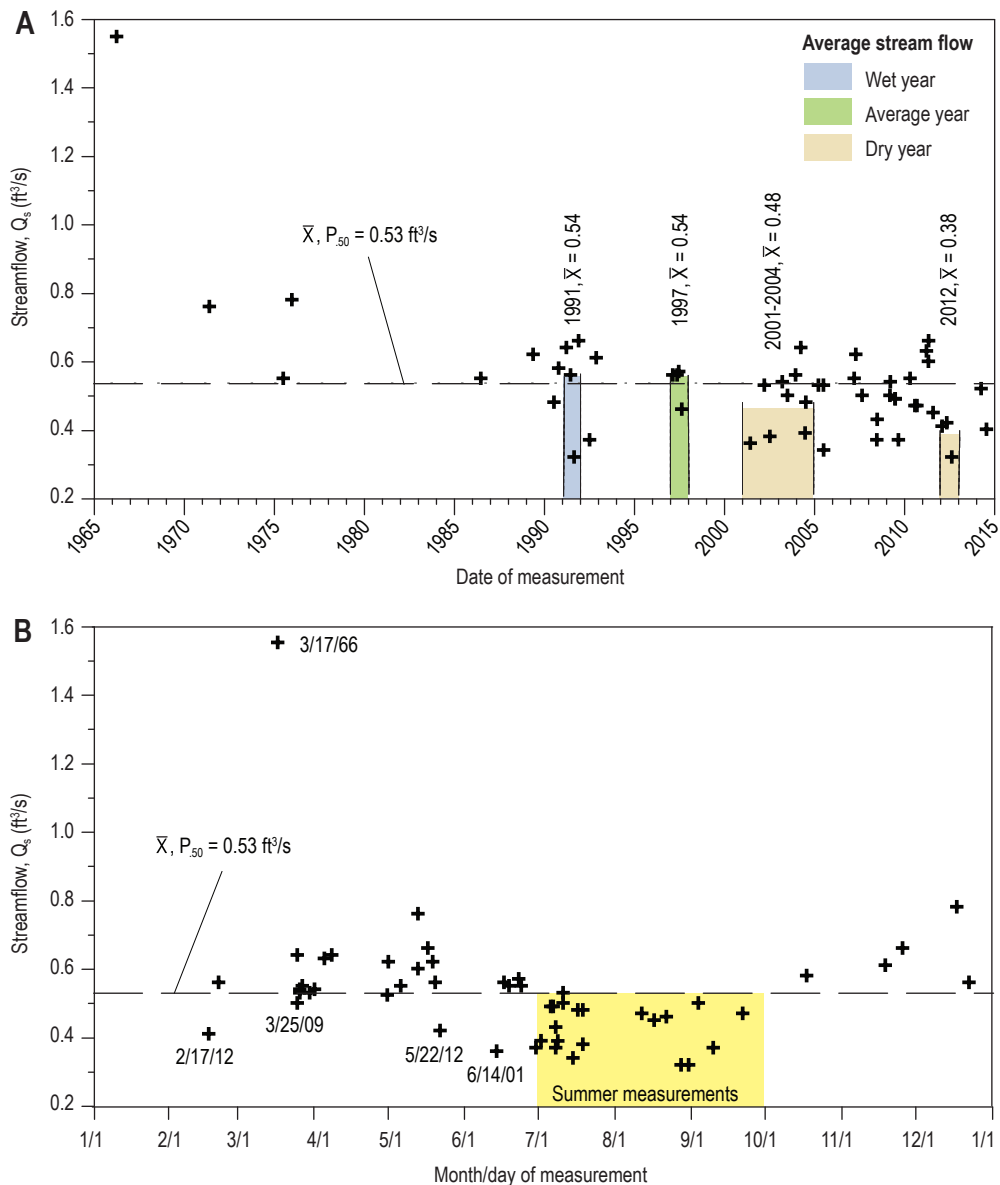


Figure 19. Stream discharge on Cienega Creek near the Acequia de la Cienega head gate, USGS station 08317150, for the period 1966–2014.

A—Streamflow over time illustrates the scatter of the data about the mean and median value of $0.53 \text{ ft}^3/\text{s}$ and highlights a temporal correlation between decreasing annual average streamflow and years with low precipitation. Wet and dry years are defined using annual precipitation in the upper (P_{75}) and lower (P_{25}) quartiles. Annual and period mean discharges are shown for wet and dry intervals. B—Stream discharge plotted by month and day illustrates the seasonal variation in streamflow where discharge is lowest during summer months and generally higher the rest of the year. Data are presented in Table 6. \bar{X} —mean discharge; P_{50} —median discharge.

The small-scale variability in streamflow measurements at the Cienega head gate is primarily associated with seasonal changes in the water balance that occur between summer months (July, August, September) and the remainder of the year. Streamflow drops during the summer, despite a substantial increase in precipitation from the summer monsoon. By considering all inflows and outflows of the wetland water balance (Fig. 15), we can reason that a summer reduction in streamflow results when outflow from ET exceeds inflow from precipitation and groundwater.

Cienega Creek and tributaries

The recent study by NM Hydrologic, LLC and the New Mexico Office of the State Engineer (2012b) provides the only estimates of stream gains and losses by stream reach along Cienega Creek and its tributaries. Streamflow measurements were made in February 2012 at multiple locations on Cienega Creek, Arroyo Hondo, Canorita de las Bacas, Guicu Creek, and Alamo Creek. The study was conducted during a period with minimal evapotranspiration, no irrigation diversions, and minimal precipitation so that baseflow gains and losses could be estimated. Flows in Cienega Creek were monitored to ensure that data were collected during periods of minimal flow variation. The results showed that Cienega Creek streamflow increased in a downstream direction (Table 7, Fig. 18), with gains attributed to tributary inflow as follows:

- Arroyo Hondo, about +0.4 ft³/s
- Cienega Creek above Arroyo Hondo, +0.6 ft³/s
- The Canorita de las Bacas ditch above Mill Pond (which flows through the Leonora Curtin Wetland Preserve and El Rancho de las Golondrinas), about +0.1 to +0.2 ft³/s
- Guicu Creek, about +0.2 to +0.5 ft³/s
- Alamo Creek, about +0.2 ft³/s

There was an additional gain in streamflow between tributaries, particularly along Cienega Creek between Canorita de las Bacas and Guicu Creek (Petronis et al., 2012).

A comparison of recent measurements of streamflow in Cienega and Alamo Creeks by Petronis et al., (2012, p. 51) provides valuable insight regarding surface water outflow from the wetlands, and those data are presented here as a series of bar charts (Fig. 20, Table 7). The figure shows three streamflow measurements in Cienega and Alamo Creeks taken in January 2007, March 2010, and February 2012 together with precipitation in the month of

measurement, in the measurement month plus two previous months (“recent precipitation”), and in the measurement month plus eleven previous months (“annual precipitation”).

Dry winter measurements of streamflow are considered to represent a stream’s baseflow or that part of stream discharge sustained solely by groundwater and not attributable to runoff from precipitation or snow melt nor affected by evapotranspiration. Groundwater discharge and stream baseflow do not remain steady throughout the year or from year to year, rather they vary in response to groundwater development, climatic cycles, and other changes in the water balance. The data presented (Fig. 20, Table 7) are the best available measurements of stream baseflow in Cienega and Alamo Creeks and provide the best estimates of groundwater discharge to streams in the La Cienega wetlands at the times of measurement.

Figure 20 demonstrates that streamflow in Cienega Creek and annual precipitation declined steadily between winter measurements in 2007, 2010, and 2012, while discharge from Alamo Creek remained relatively constant and recent precipitation varied discordantly. The reduction in Cienega Creek streamflow occurred despite an increase in recent precipitation in 2010. The data imply that the aquifer and Cienega Creek may be responding to multi-year drought, but this does not preclude declines in aquifer and stream levels due to other hydrologic factors.

Additional winter flow measurements are reported by Spiegel and Baldwin (1963) for the Santa Fe River above the confluence at La Cieneguilla (December 1951, 0.9 ft³/s) and below the confluence at the Gallegos Ranch (December 1952, 6.5 ft³/s) (Fig. 18). These data allow an estimate of 5.6 ft³/s for the combined flow from Cienega and Alamo Creeks during the early 1950s. However, the Santa Fe River is not a perennial, groundwater-fed stream, and the high variability in the two measurements, made a year apart, make the flow estimate unreliable.

Regional Groundwater Hydrology

Regional water-level maps for the southern Española Basin (Spiegel and Baldwin, 1963; Mourant, 1980; Johnson, 2009) show that groundwater south of the Santa Fe River flows west-southwest through the regional aquifer from the mountain front on the east to discharge areas on the west side of the basin that include the lower Santa Fe River, Cienega Creek and its tributaries (Fig. 21). Studies north of the Santa Fe River (Johnson et al., 2013) demonstrated that

Figure 20. A comparison of recent measurements of streamflow (cubic feet per second, ft³/s) in Cienega and Alamo Creeks during the non-irrigation season, and total precipitation (inches) reported for NOAA station SFCMA during the month of and months preceding flow measurements. The plot illustrates variability in precipitation and stream discharge from the wetlands between three measurement periods—2007, 2010, and 2012—and shows steady declines in Cienega Creek streamflow and annual precipitation. Monthly precipitation data are shown on Figure 17B and summarized in Table 5. Streamflow data are shown in Table 7.

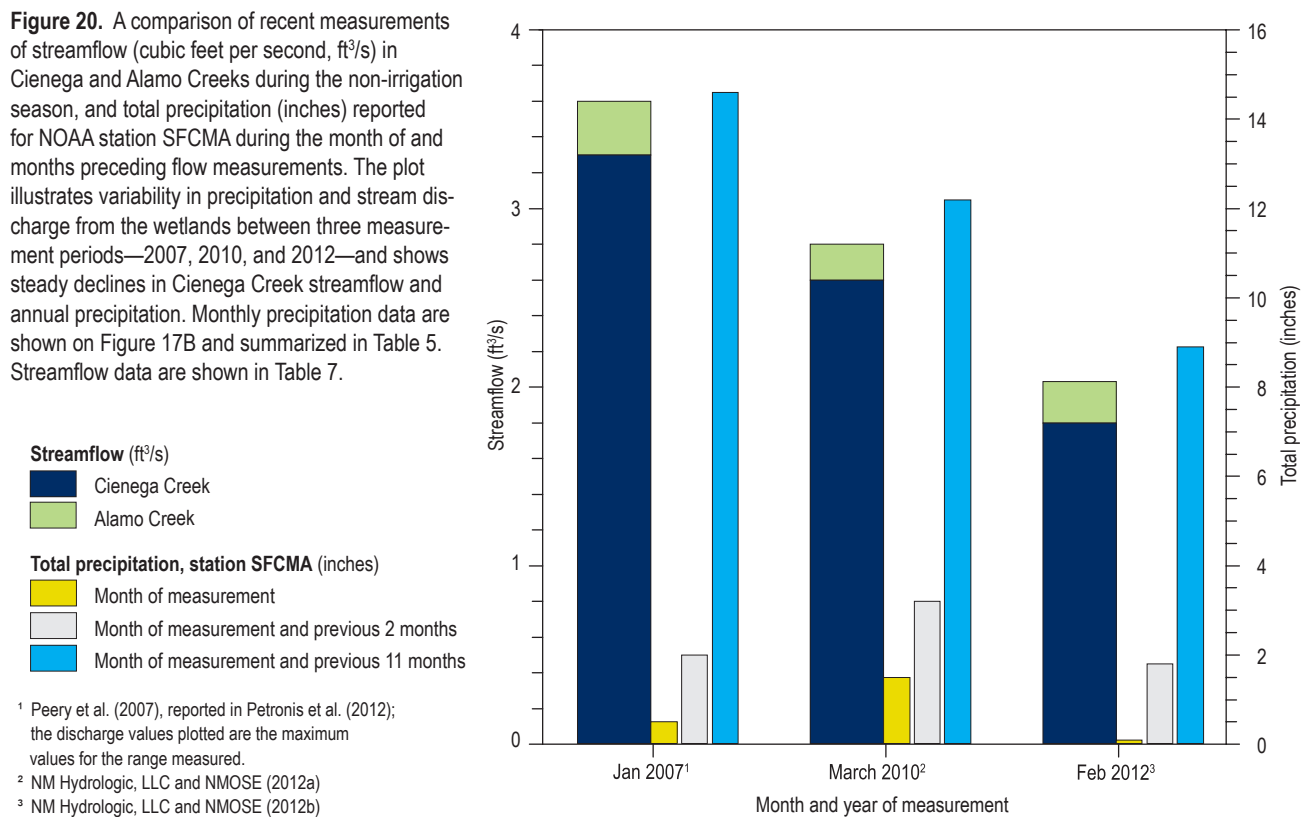


Table 7. Streamflow measurements for Cienega and Alamo Creeks from NM Hydrologic, LLC and the New Mexico Office of the State Engineer (2012a, b). The measurements identify gaining and losing reaches (Fig. 18) and are compared with historical measurements from 2007 (Fig. 20).

Surface water site ID	Site name	UTM easting NAD83	UTM northing NAD83	Date	Measured flow (ft ³ /s)
Cienega Creek and tributaries	CNG 1	400417	3937469	2/17/12	0.41
	HND 1	399805	3937524	2/17/12	0.35
	CNG 2	399851	3937451	2/17/12	0.62
	CNG 3	399607	3937263	2/17/12	0.97
	TAD 1	399616	3937017	2/21/12	0.035
	CNG 4	399348	3936993	2/17/12	1.1
	CLB 1	399490	3936784	2/21/12	0.17
	CNG 5	399165	3936900	2/21/12	1.2
	CAR 1	398998	3937137	nfo	
	GUI 1	398894	3935556	2/22/12	0.41
	GUI 2	397754	3935961	2/22/12	0.52
	CNG 6	397665	3936017	2/22/12	1.5
	CNG 7	397658	3935879	2/22/12	1.7
	CNG 8	395733	3935496	2/22/12	1.8 +
Alamo Creek	CNG 8	395733	3935496	3/26/10	2.6 +
	ALA 1	397009	3933745	2/23/12	ndc
	ALA 2	396261	3934242	2/23/12	0.26
Cienega and Alamo Creeks	ALA 3	395710	3935346	2/23/12	0.23 ^+
	CNG 8 and ALA3			3/26/10	2.8 +
				3/27/10	2.6
				3/28/10	2.4
				3/29/10	2.36

nfo—no flow observed; +—value used in streamflow discharge plotted on Figure 20; ndc—no defined channel; ^—flow computed from average of four observed gage heights

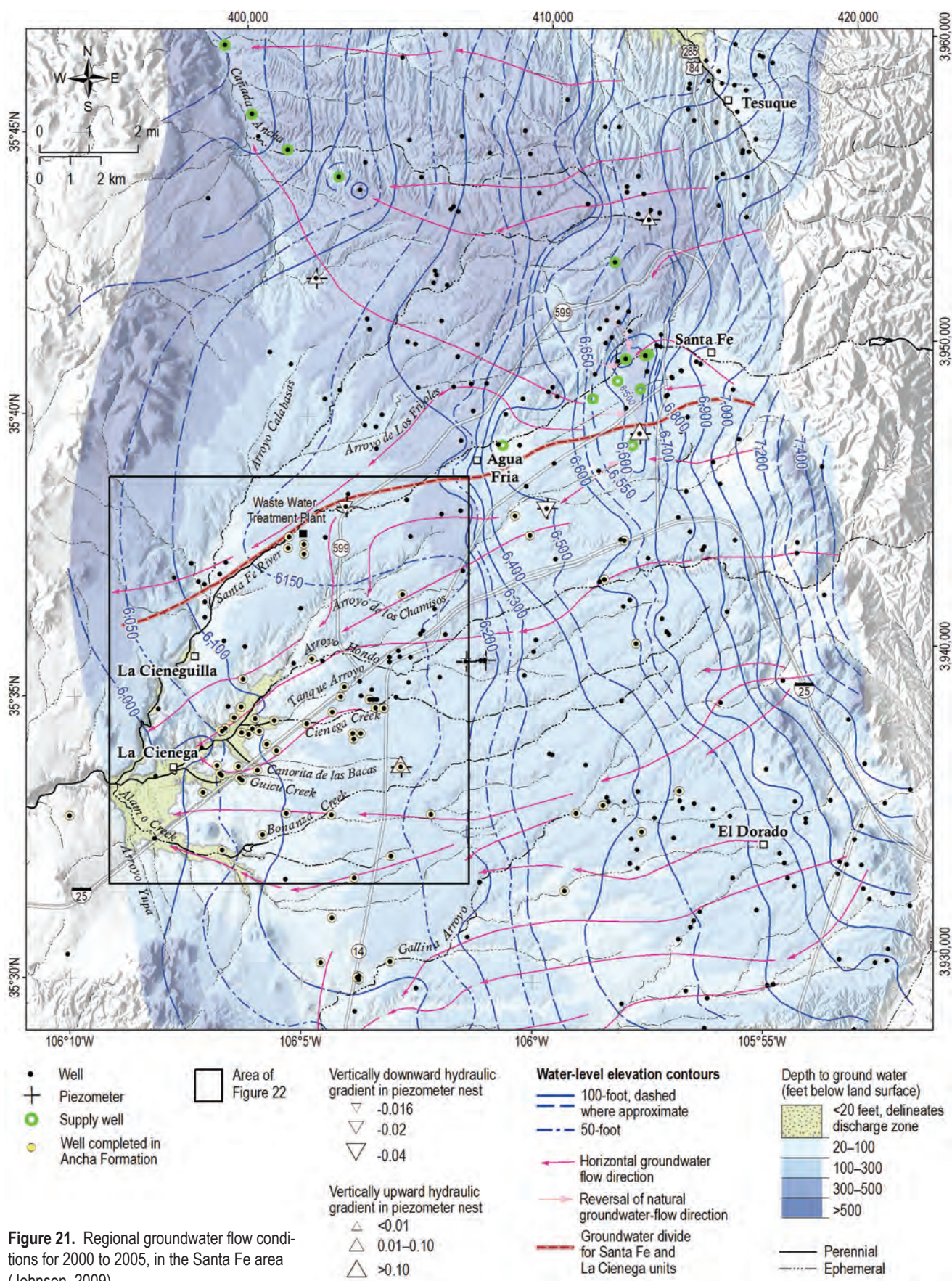


Figure 21. Regional groundwater flow conditions for 2000 to 2005, in the Santa Fe area (Johnson, 2009).

the western half of the basin (west of Agua Fria) is a discharge zone for the regional aquifer that is characterized by upward movement of warm, sodium-rich groundwater from deep within the Tesuque Formation. Groundwater levels in the SFG aquifer vary from less than 20 ft to more than 500 ft, and south of the Santa Fe River they are generally less than 300 ft.

Spiegel and Baldwin (1963) defined three groundwater units in the Santa Fe area—a northern unit north of the Santa Fe River, the Cienega unit, and a southern unit south of Gallina Arroyo—and noted that groundwater in each unit discharges, respectively, to the Rio Grande, the Santa Fe River, and Galisteo Creek. A regional map of 2000–2005 groundwater conditions (Johnson, 2009) also estimated a flow-line boundary roughly coincident with the Santa Fe River that separates the Cienega groundwater unit from the northern (Rio Grande) unit (Fig. 21). By delineating groundwater units we identify discharge zones that contribute groundwater to streams, springs, and wetlands and the recharge areas and flow paths that feed them. Groundwater divides are generally recognized as transient features affected by both pumping and recharge.

Sources of recharge to the SFG aquifer include mountain front and stream channel recharge along the Sangre de Cristo Mountains, small amounts of areal recharge through coarse surface materials, and focused recharge via streambed infiltration along ephemeral channels crossing the basin (Wasiolek, 1995). Focused recharge has been demonstrated by various methods and noted in studies that encompass the Santa Fe River, Arroyo Hondo, and Cañada Ancha (Johnson et al., 2013; Manning, 2009; Moore, 2007; Thomas et al., 2000). Focused recharge beneath the Santa Fe River creates a groundwater mound that extends west from Agua Fria toward the Santa Fe WWTP (Fig. 21). This groundwater high—a product of recharge from streambed infiltration—has been a persistent feature in historic groundwater maps representing 1952 conditions (Spiegel and Baldwin, 1963), 1977 conditions (Mourant, 1980), and 2000–2005 conditions (Johnson, 2009). The modern shape and extent of the recharge mound may be affected by discharge from the WWTP, which has been functioning since the early 1960s. Spiegel (1963, p. 152) proposed that surface drainage from the river probably provides some recharge to the La Cienega groundwater unit. The groundwater map of Johnson (2009) supports a similar interpretation.

Groundwater Hydrology in the La Cienega Area

A local groundwater map (Fig. 22) for the La Cienega area was constructed with 20-foot contours to enhance resolution of the groundwater surface in the vicinity of the wetlands. When combined with other hydrologic and geologic data, the local groundwater map provides basic information for understanding the shallow Santa Fe Group aquifer and its connection to springs and wetlands. Water-table elevations drop from 6,180 ft on the east to less than 5,860 ft at the confluence of Cienega Creek and the Santa Fe River. The direction of groundwater flow is perpendicular to the water-table contours, assuming that the aquifer is horizontally isotropic.

The water-table map indicates that groundwater enters the study area from the east and north, and flows southwest toward Cienega Creek. Flow directions vary locally where the groundwater surface is affected by stream interactions, stream incision, local topography, and changes in aquifer transmissivity. Southwest of the Rancho Viejo hinge zone (Figs. 10, 22), the basin sediments thin and aquifer thickness is dramatically reduced, forcing groundwater to discharge at streams, springs and wetlands. The mixing of deep and shallow groundwater sources, common in discharge zones, is evaluated with chemical methods in the next chapter.

Colored arrows in Figure 22 illustrate general groundwater flow direction and discharge to: 1) Cienega Creek, Arroyo Hondo and Guicu Creek (green arrows); 2) the Rio Grande and Santa Fe River (orange arrows); and 3) Alamo and Bonanza Creeks (tan arrows). Discharge to a gaining stream reach is indicated by upstream deflection of groundwater elevation contours; recharge from a losing stream is shown by downstream deflection of contours. Gaining reaches identified from the groundwater map include: 1) Cienega Creek from highway 14 to its confluence with the Santa Fe River; 2) Arroyo Hondo above its confluence with Cienega Creek; 3) Guicu Creek and Canorita de las Bacas west of I-25; and 4) the Santa Fe River at and below La Cieneguilla. Gaining reaches identified on Figure 22 are consistent with those defined through streamflow measurements by NM Hydrologic, LLC and the New Mexico Office of the State Engineer (2012a, b).

Similar to historic maps (Spiegel and Baldwin, 1963; Mourant, 1980; Johnson, 2009), the

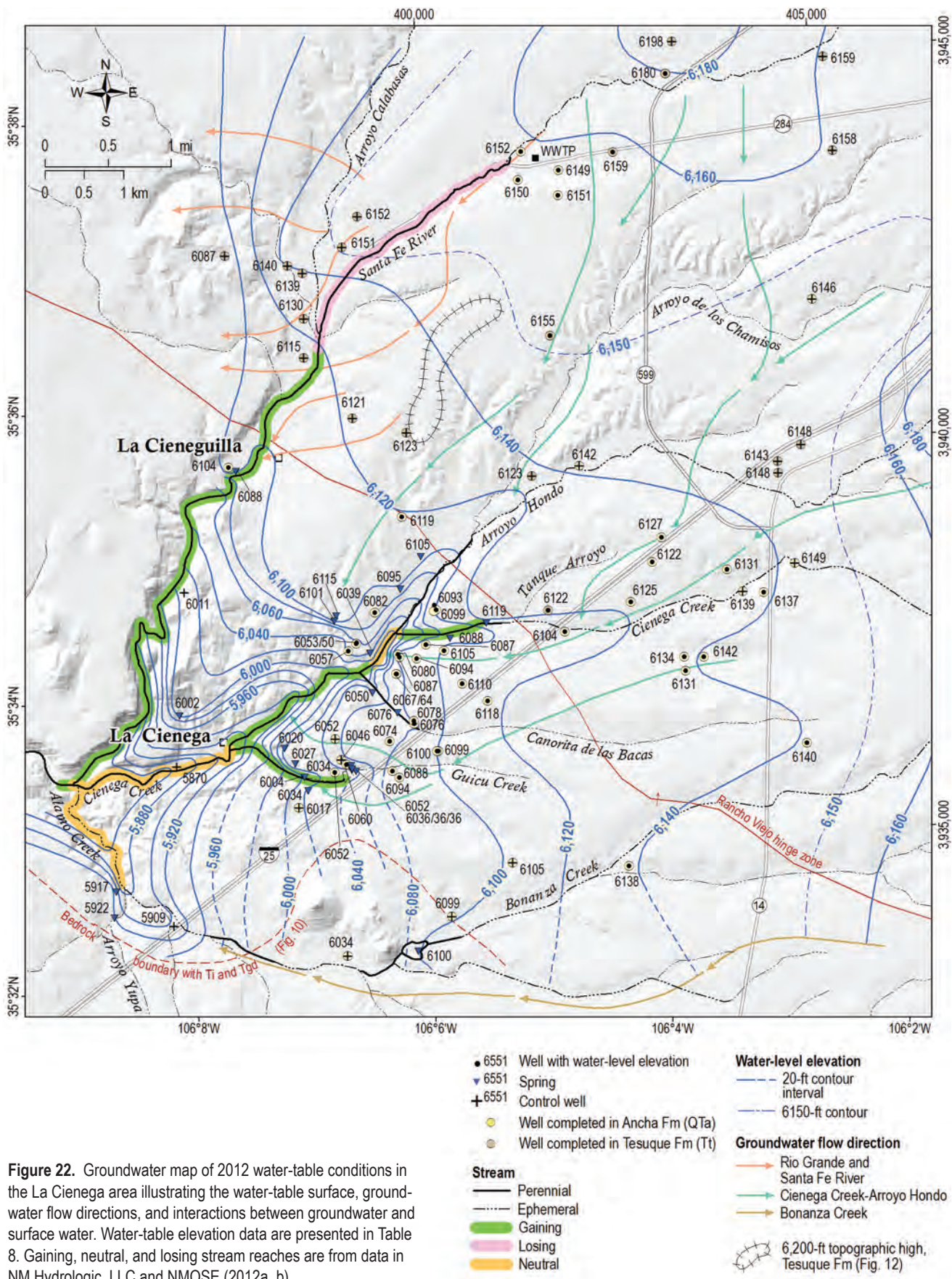


Figure 22. Groundwater map of 2012 water-table conditions in the La Cienega area illustrating the water-table surface, groundwater flow directions, and interactions between groundwater and surface water. Water-table elevation data are presented in Table 8. Gaining, neutral, and losing stream reaches are from data in NM Hydrologic, LLC and NMOSE (2012a, b).

groundwater map of 2012 conditions delineates a sizeable recharge mound beneath the Santa Fe River that extends from Agua Fria to approximately the river's confluence with Arroyo Calabasas (Fig. 22). The Santa Fe River channel is ephemeral upstream of the WWTP. Groundwater highs also exist beneath some reaches of Arroyo de los Chamisos and Arroyo Hondo. Groundwater from the eastern part of the Santa Fe River recharge mound (upstream of the WWTP) flows south-southwest toward seeps and springs along Arroyo Hondo. Groundwater from the recharge mound downstream of the WWTP flows west toward the Rio Grande and southwest along the Santa Fe River canyon. Groundwater flow appears to diverge at the paleotopographic high on the Tesuque Formation east of La Cieneguilla (Figs. 22, 12) where low permeability sediments in lithosome S of the Tesuque Formation may impede and deflect flow. Ancha Formation sediments that overlie the high Tesuque surface are entirely above the water table and the coarse deposits are unsaturated (Fig. 14).

Groundwater discharge to wetlands and springs

Springs, seeps, and phreatophytic vegetation are sustained in the valleys of Cienega Creek and its tributaries by groundwater discharge from the

Tesuque and Ancha Formations (Spiegel, 1975). A conceptual illustration of wetlands as natural groundwater discharge areas is shown in Figure 23. Groundwater-fed wetlands adjacent to streams and saturated slope and hillside wetlands cover 384 acres in the La Cienega area (Dick, 2012) (Fig. 14). Where springs and wetlands are fed from multiple aquifer zones, waters from the different sources and depths mix in the discharge area.

The persistence, size, and function of wetlands are controlled by hydrologic processes expressed in the wetland water balance (Carter, 1996). The preservation of groundwater-fed wetlands requires a relatively stable influx of groundwater throughout changing seasonal and annual climatic cycles. Stable groundwater levels are important in maintaining physical and chemical conditions in the root zone that promote healthy and stable growth of wetland plants (Hunt et al., 1999). A decline in groundwater inflow (recharge) or increase in groundwater outflow (discharge)—due, for example, to groundwater depletion, drought, altered recharge patterns, or increased ET—can lead to reductions and disruptions in spring flow, or elimination of springs and wetlands altogether. Characterizing groundwater discharge and storage is difficult, but understanding the water balance and its relation to climate, groundwater depletion, and other environmental factors is critical to

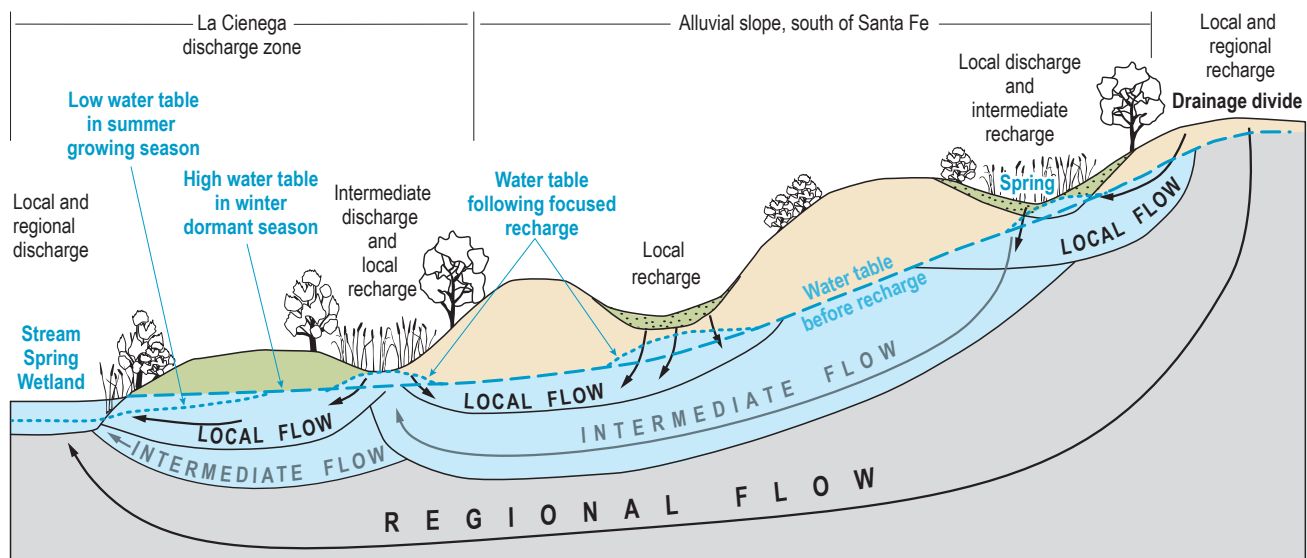


Figure 23. Conceptual illustration of groundwater-fed wetlands. In La Cienega, groundwater discharges to wetlands from a complex system of local, intermediate and regional flow paths. Regional groundwater is recharged at the major regional topographic high (the Sangre de Cristo Mountains) and discharged at the major regional topographic lows (La Cienega, the Santa Fe River, and the Rio Grande). Local recharge is focused beneath ephemeral tributary channels and depressions in the land surface where the unsaturated zone is relatively thin. In wetlands and riparian zones, evaporation from open water and saturated soils and transpiration from plants (evapotranspiration, ET) draws water from near the surface and can cause a water-table depression similar to a pumping well. In wetlands discharging groundwater from multiple systems, waters from the different sources often mix. Figure is modified for the La Cienega area from Carter (1996).

wetland conservation and restoration. Investigations of groundwater sources feeding the wetlands, the natural range in fluctuations of the water table, and potential impacts to groundwater inflow and storage are important aspects of wetland studies.

Groundwater fluctuations in wetlands

Groundwater fluctuations are controlled by the balance between recharge to, storage in, and discharge from an aquifer. A change in groundwater recharge or discharge alters the amount of groundwater in storage. These changes are reflected in fluctuations of the water-table surface and documented by measuring groundwater levels over time. The primary factors affecting groundwater fluctuations are: 1) the timing, location and amount of recharge from precipitation and surface-water seepage; and 2) groundwater discharge through evapotranspiration and pumping. A change in groundwater discharge to wetlands is a reflection of changes in the water balance. When the rate of recharge to an aquifer exceeds the rate of discharge, groundwater storage increases and water levels rise. When the rate of groundwater discharge and withdrawal exceeds the rate of recharge, then aquifer storage is depleted and water levels decline.

Water levels in most shallow, unconfined aquifers follow a natural, seasonal fluctuation, typically rising during the winter and spring due to greater precipitation and recharge and/or lower ET, then declining from early summer to fall when ET exceeds recharge (Taylor and Alley, 2001). This seasonal pattern, driven by changes in precipitation and ET, is common in wetland areas (Carter, 1996). The magnitude of seasonal fluctuations in water levels can also vary from year to year in response to varying climatic conditions and the consequent effects on ET, surface flow, and groundwater storage. Changes in groundwater recharge and storage caused by climate variability commonly occur over years to decades and groundwater levels generally have a delayed response to the cumulative effects of long-term drought (Taylor and Alley, 2001).

Wetlands can be quite sensitive to the effects of groundwater pumping, which progressively lowers the water table and increases the magnitude of seasonal changes in groundwater levels (Alley et al., 1999). The amplitude and frequency of seasonal water-level fluctuations affect wetland characteristics such as the type of vegetation, fish, and bird species present (Carter, 1996). The combined effects of pumping and seasonal fluctuations complicate

water-level changes and discharge patterns and perturb the natural seasonal and annual cycles of wetlands (Alley et al., 1999, p. 42). In the La Cienega area, we studied seasonal, short-term, and long-term changes in water levels in the shallow aquifer surrounding the wetlands.

Seasonal water-level fluctuations and evapotranspiration (ET)—Seasonal groundwater fluctuations in the Cienega Creek valley were first evaluated using repeat water-level measurements in 37 shallow wells between the summer-fall of 2011 and the winter (February) of 2012. Results show that water levels rose during the winter throughout the wetland area by +0.04 to +6.60 ft, while declining by -0.04 to -0.50 ft in wells outside of wetlands during the same time period (Fig. 24A, Table 8). Seasonal water-level variations characterized by a summer drop are common in wetland aquifers and reflect a change in evapotranspiration that occurs between growing and dormant seasons (Carter, 1996; Vincke and Thiry, 2008) (Fig. 23).

The timing and magnitude of groundwater fluctuations in the wetlands were further examined by continuous water-level measurements in two wetland wells (Fig. 25). Well LC-025, an 18-ft PVC-cased piezometer, is located in a riparian zone of the Leonora Curtin Wetland Preserve in Cañorita de las Bacas east of Cienega Creek (Fig. 26A). Well EB-306, a 43-ft steel-cased well, is located in a dry grassy upland roughly 900 ft west of the confluence of Cienega Creek and Arroyo Hondo (Fig. 26B). Seasonal water-table fluctuations occurred in both wells between October 2011 and March 2014 (Fig. 25), but the largest variations are seen in LC-025. Groundwater levels were low (12–12.8 ft bls) between late June and early October during the growing season. Groundwater highs (8.1 ft bls in 2012, 8.5 ft bls in 2013) were recorded in March of each year following winter recharge of the wetland aquifer. The maximum recorded seasonal variations were 4.93 ft in 2012 and 4.52 ft in 2013. Well EB-306 presents a similar seasonal fluctuation with significantly reduced magnitudes (1.11 ft in 2012 and 0.60 ft in 2013). The seasonal water-level cycle in shallow wetland wells is driven by discharge from ET.

The hydrographs also show large, episodic late-summer fluctuations that demonstrate recharge from precipitation and small daily fluctuations related to ET. The LC-025 hydrograph recorded a nearly six-foot rise in water level within a 12-hour period on September 15, 2103 in response to a two-inch rain

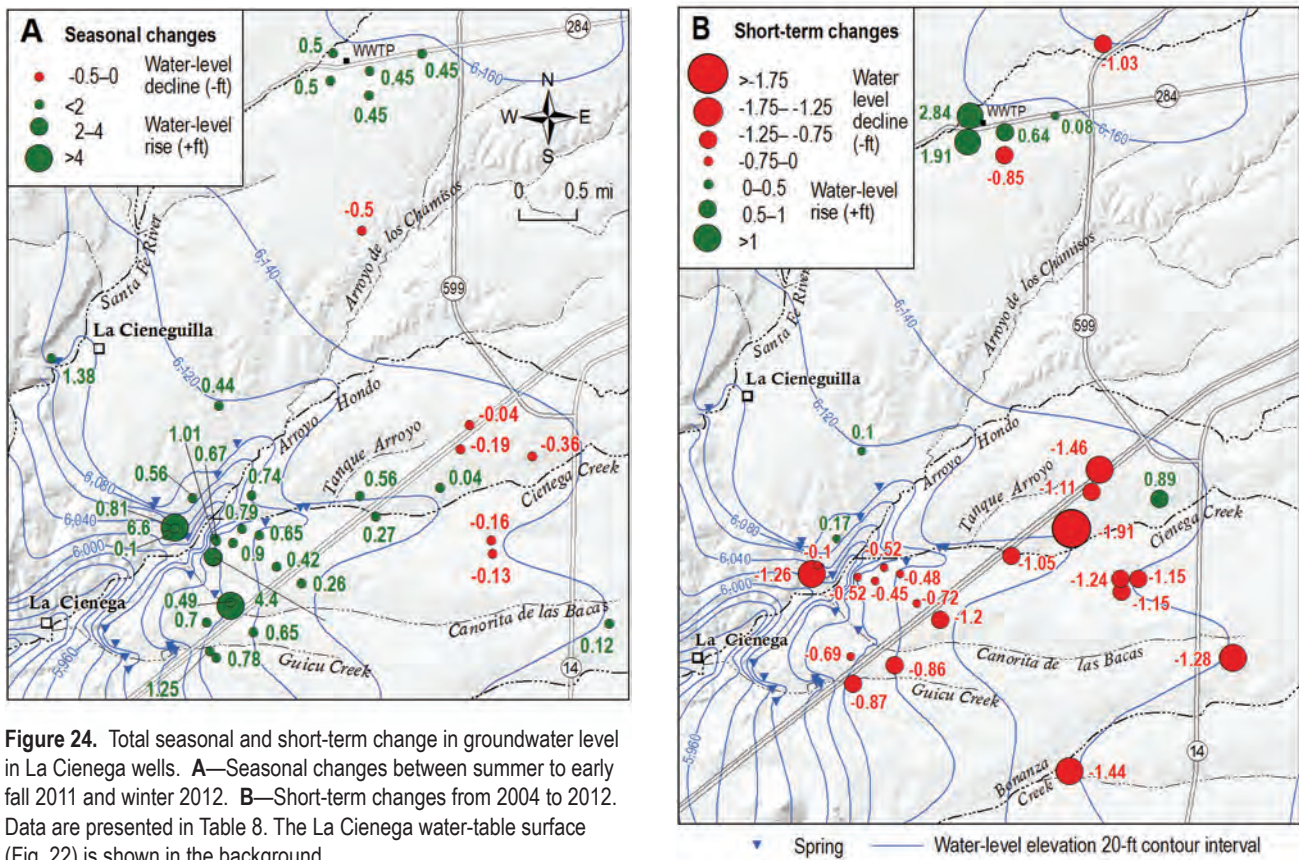


Figure 24. Total seasonal and short-term change in groundwater level in La Cienega wells. **A**—Seasonal changes between summer to early fall 2011 and winter 2012. **B**—Short-term changes from 2004 to 2012. Data are presented in Table 8. The La Cienega water-table surface (Fig. 22) is shown in the background.

event. Water levels remained high in this well (~7.4 ft bls, Fig. 25) through at least February of 2014. Daily and episodic fluctuations are discussed further in following sections.

Diurnal water-table fluctuations and evapotranspiration (ET)—Unconfined aquifers with groundwater near land surface frequently exhibit daily fluctuations that are attributed to evaporation and/or transpiration. Both processes cause a discharge of groundwater into the atmosphere and have nearly the same diurnal variation because of their correlation with temperature (Todd and Mays, 2005). Evaporation from groundwater increases as the water table approaches ground surface. For water tables within one meter of the surface, evaporation is largely controlled by atmospheric conditions (temperature, humidity, and wind). Below one meter, soil properties limit evaporation and the rate decreases significantly with depth (Todd and Mays, 2005). Transpiration occurs where the root zone of vegetation reaches saturated sediment and represents the uptake of groundwater by roots (Todd and Mays, 2005).

In a diurnal fluctuation pattern associated with ET, the shallow aquifer reacts as if a pumping well

is turned on in the morning and turned off in the evening. In response, the water table drops during the day when transpiration is at its highest and rises at night when ET is minimal. The maximum water level occurs in midmorning. From then until early evening ET losses exceed recharge from the adjacent aquifer, and water levels fall. The highest ET discharge is associated with the highest temperatures near midday. The minimum water level occurs in the evening. Thereafter, water levels rise through the night when recharge from the adjacent aquifer exceeds discharge from ET (Todd and Mays, 2005). Numerous studies have noted diurnal trends in groundwater levels in shallow aquifers and related them to evapotranspiration (Dolan et al., 1984; Healy and Cook, 2002; Hays, 2003; Loheide II et al., 2005; Nachabe et al., 2005; Vincke and Thiry, 2008).

Diurnal water-table fluctuations occur concurrently with seasonal changes in water level, and both usually begin with the appearance of foliage and cease after killing frosts (Todd and Mays, 2005). In 2012, both seasonal and diurnal water-table fluctuations in LC-025 (Fig. 25) followed this pattern. The spring water-table drop in LC-025 began in early April and coincided with the onset of a diurnal

Table 8. Water-level data for 2012 groundwater conditions (Fig. 22), and seasonal and short-term changes in depth to water in La Cienega wells (Fig. 24). Control wells with published water-level data from 1997–2007 (Johnson, 2009; NMGBMR, 2008) were used to fill data gaps and provide water-table control near study-area boundaries in Figure 22—Continued.

Site ID	Site type	MOST RECENT WATER LEVEL (USED FOR 2012 CONDITIONS)			SEASONAL CHANGE (SUMMER-FALL 2011 TO WINTER 2012)				SHORT-TERM CHANGE (~2004 TO 2012)			
		Date measured	Water depth (ft bsl)	Water depth elevation (ft asl)*	Date measured	Water depth (ft bsl)	Water depth elevation (ft asl)	Change in depth (ft) from 2011 to 2012	Date measured	Water depth (ft bsl)	Water depth elevation (ft asl)	Change in depth (ft) from ~2004 to 2012
EB-001	controlwell	1/9/2004	48.41	6016.58								
EB-002	controlwell	2/27/2004	26.95	6045.80								
EB-019	well	2/14/2012	44.20	6099.19	10/5/2011	44.85	6098.54	0.65	3/23/2004	43.34	6100.05	-0.86
EB-102	well	1/12/2012	61.79	6137.69					3/31/2004	60.35	6139.13	-1.44
EB-130	controlwell	3/24/2004	181.90	6142.51								
EB-132	well	2/15/2012	68.28	6110.29	10/5/2011	68.70	6109.87	0.42	2/10/2004	67.56	6111.01	-0.72
EB-172	controlwell	5/18/2007	303.50	6158.02								
EB-219	controlwell	5/30/2005	65.50	6152.00								
EB-220	well	2/14/2012	132.86	6126.63	9/12/2011	132.82	6126.67	-0.04	2/18/2004	131.40	6128.09	-1.46
EB-221	controlwell	5/18/2007	103.85	6139.43								
EB-222	well	1/13/2012	132.00	6137.83								
EB-223	well	2/15/2012	46.21	6119.20	7/21/2011	46.65	6118.76	0.44	2/11/2004	46.31	6119.10	0.10
EB-301	controlwell	1/9/2004	20.93	5870.18								
EB-302	spring	2/11/2004		6002.42								
EB-303	well	2/14/2012	23.49	6098.68	10/6/2011	24.23	6097.94	0.74				
EB-304	well	2/14/2012	14.85	6086.55	10/6/2011	15.64	6085.76	0.79	1/9/2004	14.33	6087.07	-0.52
EB-305	well	2/14/2012	22.65	6104.74	10/6/2011	23.30	6104.09	0.65	1/9/2004	22.17	6105.22	-0.48
EB-306	well	2/14/2012	19.23	6082.35	10/6/2011	19.79	6081.79	0.56	2/10/2004	19.40	6082.18	0.17
EB-309	controlwell	2/11/2004	106.50	6123.06								
EB-310	controlwell	2/11/2004	38.07	6142.14								
EB-312	well	2/15/2012	61.45	6117.95	10/5/2011	61.71	6117.69	0.26	2/10/2004	60.25	6119.15	-1.20
EB-313	well	2/15/2012	21.23	6053.20	10/5/2011	22.04	6052.39	0.81	2/10/2004	21.13	6053.30	-0.10
EB-314	well	2/15/2012	3.60	6056.50	10/5/2011	3.70	6056.40	0.10	2/10/2004	2.34	6057.76	-1.26
EB-315	well	2/15/2012	20.36	6093.52	10/5/2011	21.26	6092.62	0.90	2/10/2004	19.91	6093.97	-0.45
EB-316	well	2/15/2012	6.02	6085.21	10/5/2011	7.03	6084.20	1.01	2/10/2004	5.50	6085.73	-0.52
EB-321	well	2/15/2012	132.00	6131.09	10/5/2011	131.64	6131.45	-0.36	2/20/2004	132.89	6130.20	0.89
EB-323	controlwell	2/21/2004	30.00	6008.52								
EB-324	controlwell	5/21/1997	40.00	6130.14								
EB-325	controlwell	5/18/1997	35.00	6114.93								
EB-326	controlwell	6/28/2005	49.41	6151.25								
EB-327	controlwell	3/26/2004	49.25	6139.02								
EB-328	controlwell	6/7/2005	286.26	6085.66								
EB-329	controlwell	5/11/2005	90.73	6121.11								
EB-330	well	10/5/2011	8.63	6059.68								
EB-331	controlwell	2/27/2004	52.06	6052.22								
EB-332	well	2/14/2012	8.47	6087.50	7/21/2011	9.72	6086.25	1.25	2/27/2004	7.60	6088.37	-0.87
EB-333	well	2/14/2012	26.14	6095.89	10/5/2011	26.92	6095.11	0.78				
EB-334	well	2/15/2012	39.47	6104.35	10/5/2011	39.74	6104.08	0.27	2/27/2004	38.42	6105.40	-1.05
EB-335	well	2/14/2012	86.91	6125.42	7/21/2011	86.95	6125.38	0.04	2/27/2004	85.00	6127.33	-1.91
EB-338	well	3/29/2012	186.44	6180.03					1/20/2005	185.41	6181.06	-1.03
EB-339	well	2/15/2012	137.64	6121.63	10/5/2011	137.45	6121.82	-0.19	4/29/2004	136.53	6122.74	-1.11
EB-340	well	2/15/2012	52.22	6074.05	10/5/2011	52.92	6073.35	0.70	4/29/2004	51.53	6074.74	-0.69
EB-361	controlwell	6/8/2005	287.00	6158.51								
EB-362	well	2/14/2012	129.60	6150.45	10/20/2011	130.10	6149.95	0.50	6/10/2004	131.51	6148.54	1.91
EB-363	well	2/14/2012	145.15	6149.38	10/20/2011	145.60	6148.93	0.45	6/10/2004	145.79	6148.74	0.64
EB-364	well	2/14/2012	178.55	6158.76	10/20/2011	179.00	6158.31	0.45	6/10/2004	178.63	6158.68	0.08
EB-365	well	2/14/2012	119.10	6151.66	10/20/2011	119.60	6151.16	0.50	6/10/2004	121.94	6148.82	2.84
EB-366	well	2/14/2012	188.75	6150.95	10/20/2011	189.20	6150.50	0.45	6/10/2004	187.90	6151.80	-0.85
EB-373	well	2/14/2012	118.50	6154.94	10/20/2011	118.00	6155.44	-0.50				

Table 8. Water-level data for 2012 groundwater conditions (Fig. 22), and seasonal and short-term changes in depth to water in La Cienega wells (Fig. 24). Control wells with published water-level data from 1997–2007 (Johnson, 2009; NMGBMR, 2008) were used to fill data gaps and provide water-table control near study-area boundaries in Figure 22—Continued.

Site ID	Site type	MOST RECENT WATER LEVEL (USED FOR 2012 CONDITIONS)			SEASONAL CHANGE (SUMMER-FALL 2011 TO WINTER 2012)				SHORT-TERM CHANGE (~2004 TO 2012)			
		Date measured	Water depth (ft bsl)	Water depth elevation (ft asl)*	Date measured	Water depth (ft bsl)	Water depth elevation (ft asl)	Change in depth (ft) from 2011 to 2012	Date measured	Water depth (ft bsl)	Water depth elevation (ft asl)	Change in depth (ft) from ~2004 to 2012
EB-377	controlwell	6/24/2004	12.65	6034.43								
EB-378	controlwell	6/24/2004	25.15	6098.93								
EB-379	controlwell	6/24/2004	101.44	6104.70								
EB-382	controlwell	6/24/2004	186.28	6147.76								
EB-387	well	3/17/2012	100.23	6142.04								
EB-388	well	3/17/2012	90.41	6133.83	8/11/2011	90.25	6133.99	-0.16	1/1/2003	99.08	6143.19	-1.15
EB-389	well	3/17/2012	110.40	6130.87	8/11/2011	110.27	6131.00	-0.13	1/1/2003	89.17	6135.07	-1.24
EB-391	controlwell	7/11/2004	158.40	6147.68					1/1/2003	109.25	6132.02	-1.15
EB-392	controlwell	7/15/2004	125.21	6148.65								
EB-407	controlwell	3/23/2004	217.60	6146.25								
EB-509	controlwell	3/24/2005	47.59	5908.63								
EB-579	controlwell	5/30/2005	57.00	6140.24								
EB-607	well	1/5/2012	199.68	6140.09	8/19/2011	199.80	6139.97	0.12	6/30/2005	198.40	6141.37	-1.28
EB-624	spring			6099.48								
EB-671	controlwell	5/1/2007	195.00	6197.79								
EB-672	controlwell	9/10/2005	34.70	6123.35								
EB-691	well	5/24/2012	23.63	6092.82								
LC-001	spring			6036.27								
LC-002	spring			6004.07								
LC-003	spring			6020.22								
LC-004	spring			6027.17								
LC-005	spring			6119.45								
LC-006	well	2/14/2012	7.64	6103.97	8/13/2011	9.02	6102.59	1.38				
LC-007	spring			6039.02								
LC-008	spring			6050.49								
LC-009	well	2/15/2012	14.98	6066.96	10/5/2011	17.56	6064.38	2.58				
LC-010	well	2/15/2012	15.83	6086.64	10/5/2011	16.50	6085.97	0.67				
LC-011	well	2/15/2012	25.06	6050.17	10/5/2011	31.66	6043.57	6.60				
LC-012	spring			6076.34								
LC-015	spring			6115.17								
LC-016	spring			6095.31								
LC-017	spring			6052.11								
LC-018	spring			6036.27								
LC-019	spring			6036.27								
LC-020	spring			6033.75								
LC-021	spring			6087.95								
LC-022	spring			6087.97								
LC-023	spring			6104.59								
LC-024	spring			6100.77								
LC-025	well	2/16/2012	8.40	6076.09	10/4/2011	12.80	6071.69	4.40				
LC-026	well	2/15/2012	7.16	6077.84	10/4/2011	7.65	6077.35	0.49				
LC-027	well	2/14/2012	40.34	6122.49	10/4/2011	40.90	6121.93	0.56				
LC-028	well	2/15/2012	12.72	6067.45	10/5/2011	15.14	6065.03	2.42				
LC-029	well	10/5/2011	44.94	6100.31								
LC-030	well	2/15/2012	9.71	6034.37								
LC-031	spring			5917.00								
LC-032	spring			5922.00								

*—Water depth elevation used for water table map (Fig. 21), bsl—below land surface, asl—above sea level

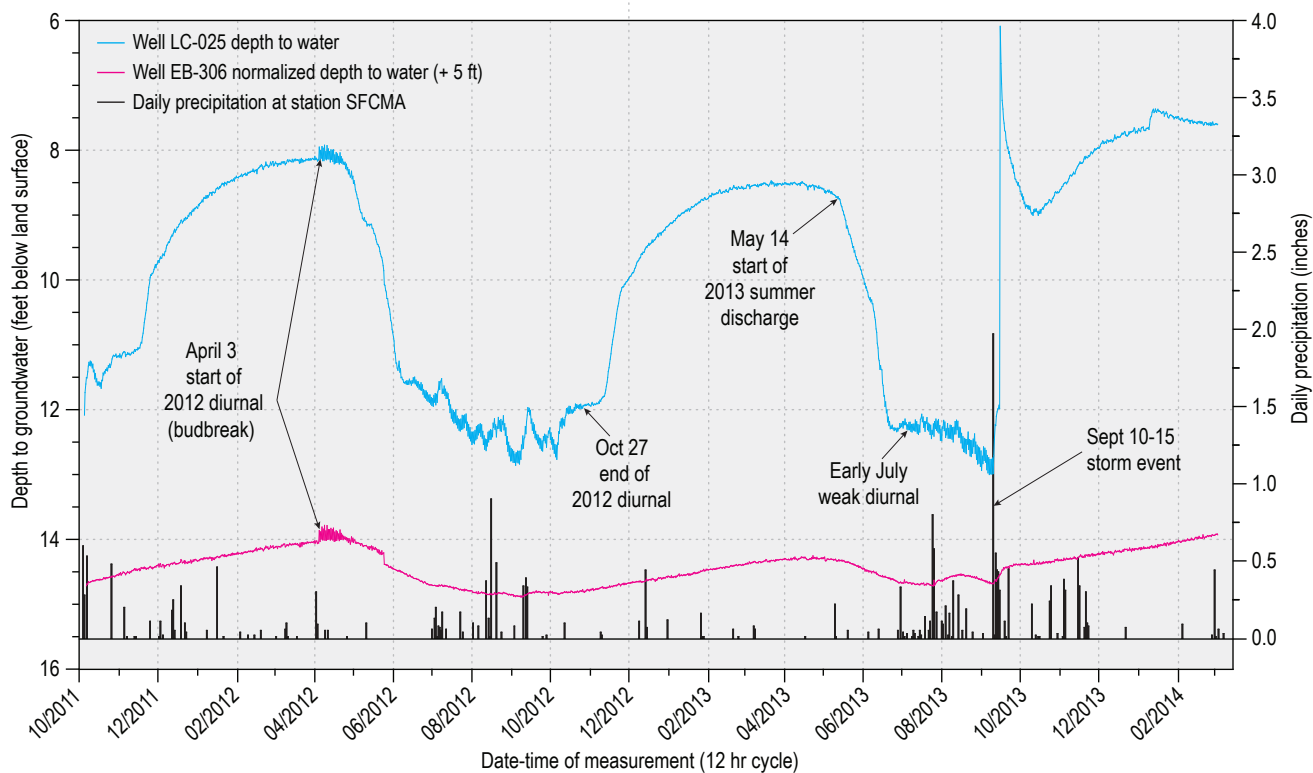


Figure 25. Hydrographs of 12-hour water-table fluctuations in two wetland wells (LC-025 and EB-306) for the period October 2011 to March 2014. Daily precipitation from NOAA Station SFCMA (vertical bars) is shown on the right Y-axis. See Figure 26 for well locations. Continuous water-level data are in Appendix 1.

fluctuation in the range of 0.1–0.2 feet. The diurnal signal continued through the growing season when the water table was low, waned in late September, and ended in late October (Fig. 25). The end of the diurnal was followed closely by a winter water-table rise as recharge from the surrounding aquifer filled the groundwater depression left by a season of ET discharge.

In contrast, the 2013 season presented a significantly different pattern of water-table fluctuations starting with lower groundwater levels at the winter's end. The data (Appendix 1, Fig. 25) clearly show that the onset of the spring water-level drop, which is one indicator of wetland ET, began about May 14, six weeks later than occurred in the previous season. Furthermore, no stable diurnal fluctuation developed until early July, following a June 30 rain event. The presence and strength of the diurnal fluctuation is directly related to many factors, including: 1) depth of the water table; 2) type of vegetation; 3) rate of foliage growth; 4) the season; 5) the weather; and 6) the amount of soil moisture available to meet the transpiration demand. For example, hot windy days produce maximum drawdowns, whereas cool, cloudy days show only small variations (Todd and

May, 2005). Late onset of ET discharge and lack of a stable diurnal fluctuation until late June 2013 indicates that the transpiration demand in the vicinity of LC-025 was either absent, severely weakened, or being met by soil moisture as opposed to groundwater. However, since spring 2013 followed more than two years of severe drought and record low rainfall in 2012, the abnormalities in ET demand were likely caused by a combination of low winter water levels and weather- or drought-related factors.

Some ET studies have investigated water-table fluctuations as a way to measure plant water use (White, 1932; Heikurainen, 1963; Rosenberry and Winter, 1997). An ET study by Vincke and Thiry (2008) applied the water-table fluctuation (WTF) method with a 30-minute measurement frequency and noted a diurnal fluctuation of 0.11–0.15 ft (3.3–4.7 cm) with a high water level at about 10:00 hours and a low water level at 21:00 to 22:00 hours (Vincke and Thiry, 2008). The diurnal fluctuations in LC-025 were depicted with a 12-hour measurement cycle (00:00 and 12:00 hours) that probably does not capture the timing or full magnitude of the diurnal signal. A higher measurement frequency applied at the LC-025 site would better define the diurnal

fluctuation. The large summer water-level drops at LC-025 (-4.93 ft in 2012) indicate that evapotranspiration is a significant part of the seasonal water balance in the wetland riparian zone. By expanding the wetland monitoring well network, and applying higher frequency water-level measurements to more clearly define diurnal variations in the water table, the WFT method could help quantify the ET component of the wetland water budget.

Short-term water-level changes—Water-level records covering months to years are important for monitoring groundwater and surface-water interactions, the effects of natural variability in precipitation and recharge, and trends in groundwater storage and depletion (Taylor and Alley, 2001; Konikow, 2015). Short-term changes in the water table near wetlands were evaluated by comparing water levels from 29 shallow wells measured in 2004 with repeat measurements in the same wells during winter 2012. Results show a consistent drop in water levels throughout the La Cienega area over the eight-year period (Fig. 24B, Table 8). Water levels declined in most (76%) wells, with the largest drops located east (up-gradient) of the La Cienega wetlands and at the Ranchos de los Golondrinas. Declines ranged from -1.9 to -0.10 ft, and averaged -1.0 ft. These water-level declines, based on winter-to-winter

measurements, do not relate to seasonal variations. The 2004–2012 drop could have been aggravated by severe drought conditions in 2011–2012, but it is difficult to explain entirely by drought as annual precipitation was near or above the post-1998 average from 2004–2010 (Fig. 17A, Table 5). This short-term depletion in aquifer storage is consistent with the long-term trends in groundwater declines discussed in the following section.

Locally, water levels rose from +0.08 to +2.84 feet in several shallow wells near the WWTP, near Arroyo Hondo north of El Rancho de las Golondrinas, and near Cienega Creek east of Interstate 25. As noted by Spiegel (1975), the water-table rise near the WWTP (average +0.95 ft) likely reflects channel recharge from WWTP outflow and the Santa Fe River. The water-table rise near Cienega Creek (+0.89 ft) is more ambiguous and could reflect either a response to channel recharge from Cienega Creek, a reduction in local groundwater pumping, or both.

Long-term water-level changes—Water-level records covering years or decades are critical to understanding long-term changes in groundwater recharge and storage due to effects of climatic variability and regional groundwater development (Taylor and Alley, 2001). Multi-decadal groundwater hydrographs and periodic water-level measurements

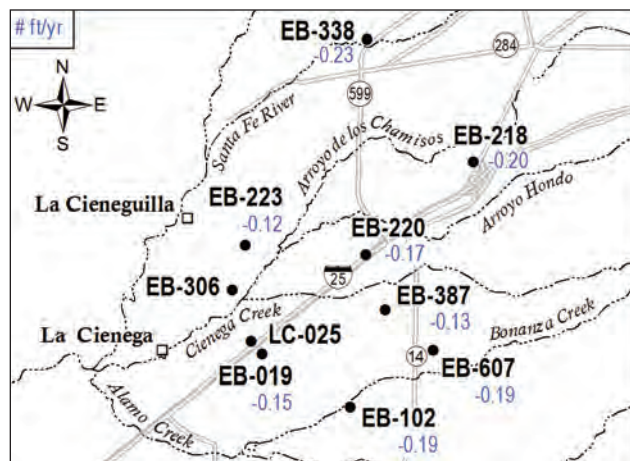


Figure 26. Location map and photos for wells with hydrographs (Figs. 25, 27, 28, and 30). **A**—Photo of well LC-025, visible at the right of the photo near the orange pole, and the surrounding wetland riparian zone. **B**—Photo of well EB-306 located in a grassy upland west of Cienega Creek, with the floodplain riparian zone visible in the background. Rates of water-level decline (ft/yr) are shown for sites with long measurement records.



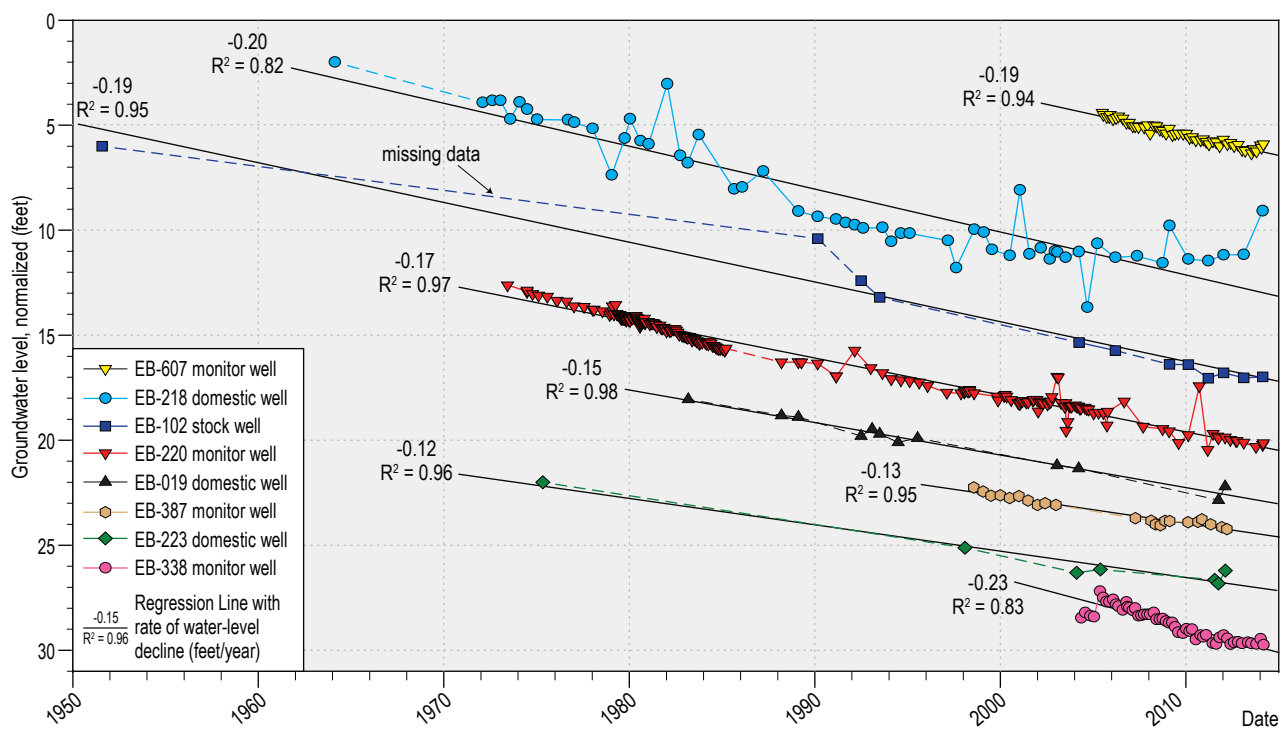


Figure 27. Groundwater hydrographs from shallow wells in the La Cienega area show a persistent decline in water levels over time. The rate of groundwater decline (ft/yr) is the slope of the regression line. Well information is shown in Table 1. Well locations are shown on Figure 26. Water-level data are presented in Appendix 2.

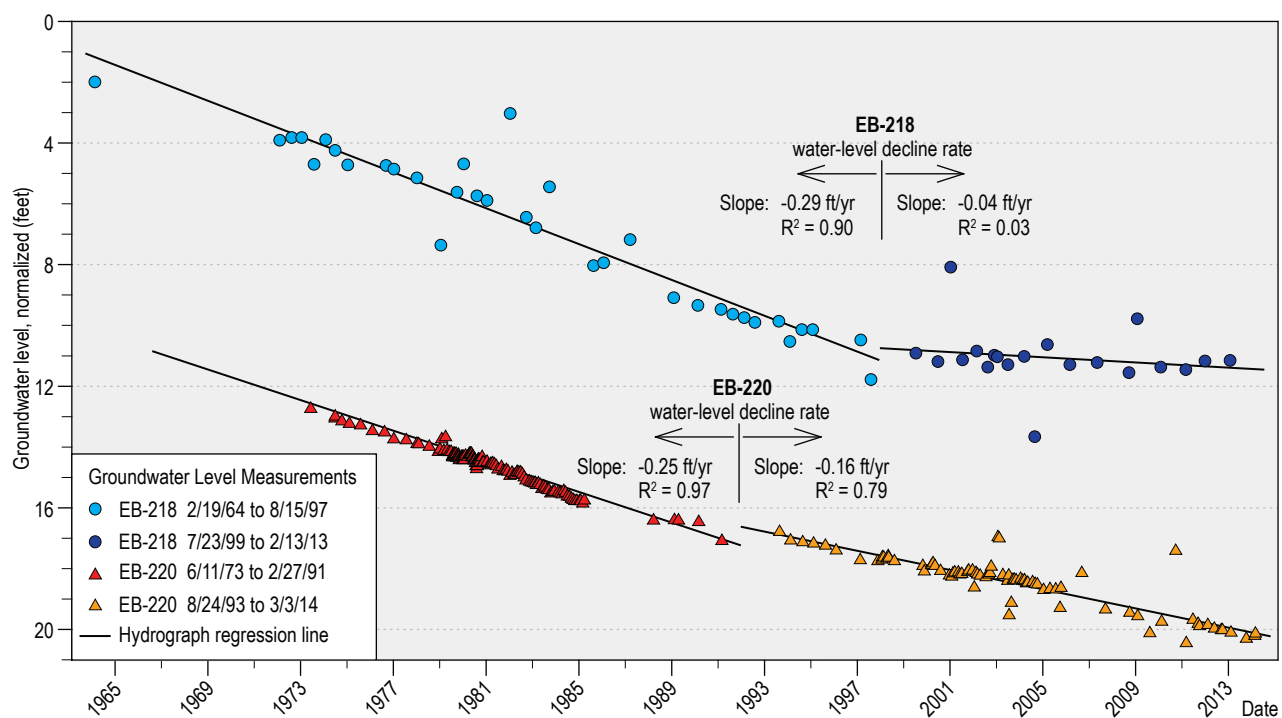


Figure 28. Groundwater hydrographs for two wells east and northeast of the Cienega Creek wetlands show that rates of water-level decline shifted in the early and late 1990s. Trend lines based on linear regression of water levels and time indicate that decline rates decreased in ~1998 in well EB-218 (from -0.29 to -0.04 ft/yr) and in ~1992 in well EB-220 (from -0.25 to -0.16 ft/yr). The shifts in water-level decline rates could be a response to changes in local or regional groundwater pumping.

from wells near La Cienega are examined for indicators of water-table changes related to large precipitation events, drought, and well depletions.

Groundwater hydrographs. Long records of groundwater levels in shallow wells east and north of La Cienega are shown in hydrographs from four dedicated monitor wells, three domestic wells, and one windmill (Fig. 27). The monitor wells provide high-frequency measurements spanning 9 to 41 years. Domestic and stock wells have sporadic measurements with some significant gaps. Three hydrologic localities are covered by the water-level records (Fig. 26): 1) the center of the Ancha zone of saturation near the El Dorado buried valley east of the wetlands (wells EB-220, EB-387, EB-607, EB-102 and EB-019); 2) the edge of the Ancha saturation zone near the ancestral Santa Fe River buried valley north and northwest of the wetlands (well EB-223); and 3) the Tesuque Formation northeast of La Cienega (wells EB-218 and EB-338).

The hydrographs generally demonstrate a widespread, persistent trend of declining groundwater levels starting as early as the 1970s (Fig. 27). In the Ancha zone of saturation east of the Cienega Creek wetlands, hydrographs record dropping groundwater levels with rates of -0.13 to -0.19 ft/yr. North of the wetlands, in the ancestral Santa Fe River buried valley of the Ancha aquifer, a single well shows a decline rate of -0.12 ft/yr (EB-223). In the Tesuque aquifer near Santa Fe, the water-level decline rates have been similar at two locations—-0.23 ft/yr at the Santa Fe River (EB-338) and -0.20 ft/yr near the Cerrillos interchange (EB-218)—over the past 10 to 40 years. Some hydrographs from monitor wells with low-frequency measurements (Appendix 2) show similar declining trends. The long-term trend of declining groundwater levels near La Cienega documents a persistent depletion in aquifer storage. Aquifer depletion occurs when total outflow from the aquifer exceeds inflow.

Reductions in water-level decline. A closer look at these hydrographs (Fig. 27) shows that average rates of decline in some wells have not been constant through time. A noticeable change in an otherwise steady decline is evident midway through hydrographs for EB-218 and EB-220. Regression analysis of the EB-218 data (Fig. 28) shows that the rate of water-level decline changed from -0.30 ft/yr to essentially flat (-0.04 ft/yr) in about 1998. In EB-220, adjacent to the Cienega Creek wetlands, the decline rate dropped from -0.25 to -0.16 ft/yr in about 1992. This observation is consistent with the findings of HydroScience Associates, Inc. (2004) and this report that most of

the streamflow decline at the nearby Acequia de La Cienega gage site occurred prior to 1991 (see prior discussion of streamflow at the Cienega head gate, page 43). Water-level declines in some wells near the perimeter of the study area (EB-218, EB-102, EB-223 and EB-338) appear to have stabilized since the early to late 2000s, with essentially no change over the last 4 to 10 years. Changes in the rates of long-term water-level decline may reflect changes in local or regional groundwater pumping. If this is the case near La Cienega, it suggests that aquifer depletion (and streamflow reductions) might be attenuated through effective management of the timing and location of groundwater withdrawals or by enhancing aquifer recharge. Such remedies might provide a valuable contribution to aquifer and wetland management, and should be considered when developing plans for wetland conservation and restoration.

Historic water-level changes. Periodic water-level measurements from a limited number of wells provide additional information concerning aquifer depletion near La Cienega. We compare water-level data from three historic measurement periods—2004–2012 (this study and Johnson, 2009), the mid-1970s (Mourant, 1980), and the 1950s (Spiegel and Baldwin, 1963)—and calculate rates of water-level change. The results, presented in Figure 29 and Table 9, quantify water-level declines due to aquifer depletion up-gradient of springs and wetlands, particularly in the Ancha zone of saturation and the area between La Cienega and Santa Fe. The significant spatial and temporal patterns gleaned from historic groundwater-level records are summarized here.

1. In wells located between La Cienega and the City of Santa Fe, near state road 599 and I-25 (EB-130 and EB-407, Fig. 29), groundwater levels consistently declined at a rate of -0.11 ft/yr between 1952 and 2004. Total declines were -5.6 ft and -5.8 ft respectively.
2. Large groundwater declines were recorded in the Valle Vista area along the Cienega Creek arroyo between measurements by Mourant and the USGS (mid-1970s to mid-1980s) and those by Johnson (2004–2012). Water-level declines ranged from -7.2 to -8.9 ft for the period, and decline rates varied from -0.19 to -0.31 ft/yr. The Valle Vista community overlies the northern edge of the Ancha zone of saturation (Fig. 29B).
3. A large drop in groundwater levels (-10.8 ft, at a rate of -0.18 ft/yr) occurred in well EB-102, located near Bonanza Creek south of the state

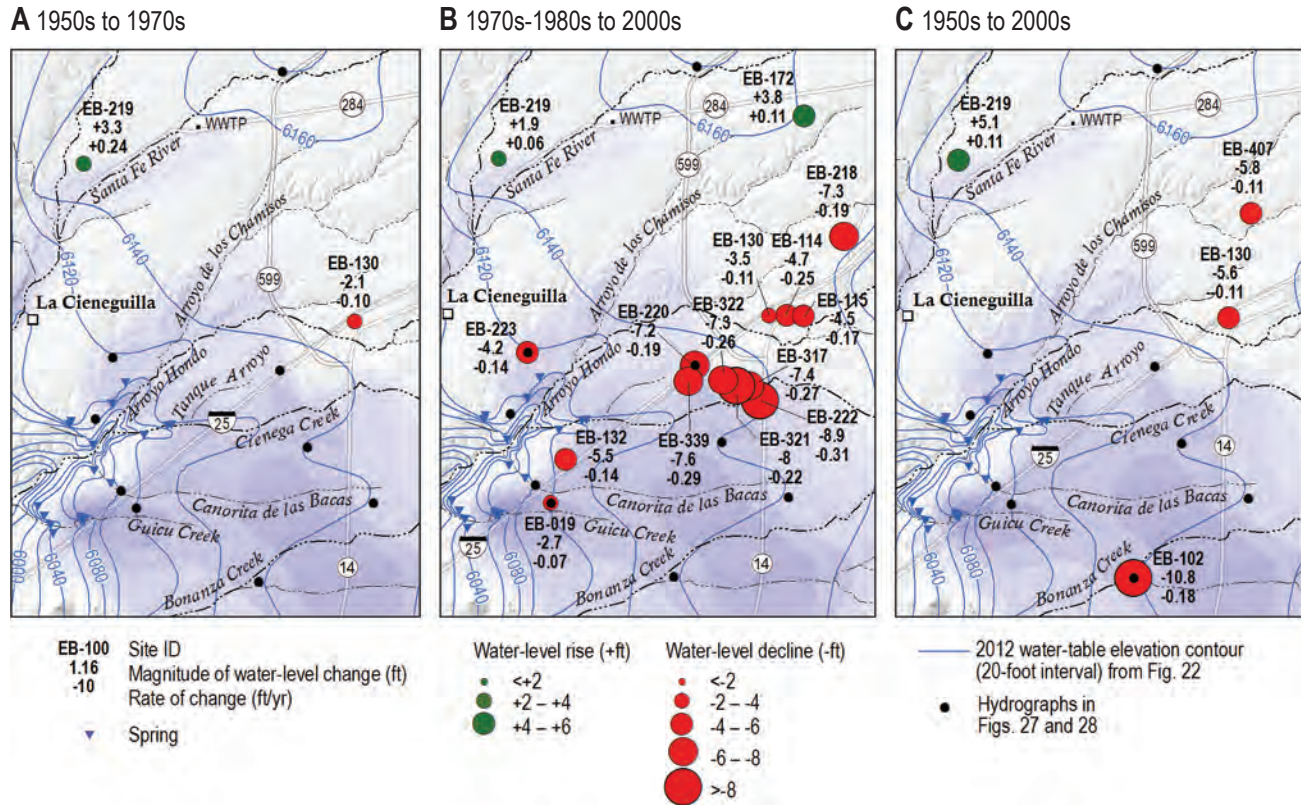


Figure 29. Maps showing the magnitude and rate of change (in feet and feet/year) in water levels between three historic measurement periods: (1) period one, 1951–1959 (Spiegel and Baldwin, 1963); (2) period two, 1973–1976 (Mourant, 1980); and (3) period three, 2004–2012 (Johnson, 2009). **A**—Water-level changes between the 1950s and the 1970s. **B**—Water-level changes between the 1970s–1980s and the 2000s. **C**—Water-level changes between the 1950s and the 2000s. The extent of groundwater saturation in the Ancha Formation (from Fig. 14) is shown in the background. Water-level data for the three measurement periods are presented in Table 9.

penitentiary, between 1951 and 2012 (Fig. 29C, Table 9). This well is situated at the southern edge of the Ancha zone of saturation.

- Large increases in water level are recorded in wells near the Santa Fe River at the WWTP (EB-219) and east of state road 599 between the Santa Fe River and Arroyo de los Chamisos (EB-172). The water level rose over 5 feet (+0.11 ft/yr) in well EB-219 between 1959 and 2005 (Fig. 29C) and 3.8 ft (also +0.11 ft/yr) in EB-172 between 1973 and 2007 (Fig. 29B). The highest rate of rise in EB-219 (+0.24 ft/yr) occurred between 1959 and 1973 (Fig. 29A). The rate decreased to +0.06 ft/yr between 1973 and 2005 (Fig. 29B). The WWTP began to discharge recycled wastewater into the Santa Fe River channel in the early 1960s.

A decline or rise in water level in a well is a net effect of all natural and man-made recharges to and withdrawals from the aquifer. This simple analysis of historic water levels illustrates the decline and rise of

the water table in different areas, at variable rates. The largest documented declines (Fig. 29) occurred in the Valle Vista and penitentiary areas, east and up-gradient of the La Cienega wetlands and along the margins of the Ancha zone of saturation. No data on the location, volume or timing of pumping were compiled for this study. However, the persistent water-level declines seen in well hydrographs (Fig. 27) and periodic historic measurements (Fig. 29) are consistent with aquifer depletion associated with groundwater pumping in excess of recharge (Taylor and Alley, 2001; Konikow, 2015). The rise in water levels near the Santa Fe River and Arroyo de los Chamisos are typical of focused recharge, likely from natural runoff and WWTP return flow. These storage gains attenuate with distance from the channels. Changes in surface runoff and pumping patterns can also force fluctuations in the water table and variations in the rate of change in water-table decline as shown in Figure 28.

These historic water-level records provide valuable data for calibration of numerical

Table 9. Water-level-change data for three historic measurement periods (Figure 29). Hydrographs and water-level data are included in Appendix 2 and on Figure 27.

WELL SITES	WELL LOCATION	FIRST WATER-LEVEL PERIOD 1950s	SECOND WATER-LEVEL PERIOD 1970s	THIRD WATER-LEVEL PERIOD 2000s	Hydrograph	x	x	x	x	x	x	x	x	x	x	x	x	x	x	x	x	x
					Water-level change period 1–3 (ft)																	
EB-019	RG-27637S	400304	3935932	6144	Water-level change period 2–3 (ft)																	
EB-102	Unknown	402734	3934466	6199	Water depth elevation (ft asl)																	
EB-114	RG-35281	404980	3935648	6337	Water depth (ft bsl)																	
EB-115	RG-35282	405319	3935633	6352	Measurement period 2004–2012																	
EB-130	Unknown	404633	3935633	6325	Water-level change period 1–2 (ft)																	
EB-132	RG-08223	400609	3936794	6180	Water depth elevation (ft asl)																	
EB-172	RG-24042	405330	3945594	6462	Water depth (ft bsl)																	
EB-218	RG-09982	406118	3941215	6409	Measurement period 1973–1985																	
EB-219	RG-00590	399267	3942749	6218	Water depth elevation (ft asl)																	
EB-220	RG-03824T	403153	3938661	6260	Water depth (ft bsl)																	
EB-222	RG-22251	404457	3937957	6269	Measurement period 1951–1964																	
EB-223	RG-25952	399840	3938918	6165	Surface elevation (ft asl)																	
EB-317	RG-22251x6	404232	3938253	6261	Water-level change period 1–3 (ft)																	
EB-321	RG-22251x2	403986	3938251	6263	Water-level change period 2–3 (ft)																	
EB-322	RG-22251x7	403716	3938365	6270	Water depth elevation (ft asl)																	
EB-339	RG-44219	403035	3938347	6259	Water depth (ft bsl)																	
EB-407	RG-26718	405069	3941697	6365	Measurement period 2004–2012																	
					Water-level change period 2–3 (ft)																	
					Water depth elevation (ft asl)																	
					Water depth (ft bsl)																	
					Measurement period 2004–2012																	

asl=above sea level; bsl=below land surface

groundwater-flow models, which can incorporate pumping, recharge, and other outflows and inflows in a predictive mode and are rigorous analytical and management tools. This analysis is a preliminary exploration of the data and is not a substitute for more rigorous numerical methods.

The water-table response to extreme climatic events. Understanding how climate and groundwater development affect the water table is important when developing wetland restoration and management plans. Drought, recharge and groundwater pumping each affect groundwater levels and are observable in hydrographs (Alley et al., 1999) when the individual effects do not interfere and measurement frequencies are sufficiently high. We evaluate the effects of climatic events on groundwater levels near La Cienega by identifying extreme periods of rainfall and drought that coincide with water-table inflections. The graphic analysis (Fig. 30) uses hydrographs from three wells that have high-frequency measurements and show long-term declines associated with groundwater depletion. In Figure 30, the hydrographs are superimposed on extreme wet and dry periods (highlighted in Table 10) defined from upper and lower quartiles of monthly precipitation (P_{90} and P_{10} values, Table 5). Wet periods are indicated by monthly precipitation exceeding the 90th percentile value. Droughts are defined by recurring monthly precipitation less than the 10th percentile value in at least three months of a 12-month period.

In this comparison of water-level fluctuations with the 10% wettest months on record, we identify precipitation thresholds that produce a water-table rise that documents recharge (Fig. 30). Two significant water-table spikes captured in the hydrographs correlate to precipitation and spring runoff. The first occurred in EB-220 near the head of Cienega Creek where a rise of +1.23 ft was associated with a record monsoon in 1991 (9.96 inches,

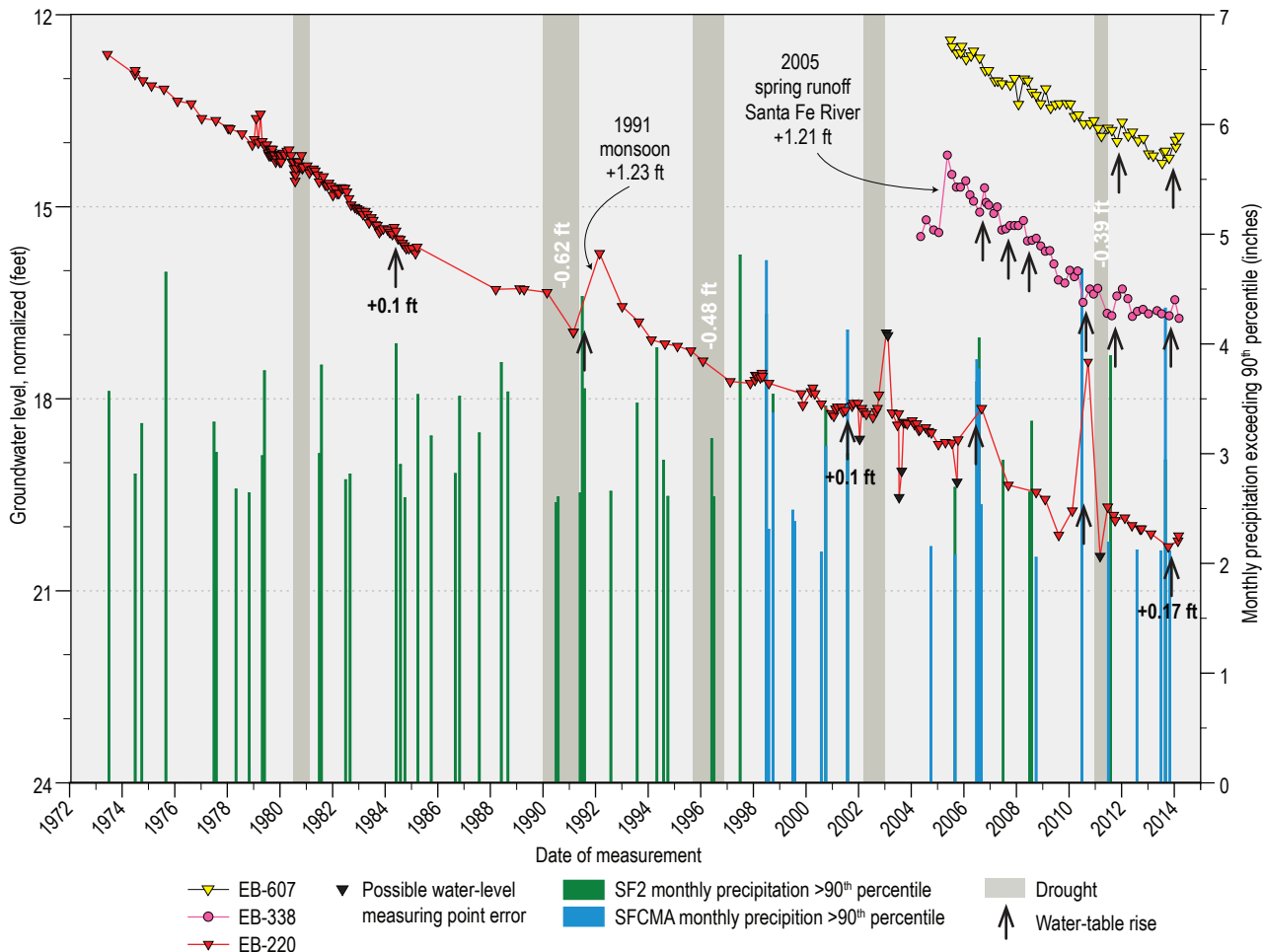


Figure 30. Graph showing a time-series comparison of groundwater levels in wells (left Y-axis) and monthly precipitation during the 10% wettest months recorded at nearby NOAA weather stations (colored bars, right Y-axis). Wet periods (green and blue bands) are defined by monthly precipitation greater than the 90th percentile value. Drought periods (gray bands) are defined where monthly precipitation is less than the 10th percentile value in three or more months during a 12-month period. Arrows mark a water-table rise coincident with an extremely wet month. Extreme wet and dry periods that correlate to a water-table rise or fall are highlighted in Table 10. Water-level data are presented in Appendix 2. Streamflow data for the Santa Fe River showing high discharge in spring 2005 are presented in Appendix 4. Well locations are shown on Figure 26.

July–September). The second event appeared in EB-338—located adjacent to the Santa Fe River west of State Road 599—where a rise of +1.21 ft coincided with high spring runoff in 2005. (Streamflow data from the lower Santa Fe River are presented in Appendix 4.) A water-table rise of +0.1 to +0.4 inches occurred at all sites when monthly precipitation exceeded 4 inches, or with two to three consecutive months of high cumulative precipitation. Most of these events produced a high water level in the fall, following a summer monsoon. These fall water-table highs are prominent in EB-338 near the Santa Fe River and periodic in EB-607 and EB-220.

The local wetland water-table response to recharge can be dramatic. The hydrograph from well LC-025 (Fig. 25) recorded a water-table rise of

nearly 6 ft within a 12-hour period on September 15, 2103 in direct response to a 2-inch rain event. Water levels remained high at this site through at least February of 2014.

A similar comparison of hydrographs and drought periods indicates that droughts lasting a year or more have a negative effect on the water table. Three of five drought periods identified corresponded with a water-table drop of 0.4 to 0.6 ft EB-220. The drought-depressed water table was usually restored by post-drought rainfall. Between fall 2013 and winter 2014, drought-depressed groundwater levels rebounded in response to strong monsoon storm events in September 2013 (Figs. 25 and 30, Table 10). In the hydrographs examined, a water-table rise caused by rain-derived recharge was

typically overcome by water-table recession due to persistent groundwater depletion within a few months to a few years.

Summary of Hydrologic Investigations

Information on precipitation, streamflow, and groundwater levels advances our understanding of the hydrologic factors that affect wetland function. Those aspects of wetland hydrology relevant to planning and conservation are considered here in the context of the wetland water balance (Fig. 15).

1. Precipitation, climate and groundwater fluctuations

The natural variability in precipitation and recharge produces a short-term response in the water table (Taylor and Alley, 2001; Konikow, 2015). Periods of extreme rainfall and drought are scattered throughout the precipitation record (NOAA station SF-2, Fig. 17A). The years 1998–2013 were notably dry (annual mean of 11.8 inches), compared with the period 1972–1997 (annual mean of 14.1 inches). Our time-series comparison of groundwater levels and precipitation from wet and dry periods links short-term water-table inflections near the wetlands to climate variability (Fig. 30). Findings indicate that climate-related water-table fluctuations are generally short lived and insignificant compared to the persistent long-term trend of groundwater decline. Large water-table spikes (+1.2 ft) occurred near Cienega Creek following a record monsoon in 1991, and near the Santa Fe River following a record snowmelt in spring 2005. Small water-table increases (+0.1 to +0.4 inches) are fairly regular when monthly precipitation exceeds 4 inches. Fall water-level highs following summer monsoons occur periodically near the Santa Fe River (EB-338) and in wells east of La Cienega (EB-607 and EB-220). A water-table rise of nearly 6 ft occurred in a wetland well over a 12-hour period on September 15, 2103 in response to a 2-inch rain in the midst of a 5-day monsoon event, and the water table remained high through the winter of 2014. Droughts lasting a year or more generally corresponded with declines of 0.4 to 0.6 ft (EB-220) that rebounded with post-drought rainfall.

2. Cienega Creek streamflow

Perennial streamflow in Cienega Creek is fed by groundwater discharging from springs and

Table 10. Monthly precipitation data used to define drought periods (less than the 10th percentile value) and wet periods (greater than the 90th percentile value) from NOAA stations SFCMA and SF2. Highlighted wet periods coincide with a visible rise in local groundwater levels (Fig. 30).

NOAA STATION SFCMA		NOAA STATION SF2	
DROUGHT PERIODS	WET PERIODS	DROUGHT PERIODS	WET PERIODS
Month-year	Precipitation <0.043 inches [†]	Month-year	Precipitation >0.065 inches [‡]
5/1/1998	0.01	7/1/1998	4.76
12/1/1998	0.01	8/1/1998	2.31
2/1/1999	0.01	10/1/1998	3.37
11/1/1999	0	7/1/1999	2.48
2/1/1900	0.02	8/1/1999	2.38
6/1/1901	0.04	8/1/2000	2.10
2/1/2002	0.01	10/1/2000	3.06
3/1/2002	0.02	8/1/2001	4.12
1/1/2003	0	10/1/2004	2.15
5/1/2004	0	9/1/2005	2.07
12/1/2005	0.04	7/1/2006	3.85
1/1/2006	0.04	8/1/2006	3.77
2/1/2006	0	9/1/2006	2.53
1/1/2009	0.02	10/1/2008	2.05
2/1/2009	0.03	7/1/2010	4.68
1/1/2011	0.02	7/1/2011	2.19
2/1/2011	0	8/1/2012	2.12
6/1/2011	0.03	7/1/2013	2.11
6/1/2012	0	9/1/2013	4.32
4/1/2013	0.01	11/1/2013	2.11
		12/1/2013	0.07
		1/1/2014	0.00
		2/1/2014	0.11
[†] 10 th percentile value for monthly precipitation [‡] 90 th percentile value for monthly precipitation			
Drought period (Fig. 30)			
Wet period with coinciding water-table rise (Fig. 30)			

wetlands. Thus, changes in streamflow measured during dry times with minimal ET reflect changes in groundwater discharge and water levels. Seasonal variability and long-term decline are the most notable characteristics of the discontinuous streamflow record at the Cienega head gate (1966–2014) (Table 6, Fig. 19). Seasonal measurements in years since 1991 show a consistent flow variation, where discharge is low during summer months (July–September) and generally higher the rest of the year. The summer drop in streamflow occurs despite a substantial increase in precipitation from the summer monsoon. The streamflow record also indicates that discharge has generally declined since 1966, possibly by as much as 1 ft³/s (or 64%). Average streamflow during recent dry intervals (0.48 ft³/s in 2001–2004 and 0.38 ft³/s in 2012) fell considerably below the long-term mean of 0.53 ft³/s. This implies that multi-year drought cycles contribute to streamflow declines. We also show that short-term drought-related declines in surface water and groundwater are restored during subsequent wet intervals (Figs. 19A and 30).

3. Evapotranspiration

Groundwater levels inside the wetland area fluctuate on both a seasonal and daily cycle in response to evapotranspiration (ET). Measurements from 24 wetland wells in 2011–2012 show that the wetland water table was higher during the winter by +0.04 to +6.60 (Fig. 24A). Seasonal water-level fluctuations are driven by changes in ET between growing and dormant vegetation stages (Carter, 1996; Vincke and Thiry, 2008). In 2012, the summer water-table low at the Leonora Curtin Wetland Preserve coincided with daily water-table fluctuations of 0.1 to 0.2 ft (Fig. 25, LC-025). In this diurnal water-level pattern, typical of wetlands, the water table drops during the day when ET is highest and recovers at night when ET is minimal. At LC-025, seasonal and daily fluctuations began in early April, continued through the growing season, and ended in late October. In 2013, the diurnal ET signal was absent until early July, perhaps due to drought, low humidity and extreme temperatures, which suppress vegetative growth. Large summer water-level drops in the wetland aquifer (-4.9 ft at LC-025 in 2012) indicate that ET produces a significant summer water depletion in the wetland riparian zone.

4. A declining water table

Groundwater hydrographs from near La Cienega,

spanning 9 to more than 40 years (Fig. 27), show a widespread, persistent decline in water levels starting as early as the 1970s. A long-term hydrograph representative of the area east of the wetlands, EB-220 near I-25 at the racetrack, shows the water level has declined by 7.5 feet since 1973, leaving a current saturated thickness in the Ancha Formation of 31 ft. Rates of water-level decline from -0.13 to -0.19 ft/yr have occurred for decades east of the wetlands. A smaller decline—4.2 ft over the last 30 years (rate of decline -0.12 ft/yr)—is seen west of Cienega Creek in the ancestral Santa Fe River buried-valley aquifer (EB-223). Water levels measured between the historic measurement periods of the 1950s, 1970s, and 2000s show that the largest depletions and decline rates occurred in the Valle Vista area and south of the penitentiary, near the edges of the Ancha saturation zone (Fig. 29). Declines in some wells at the study-area perimeter (EB-218, EB-102, EB-223 and EB-338) stabilized in the last 5 to 15 years.

5. Groundwater depletion

Groundwater depletion is manifested by water-level declines (Konikow, 2015). Long-term trends of declining groundwater levels (Fig. 27) and stream discharge (Fig. 19A) near La Cienega document a persistent depletion in aquifer storage, which occurs when total outflow from the aquifer exceeds inflow. We can place local groundwater depletion in the context of aquifer inflows and outflows using the wetland water balance (Fig. 15). The two sources of water in the wetlands are groundwater inflow from the regional aquifer (Gin) and local recharge from precipitation (Pin). Groundwater leaves the system as surface water (Qout), evaporation and transpiration (ET), leakage from the regional aquifer (Gout), and withdrawals from wells (Gd). Depletions from evapotranspiration produce local, seasonal water-level fluctuations (Figs. 24A and 25). Variability in precipitation and recharge are expressed in short-term water-level fluctuations (Fig. 30). Groundwater leakage out of the aquifer is static. The long-term water-level declines seen in area hydrographs are of the style discussed by Konikow (2015), which link groundwater depletion to the unsustainable withdrawal of groundwater from wells. The coarse nature and relatively high hydraulic conductivity of the buried-valley aquifers increase the vulnerability of the aquifers and associated wetlands to excessive drawdowns and depletion.

V. CHEMICAL CHARACTERISTICS AND AGE OF GROUNDWATER

Chemical and isotopic characteristics of groundwater from wells and springs were examined to address questions of the water's source, flow path, recharge, mixing, and residence time. Parameters evaluated in groundwater include total dissolved solids (TDS), calcium (Ca), sodium (Na), magnesium (Mg), sulfate (SO_4), chloride (Cl), bromide (Br), and stable isotopes of hydrogen (deuterium, D, $\delta^2\text{H}$) and oxygen (oxygen-18, $\delta^{18}\text{O}$). Groundwater residence time was evaluated using a combination of isotopes, including carbon-14 (^{14}C), tritium (^3H), and the stable isotopes deuterium and oxygen-18. Results of these studies are discussed below. Data are presented in Tables 11, 12 and in Appendix 3.

Major Ion Chemistry and Water Type

Concentrations of TDS, calcium, and sodium in groundwater are generally representative of the water's residence time. This is particularly true in the region west of Santa Fe where TDS and sodium increase with depth in the SFG aquifer (Johnson and others, 2013). Elevated TDS and sodium indicate mineralized groundwater with a long residence time and deep circulation. We use this simple concept as a first step to evaluate the origin of waters supporting springs and wetlands.

Groundwater from the SFG aquifer near La Cienega is relatively dilute in dissolved minerals, with TDS values of 92–391 mg/L (Fig. 31A, Table 11). Geographic variations demonstrate groundwater mixing and localized discharge of deep water sources. Wells and springs at the edge of the basin southwest of the Rancho Viejo hinge zone have the highest concentrations of dissolved solids (>250 mg/L), particularly in the groundwater discharge zone along lower Cienega Creek. Low TDS (92 to 152 mg/L) is characteristic of shallow groundwater everywhere in the basin northeast of the Rancho Viejo hinge zone and is noted southwest of the hinge zone near buried valleys in east of Cienega Creek (140 to 180 mg/L). Wetland springs

have an intermediate TDS content (175–305 mg/L) with higher Na, Mg and SO_4 , indicating a mixture of shallow and deep water sources. Discharge from the WWTP has a TDS concentration of 454 mg/L, which is significantly higher than observed in the surrounding aquifer.

The distribution of calcium and sodium is illustrated as a calcium-to-sodium ratio (Fig. 31B), where values greater than 1 indicate calcium dominance and values less than 1 indicate sodium dominance. Enrichment of sodium in the SFG aquifer is a product of cation exchange and demonstrates a long residence time with deep circulation through clay-rich materials (Johnson and others, 2013). Most groundwater (80% of samples) in the SFG aquifer near La Cienega is calcium rich with lesser amounts of sodium and magnesium (Table 11). Calcium concentrations range from 2 to 86 mg/L, and sodium ranges from 7 to 125 mg/L. Calcium-rich groundwater (Ca/Na ratio >2.0), like low TDS, is characteristic of shallow groundwater northeast of the Rancho Viejo hinge zone, particularly beneath the Santa Fe River and the upper valleys of Arroyo Hondo and Arroyo de los Chamisos, and is noted southwest of the hinge zone near buried valleys in the Ancha Formation near Cienega and Guicu Creeks. A stream sample from the Santa Fe River above the WWTP is exceptionally rich in calcium (a Ca/Na ratio of 3.7, Fig. 31B). Shallow Ca-rich zones typically denote groundwater recharge and flow unaffected by clay-rich sediments.

Sodium-rich groundwater (Ca/Na ratio <1.0) is characteristic of deep basin wells drawing water from the Tesuque Formation (for example EB-605, -606, -336, -337, -328) (Johnson et al., 2013), and also occurs in the western spring zone of the ancestral Santa Fe River buried valley and discharge from the WWTP. Many of the groundwater samples near La Cienega have an intermediate calcium-sodium signature (Ca/Na ratio between 2 and 1), which is consistent with mixing of shallow Ca-rich and deep Na-rich sources of groundwater.

Table 11. General chemistry data for well, spring and stream waters shown on Figures 31 through 33. Sample sites are shown on Figure 4. Units are mg/L (ppm) unless otherwise noted. Additional chemical data are presented in Appendix 3.

Site ID	Site type	GENERAL CHEMISTRY			MAJOR IONS								SAMPLE INFORMATION						
		SC ($\mu\text{S}/\text{cm}$)	Lab pH	TDS	Water type	Ca	Na	Ca:Na Ratio	Mg	K	HCO_3	CO_3	SO_4	Cl	Br	Cl:Br ratio	Analyzing laboratory	Sample date	
EB-001	well	355		Ca-Na-Mg-HCO ₃ -SO ₄	61	41	1.7	15		197	5	59	26				Unknown	4/1/95	
EB-019	well	354	8.4	188	Ca-Na-HCO ₃	39	20	2.2	7	1.7	149		16	19				Hall Environmental	3/1/96
EB-131	well	230	7.0	92	Ca-Na-HCO ₃	23	21	1.3	4		142	0	15	4				Environmental Biochemists	11/9/77
EB-134	well	230	7.3	150	Ca-Na-HCO ₃	37	36	1.2	5		152	<1	8	6				Albuchemist, Inc.	9/24/79
EB-135	well	225	8.2	166	Ca-Na-HCO ₃	34	27	1.4	3		150	<1	11	4				Albuchemist, Inc.	9/24/79
EB-219	well	125		Ca-Mg-HCO ₃	27	9	3.4	8	1.2	113		9	7				Scientific Lab. Div. of NM	9/13/84	
EB-223	well	255	7.9	163	Ca-Na-HCO ₃	26	23	1.3	3	1.2	120		19	5	0.12	40		NMBGMR	10/4/11
EB-293	well	8.2	144	Ca-Na-HCO ₃	32	13	2.9			119		11	5				Inter Mountain Lab. Inc.	1/30/01	
EB-303	well	565	7.8	391	Ca-HCO ₃ -SO ₄ -Cl	86	25	3.9	10	2.4	170		97	47	0.64	73		NMBGMR	6/22/11
EB-304	well	7.8	141	Ca-Na-HCO ₃	24	14	2.0	4		116		12	8				Assaigai Analytical Lab.	5/18/04	
EB-313	well	255	7.4	180	Ca-Na-HCO ₃ -SO ₄	25	27	1.1	4	1.3	130		32	5	0.10	48		NMBGMR	6/22/11
EB-315	well	240	8.2	160	Ca-Na-HCO ₃	31	13	2.7	5	1.6	120		15	8	0.12	66		NMBGMR	5/11/05
EB-319	well	324	8.0	182	Ca-Na-HCO ₃	32	30	1.2	8	5	167		16	10				NMDWB	9/25/97
EB-323	well	350		Na-Ca-Mg-HCO ₃	54	67	0.9	17	4.3	314		18	32				Scientific Lab. Div. of NM	9/13/84	
EB-328	well	235	8.3	155	Na-Ca-HCO ₃	16	33	0.6	3	1.8	110	4	14	6	<0.1			NMBGMR	6/7/05
EB-329	well	220	8.1	152	Ca-Na-HCO ₃	24	19	1.4	3	1.2	120		11	6	<0.1			NMBGMR	5/11/05
EB-332	well	260	7.4	180	Ca-Na-HCO ₃	28	22	1.5	7	2.2	140		11	8	0.110	72		NMBGMR	7/21/11
EB-336	well	550	8.5	316	Na-HCO ₃	2	125	0.02	<1	1	275	12	22	6	0.140	44		NMBGMR	4/8/05
EB-337	well	270	8.2	191	Na-HCO ₃	11	54	0.2	<1	1.8	150		21	3	0.110	27		NMBGMR	4/8/05
EB-338	well	150	8.0	108	Ca-HCO ₃	22	7	3.7	3	0.9	95		4	2	<0.1			NMBGMR	4/9/05
EB-339	well	239	7.8	128	Na-Ca-HCO ₃ -SO ₄	15	39	0.4	1		122	0	28	1			Controls for Envir. Poll., Inc.	10/2/87	
EB-363	well	130		Ca-HCO ₃	24	7	3.9	0	1.6	102		10	4				Scientific Lab. Div. of NM	12/27/84	
EB-364	well	185	7.9	125	Ca-HCO ₃	27	9	3.4	4	1	105		4	3	0.036	75		NMBGMR	10/20/11
EB-366	well	220	7.9	140	Ca-HCO ₃	31	8	4.2	4	1.0	115		7	7	0.077	84		NMBGMR	10/20/11
EB-370	well	440	7.9	252	Ca-Na-HCO ₃ -SO ₄	79	23	4.0	6		144	<5	62	14				Assaigai Analytical Lab.	1/13/88
EB-373	well	265	7.9	164	Ca-Na-HCO ₃	35	13	3.1	5	1.4	125		17	8	0.089	84		NMBGMR	10/20/11
EB-383	well			Na-Ca-HCO ₃	21	34	0.7	2	1.8	130	0	18	4				NMDWB	4/1/97	
EB-391	well	8.0	177	Ca-HCO ₃	38	11	4.2	4		144		7	3				Assaigai Analytical Lab.	5/5/04	
EB-459	well	162		Na-HCO ₃ -SO ₄	11	58	0.2	0	0	155		32	9				Scientific Lab. Div. of NM	12/27/84	
EB-569	well	254	7.0	Ca-HCO ₃	36	9	4.6	4	2.6	142	<1	<2	5				NMDWB	3/17/97	
EB-579	well	6.9	135	Ca-Na-HCO ₃	30	14	2.5	4		115		6	5				Assagai Analytical Lab.	6/21/00	
EB-595	stream	230	8.4	141	Ca-HCO ₃	31	10	3.7	5	1.6	87	4	23	12	<0.1			NMBGMR	5/12/05
EB-605	well	8.1	2539	Na-Cl-SO ₄	19	824	0.03	2	4.6	231	8	768	632	0.94	672		LANL	9/24/06	
EB-606	well	449	9	368	Na-HCO ₃ -SO ₄	2.3	93	0.03	0.5	0.9	203	8	32.7	8.6				LANL	9/25/06
EB-607	well	8.1	227	Na-Ca-HCO ₃	16	32	0.6	1	1.4	134	0	15	2	0.020	82		LANL	9/26/06	
EB-624	spring	322	7.6	274	Ca-Na-Mg-HCO ₃	47	27	2.0	12	3.5	231	<1	16	7				Unknown	9/8/98
LC-001	spring	275	7.7	175	Ca-Na-HCO ₃	28	20	1.6	6	2.4	145		14	6	0.066	83		NMBGMR	6/1/11
LC-003	spring	470	7.3	296	Ca-Na-Mg-HCO ₃ -SO ₄	56	25	2.6	12	2.6	155		54	34	0.330	103		NMBGMR	6/1/11
LC-005	spring	380	7.6	236	Ca-Na-HCO ₃	49	19	3.0	6	1.1	175		23	15	0.130	115		NMBGMR	6/1/11
LC-006	well	275	7.5	189	Ca-HCO ₃	35	12	3.3	7	1.7	115		10	17	0.130	131		NMBGMR	6/21/11
LC-007	spring	440	7.6	305	Ca-Na-HCO ₃ -SO ₄	43	46	1.1	7	2.2	180		65	15	0.160	94		NMBGMR	6/22/11
LC-008	spring	390	7.5	263	Ca-Na-HCO ₃	45	26	2.0	10	3.8	180		32	25	0.210	119		NMBGMR	6/22/11
LC-016	spring	307	7.4	206	Na-Ca-HCO ₃	29	34	1.0	4	1.9	155		24	8	0.110	74		NMBGMR	6/22/11
LC-023	spring	305	7.4	212	Na-Ca-HCO ₃	23	45	0.59	3.2	2.6	145		29	10	0.380	26		NMBGMR	7/20/11
LC-026	well	565	7.4	344	Ca-Na-HCO ₃ -Cl-SO ₄	69	28	2.83	11	4.6	155		63	57	0.620	92		NMBGMR	10/4/11
LC-033A	effluent	736	7.8	454	Na-Ca-HCO ₃ -Cl	45	90.5	0.57	7	21.5	239	<5	48	75.3	0.170	443		NMBGMR	8/30/12
LC-033B	effluent		598	Na-Ca-HCO ₃ -Cl	48.6	116	0.48	6.2	18.8	285		45.2	77.7				U.S. EPA, STORET database	3/1/06	
LC-033C	effluent		457	Na-Ca-HCO ₃ -Cl	31.9	96.9	0.38	2.9	18.4	197		43.6	65.5				U.S. EPA, STORET database	8/16/05	
LC-033D	effluent		482	Na-Ca-HCO ₃ -Cl	39	98.8	0.46	3.2	19.6	206		42.4	72.4				U.S. EPA, STORET database	7/12/05	
LC-033E	effluent		340	Na-Ca-HCO ₃ -Cl	30.6	55.7	0.63	3.6	10.5	156		33.6	49.6				U.S. EPA, STORET database	6/14/05	

Mixing of deep and shallow groundwater sources

A plot of the proportions of major cations (calcium [Ca], magnesium [Mg], sodium [Na], potassium [K]) and anions (bicarbonate [HCO_3^-], carbonate [CO_3^{2-}], sulfate [SO_4^{2-}], chloride [Cl]) in water is shown on a Piper diagram in Figure 32. The Piper plot illustrates water type and ion chemistry for all well, spring and surface waters sampled near La Cienega, grouped geographically (Cienega Creek, Guicu Creek, Arroyo Hondo or El Rancho de las Golondrinas) and by aquifer zone (shallow or deep). The trends in ion chemistry observed on the Piper diagram, together with the distributions of TDS and Ca/Na (Fig. 31), support hydrologic interpretations of groundwater sources, mixing, recharge and flow paths for the La Cienega springs and wetlands.

The prominent cation trend in the Piper diagram shows Ca-rich groundwater evolving toward Na-rich

groundwater (Fig. 32, left triangle) as a result of cation exchange, wherein dissolved Ca and Mg are exchanged for Na on clays (Johnson et al., 2013). The trend is prominently expressed by groundwater from two well groups: 1) shallow wells near streams and arroyos that produce Ca-HCO₃ (blue circles near the Ca-apex of the cation, or left, triangle); and 2) deep wells in the Tesuque Formation that tap Na-HCO₃ or mixed Na-Ca-HCO₃ water (red circles near the Na-apex of the left triangle).

Springs and shallow wells near wetlands primarily plot between these two well groups (Fig. 32), demonstrating that spring and wetland waters are mixtures of two general sources: 1) calcium-rich shallow groundwater from focused recharge along streams and arroyos; and 2) sodium-rich deep groundwater from regional flow in the Tesuque Formation. Progressive mixing of these two primary sources manifests in a gradational variation of the

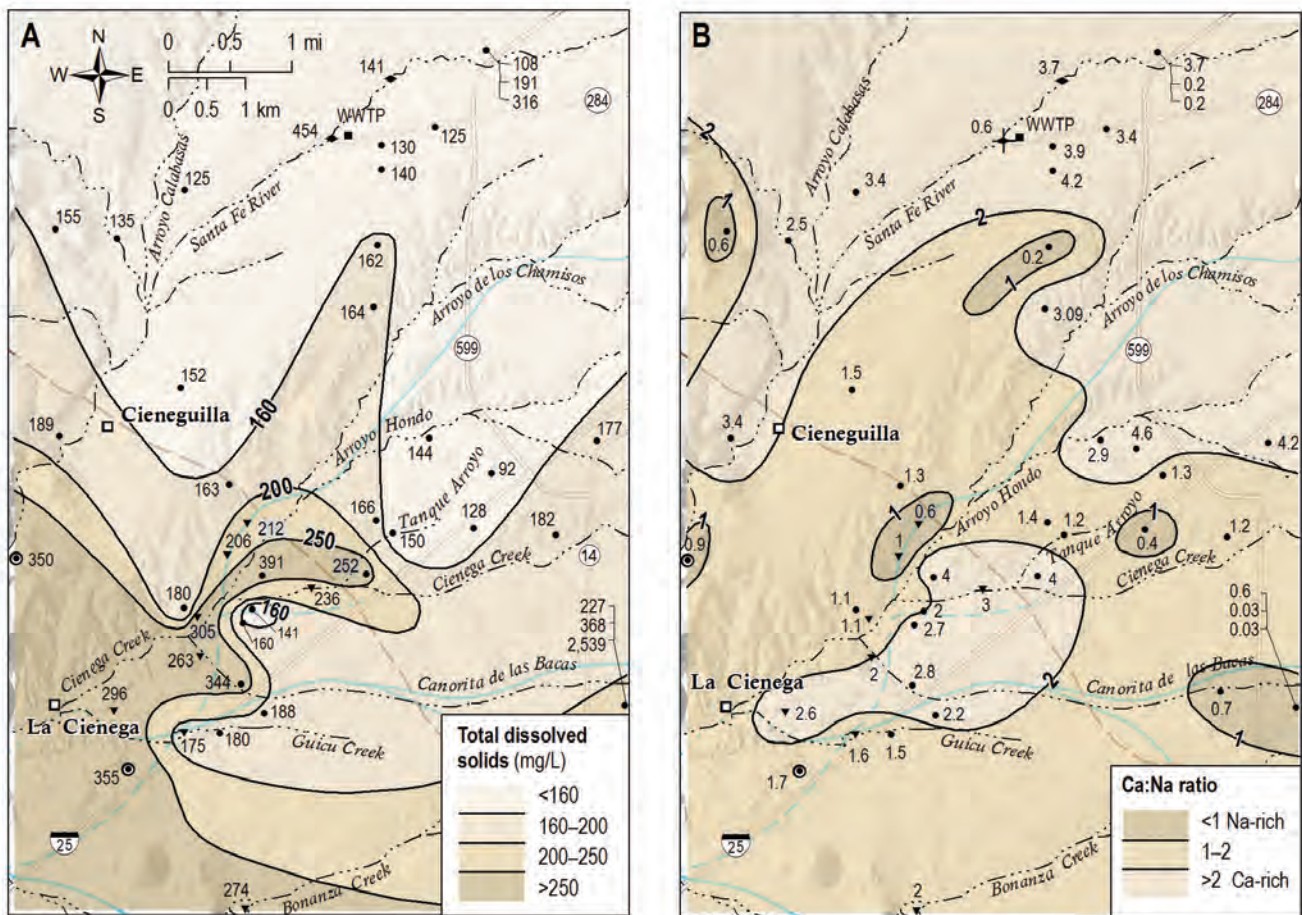


Figure 31. Maps showing distribution of: A—total dissolved solids (TDS), and B—ratios of calcium to sodium, in groundwater from wells and springs. These parameters are general indicators of relative groundwater residence time in the SFG aquifer. Results demonstrate mixing of shallow and deep sources of groundwater near the hinge zone. Chemistry data are presented in Table 11.

- Well, Santa Fe Group
- Well, Galisteo Fm
- ▼ Spring
- ◆ Surface water
- Rancho Viejo hinge zone (Fig. 5)
- Buried valley (Fig. 12)
- Stream or arroyo

Table 12. Isotopic and groundwater age data for well, spring and stream waters shown on Figures 34–36. Sample sites are shown on Figure 4.

Site ID	Site type	Sample date	$\delta^{2\text{H}}$ (‰)	$\delta^{18\text{O}}$ (‰)	${}^3\text{H}$ (TU)*	$\delta^{13\text{C}}$ (‰)	${}^{14}\text{C}$ activity (pmC)	${}^{14}\text{C}$ error (pmC)	${}^{14}\text{C}$ apparent age (RCYBP)	${}^{14}\text{C}$ apparent age error (RCYBP)
EB-223	well	10/4/11	-80.10	-12.17	0.03	-9.9	26.13	0.16	10,780	50
EB-303	well	6/22/11	-74.68	-10.33	0.90	-14.5	58.70	0.21	4,280	30
EB-313	well	6/22/11	-86.54	-12.06	0.01	-10.1	40.6	0.2	7,240	40
EB-315	well	5/11/05	-83.40	-12.01						
EB-328	well	6/7/05	-94.12	-12.89						
EB-332	well	7/21/11	-79.98	-11.53	0.04	-10.6	43.37	0.21	6,710	40
EB-336	well	4/8/05	-103.58	-14.27		-5.53			36,800**	
EB-337	well	4/8/05	-113.33	-15.65		-8.16			38,400**	
EB-338	well	4/9/05	-83.23	-12.34	<0.02**	-11.6			5,300**	
EB-364	well	10/20/11	-77.13	-11.66	-0.01	-14.1	47.03	0.23	6,060	40
EB-366	well	10/20/11	-78.14	-11.72						
EB-373	well	10/20/11	-77.53	-11.75	-0.05	-13.2	34.03	0.17	8,660	40
EB-386	well	6/1/05	-99.60	-14.20						
EB-607	well	9/26/06	-81.18	-11.49						
LC-003	spring	6/1/11	-80.52	-11.24	0.42	-11.6	65.41	0.24	5,720	30
LC-006	well	6/21/11	-79.47	-11.10	1.73	-10.6	82.45	0.30	5,140	
LC-007	spring	6/22/11	-84.83	-11.89					3,410	30
LC-008	spring	6/22/11	-79.36	-11.13	0.41	-14.2	73.44	0.27	3,390	30
LC-016	spring	6/22/11	-84.93	-11.89	0.05	-12.1	50.93	0.19	1,550	30
LC-017	spring	3/25/11	-79.43	-10.87						
LC-018	spring	3/25/11	-81.36	-11.27					2,480	30
LC-019	spring	3/25/11	-80.77	-11.15					5,420	30
LC-020	spring	3/25/11	-80.77	-11.07						
LC-021	spring	3/25/11	-80.26	-11.11						
LC-022	spring	3/25/11	-77.49	-10.43						
LC-026	well	10/4/11	-77.36	-11.6						
LC-033	effluent	8/30/12	-86.53	-12.12						
LC-001A	spring	6/1/11	-80.98	-11.41	0.04	-11.2	49.06	0.18		
LC-001B	spring	11/8/13	-78.60	-11.27	0.10	-16.1	52.7	0.2	4,860	30
LC-005‡	spring	6/1/11	-80.70	-11.37	0.11	-16.1	65.57	0.24	2,880	
LC-037‡	spring	11/8/13	-78.90	-11.09	0.14	-19.7	83.6	0.3		
LC-023A	spring	7/20/11	-83.47	-11.62	0.13	-12.6	54.61	0.20		
LC-023B	spring	11/8/13	-82.40	-11.74	0.33	-17.7	69.9	0.3	1,440	

‰ – per mil (parts per thousand)

TU – tritium units

* Standard analytical error for ${}^3\text{H}$ in all samples is 0.09 TU. Results less than 0.1 TU are effectively below the method detection limit.

pmC = percent modern carbon

RCYBP = radiocarbon years before present (1950), Cambridge half-life 5,730 +/-40 yr

** Manning (2009); Adjusted ${}^{14}\text{C}$ age (RCYBP) calculated using Libby half-life, 5568 +/-30 yr: EB-336, 35,400; EB-337, 33,700; EB-338, 400–4700

‡ LC-005 was resampled at upstream location as LC-037 in Nov. 2013. The first emergence of groundwater migrated upstream following September 2013 monsoon storm events.

calcium-sodium content in La Cienega waters. The variation is expressed spatially in compositional zones of increasing sodium across the Rancho Viejo hinge zone, where thickness of the SFG aquifer changes most dramatically. The region of highest calcium content lies between Cienega Creek (yellow dots and triangles) and Guicu Creek (orange dots and triangles), which is southwest of the hinge zone where the SFG aquifer is thinnest. Wells and springs with the largest sodium content (green dots and triangles near Arroyo Hondo) are located along the ancestral Santa Fe River buried valley or northeast

of the hinge zone. These Na-rich wells and springs have a similar chemistry as some deep wells in the Tesuque Formation. Spatial differences in the ion chemistry result from mixing different proportions of shallow and deep water sources where flow paths from multiple depths converge. Buried valleys in the Ancha Formation and the Rancho Viejo hinge zone influence the upward movement of deep Na-rich groundwater and the compositional differences between wetland zones. Mixing of groundwater from different sources, depths and pathways is conceptually illustrated in Figure 23.

Chloride in shallow groundwater and waste-water discharge

The movement of chloride in groundwater is conservative in most natural systems. The regional study by Johnson et al., (2008) showed that chloride is generally present in the SFG aquifer near Santa Fe at concentrations below 10 mg/L, with higher concentrations (10 to 60 mg/L) near the mountain front and around the perimeter of the basin. Chloride distribution near La Cienega follows a similar pattern (Fig. 33A). Concentrations are generally lower than 10 mg/L, but increase with depth in the SFG aquifer, near the basin margin, and in the Cienega Creek discharge zone. The presence of elevated chloride, TDS and sodium focused in the Cienega Creek wetlands is another indicator that groundwater discharging to wetlands is a mixture of shallow and deep sources.

Discharge water collected near the outlet of the Santa Fe WWTP in August 2012 (LC-033, Table 11)

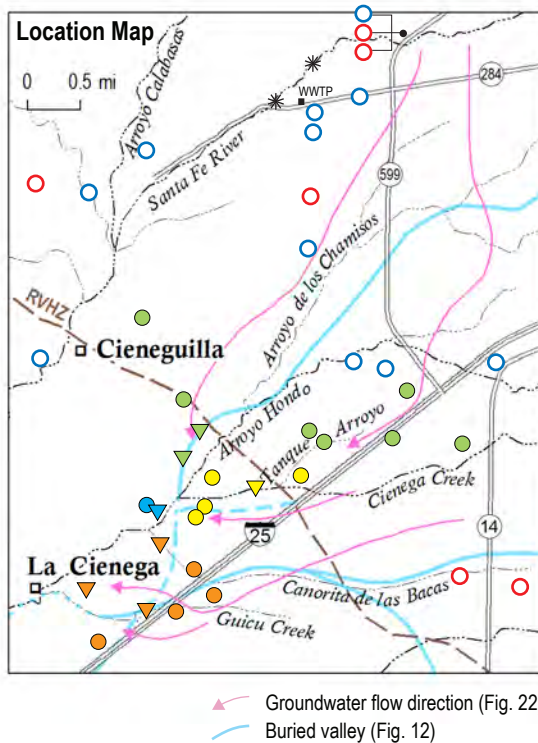
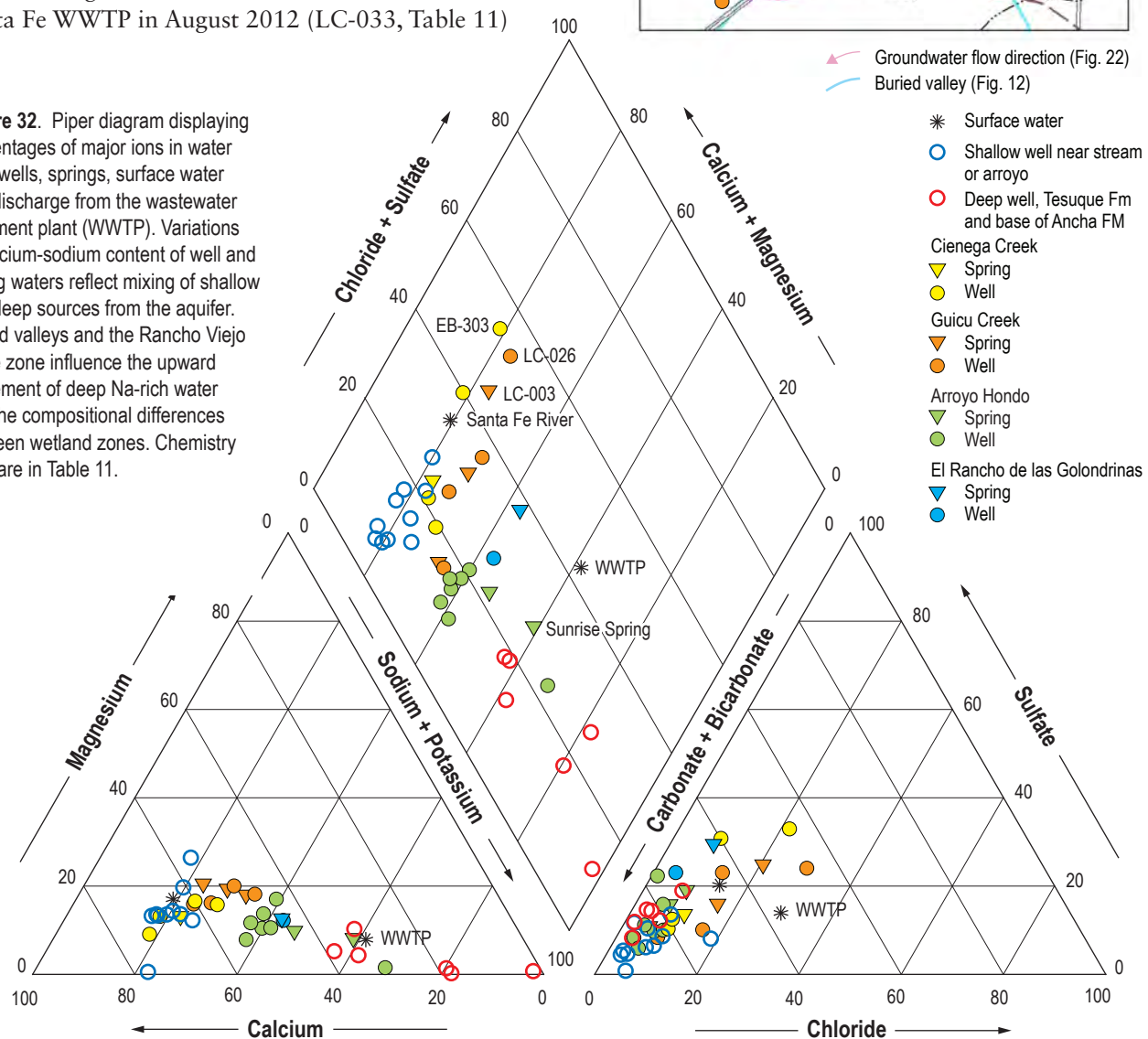


Figure 32. Piper diagram displaying percentages of major ions in water from wells, springs, surface water and discharge from the wastewater treatment plant (WWTP). Variations in calcium-sodium content of well and spring waters reflect mixing of shallow and deep sources from the aquifer. Buried valleys and the Rancho Viejo hinge zone influence the upward movement of deep Na-rich water and the compositional differences between wetland zones. Chemistry data are in Table 11.



has a unique ion signature compared with well and spring waters near La Cienega (Figs. 32 and 33). It contains sodium, calcium, bicarbonate, and the highest Cl content observed in waters of the study area. Chloride is typically elevated in wastewater (Linsley et al., 1992) and was notably high (75 mg/L) in the 2012 discharge sample. The concentration of chloride in five discharge samples collected between June 2005 and March 2006 varied from 50 to 72 mg/L, with a mean of 63 mg/L (A. Lewis, written communication).

From the Piper diagram (Fig. 32), we can evaluate whether treated wastewater discharge mixes with groundwater near La Cienega. With mixing, the compositions of both contributing waters and their mixture display along a line, in the same proportions, on each plot of the Piper diagram (Hounslow, 1995). If simple mixing were occurring between chloride-rich WWTP discharge and low-chloride groundwater,

this would be clearly demonstrated on the Piper plot. A mixing scenario for WWTP discharge is not visible in the La Cienega Piper diagram.

Applying chloride, in conjunction with the bromide ion (Br), is useful in reconstructing the origin and movement of groundwater (Davis et al., 1998). The spatial distribution of Cl and Cl/Br ratios (Fig. 33B) is used in this study to assess the movement of groundwater, treated wastewater, and natural recharge through the aquifer near La Cienega. Bromide, like chloride, behaves conservatively in groundwater, but bromine is generally 40 to 8,000 times less abundant in the environment than chlorine (Davis et al., 1998). Consequently, relatively small changes in the total mass of bromide in water give rise to large variations in ratios of Cl/Br, which are distinct for various natural and anthropogenic sources. Atmospheric precipitation generally has mass ratios between 50 and 150, but published values are

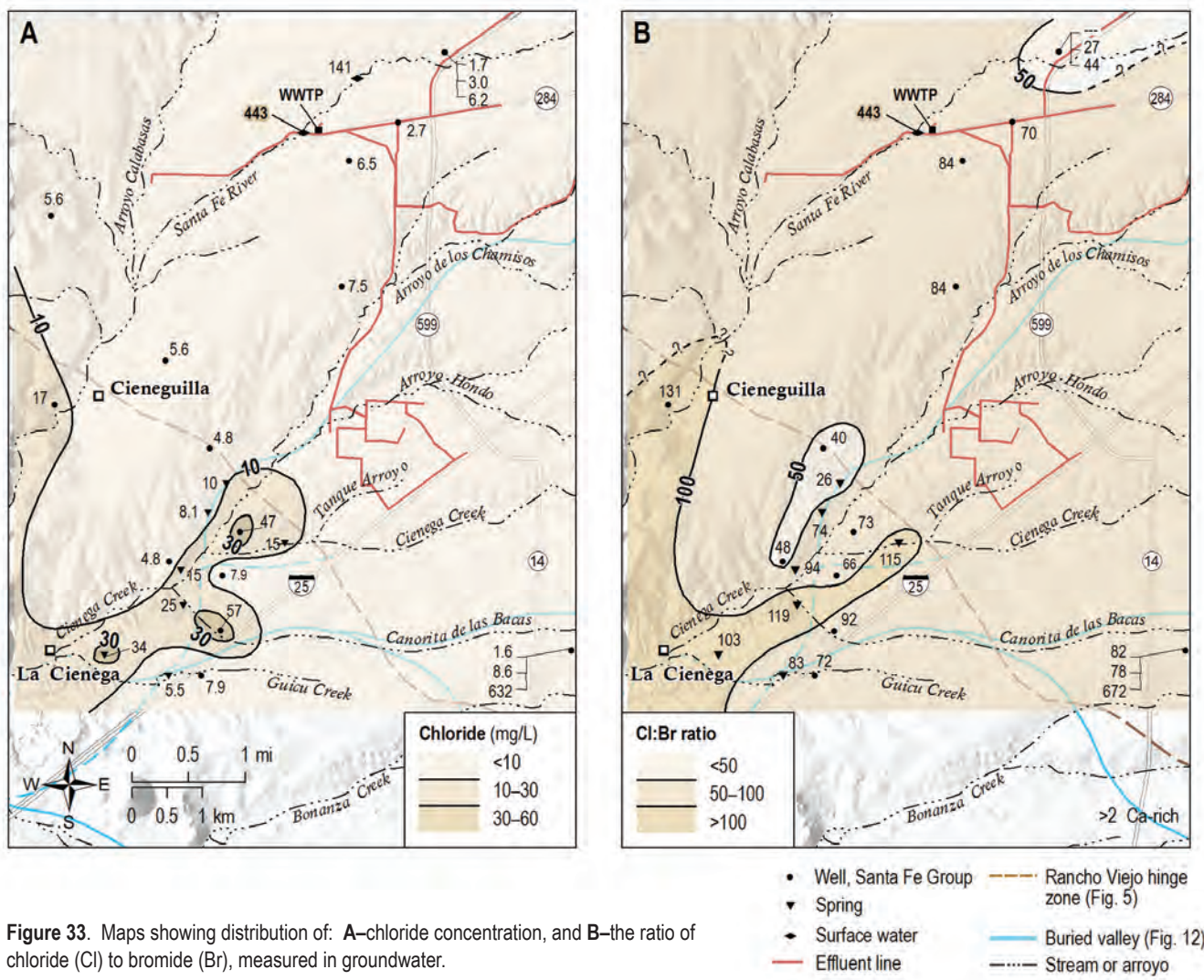
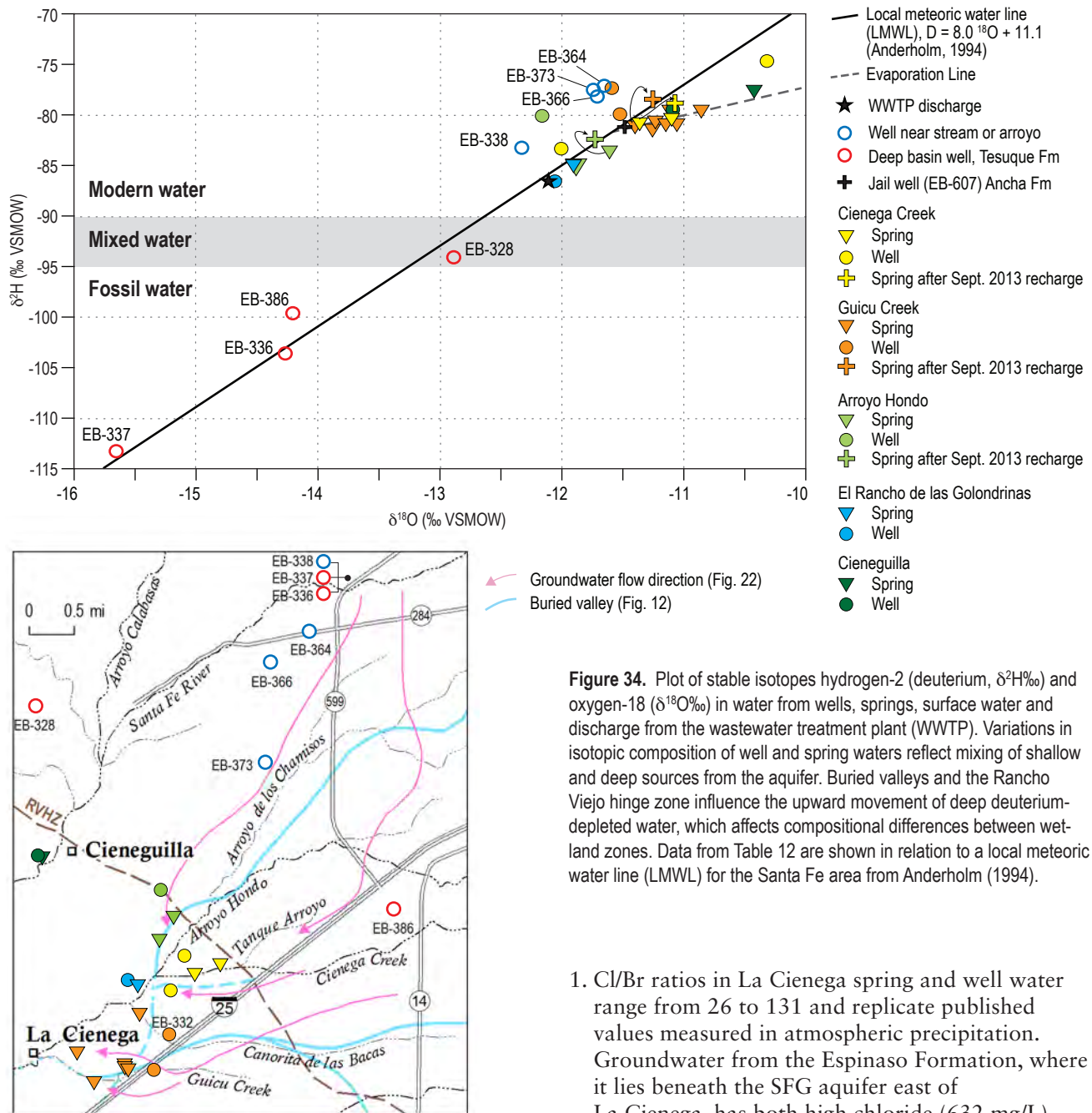


Figure 33. Maps showing distribution of: A—chloride concentration, and B—the ratio of chloride (Cl) to bromide (Br), measured in groundwater.



as low as 24 for rain and 3 for snow (Davis et al., 1998; Harriss and Williams, 1969). Shallow groundwater is between 100 and 200, but can be lower; urban runoff unaffected by salt, between 10 and 100; domestic sewage, between 300 and 600; volcanic rocks, between an average of 500 and 545; and water affected by halite, between 1,000 and 10,000 (Davis et al., 1998). Our conclusions regarding the movement of groundwater, wastewater and recharge in the aquifer near La Cienega wetlands, drawn from Figure 33 and published values of Cl/Br ratios, are summarized below.

1. Cl/Br ratios in La Cienega spring and well water range from 26 to 131 and replicate published values measured in atmospheric precipitation. Groundwater from the Espinaso Formation, where it lies beneath the SFG aquifer east of La Cienega, has both high chloride (632 mg/L) and a high Cl/Br ratio (672), which are consistent with volcanic deposits (EB-605, Table 11). A spring (LC-003) and well (LC-026) near wetlands east of Cienega Creek show high values of Cl and Cl/Br ratios, but there is no conclusive evidence that deep saline water from the Espinaso Formation mixes with wetland groundwater.
 2. The Cl content and Cl/Br ratio for discharge from the WWTP is significantly higher than any ground-water sampled in the study area. There is no chloride-bromide signature of WWTP discharge in the local aquifer system.

3. The recharge mound beneath the Santa Fe River corridor, upstream of the WWTP, and a shallow groundwater zone near Sunrise Springs have similar Cl/Br ratios that range between 26 and 48. These notably low Cl/Br ratios correspond to values reported for inland rain and snow. The low Cl/Br zone near Sunrise Springs, which coincides with the ancestral Santa Fe River buried valley, could represent focused recharge along Arroyo Hondo and/or movement of groundwater originating from the Santa Fe River recharge mound.

Isotopic Characteristics and Groundwater Residence Time

Stable isotopes of hydrogen ($\delta^2\text{H}$) and oxygen ($\delta^{18}\text{O}$)—Stable isotope values for hydrogen and oxygen in groundwater and WWTP discharge (Table 12) are plotted in Figure 34 with a local meteoric water line (LMWL) developed by Anderholm (1994) from precipitation collected near Santa Fe. Values for the waters vary from 74.7 to 113.3‰ $\delta^2\text{H}$ and 10.3 to 15.6‰ $\delta^{18}\text{O}$. The isotopic composition of springs and shallow well waters varies over a small range (86.5 to 74.7‰ $\delta^2\text{H}$ and 12.1 to 10.3‰ $\delta^{18}\text{O}$) that overlaps with the composition of modern surface flow in the Santa Fe River and Arroyo Hondo reported by Anderholm (1994) (-92 to -68‰ $\delta^2\text{H}$ and -13.2 to -10‰ $\delta^{18}\text{O}$). The isotopic similarity between surface water and shallow groundwater is consistent with the general view that groundwater discharging at La Cienega originates as runoff from the southern Sangre de Cristo Mountains, specifically through these two major drainages.

Deuterium depletion ($\delta^2\text{H}$ more negative than -95‰) in deep groundwater from the Tesuque Formation indicates that these waters were recharged during a much colder climate in the late Pleistocene (see EB-336, EB-337, and EB-386, Fig. 34 and Table 12). Using a regression of ^{14}C age data for groundwater by Manning (2009) and new deuterium data from the same well sites, Johnson et al., (2013) demonstrated that a deuterium composition in the Española Basin of <-95‰ corresponds to fossil groundwater with residence times between about 13,000 and 30,000 RCYBP. Deuterium enrichment ($\delta^2\text{H}$ less negative than -90‰) in groundwater from springs and wells in La Cienega indicates that these shallow waters were recharged after the end of the Pleistocene, or more recently than about 10,000 years ago. Groundwater compositions falling between fossil groundwater and modern

surface water in Figure 34 (EB-328, -94‰ $\delta^2\text{H}$, for example) reflect a mixture of old and young waters.

The plot of isotopic composition (Fig. 34) informs us about two hydrologic processes that affect wetland waters: evaporation and mixing. Data grouped below a meteoric water line generally reflect the effects of intensive evaporation (Craig, 1961). In Figure 34, most well water lie at or above the LMWL, whereas all spring water lies below the LMWL. Spring samples from Guicu Creek (orange triangles) and east of Cienega Creek (yellow triangles) group below the LMWL along a line with a slope of 2.7, which indicates that this groundwater has been altered by evaporation from the shallow water table prior to or during discharge.

Evaporative loss from shallow groundwater is typical of arid-region alluvial aquifers (Clark and Fritz, 1997). The springs most affected by evaporation are LC-003, LC-017, LC-018, LC-019 and LC-020 in Guicu Creek and LC-021 in Cienega Creek (see Fig. 4 for locations). Some of these same spring samples also show enrichment of Cl and SO_4 , which is consistent with evaporation from shallow wetland groundwater (Fig. 32, LC-003 for example). The evaporation line indicates that spring waters in Guicu and Cienega Creeks evaporated from groundwater with a composition the same as that measured in well EB-607 (black cross), which is located east of state road 14 in the thick Ancha saturation zone (Figs. 4 and 14).

Mixing of shallow and deep water sources at the wetlands is shown by spatial groups of isotopically depleted and enriched waters that vary in their ^2H and ^{18}O content across the Rancho Viejo hinge zone. Waters from Guicu Creek and Cienega Creek on the eastern slopes of the Cienega Creek valley are enriched in ^2H and ^{18}O and group together at the top of the LMWL (Fig. 34). These waters lie southwest of the hinge zone near buried valleys in the Ancha Formation. Wells and springs that are depleted in ^2H and ^{18}O (more negative values) are located west of Cienega Creek in El Rancho de las Golondrinas and lower Arroyo Hondo. These isotopically depleted waters lie along the ancestral Santa Fe River buried valley or northeast of the hinge zone, and contain a larger portion of deep ground-water from the Tesuque Formation. Spatial differences in isotopic content result from mixing different proportions of shallow and deep water sources, and mirror similar differences in ion content shown on the Piper diagram (Fig. 32).

Radioisotopes (^3H and ^{14}C) and groundwater

residence time—The tritium and carbon-14 data from wells and springs surrounding the wetlands indicate that groundwater of different ages intermixes in the La Cienega area. Groundwater has ^{14}C ages between 10,780 and 1,550 RCYBP and ^3H contents of 0.01 to 1.73 TU, indicating the presence of very old water that in places is combined with modern, or post-1952, recharge (Fig. 35, Table 12). The oldest groundwater (>6,500 RCYBP) comes from wells in the Tesuque and Ancha Formations north of La Cienega, between the Santa Fe River and Arroyo Hondo. Well EB-332 in the upper Guicu Creek drainage, east of Interstate 25, also produced water with an older ^{14}C age. Tritium contents for these older well waters are below detection limits (≤ 0.05 TU). The youngest groundwater from a shallow well adjacent to the Santa Fe River in La Cieneguilla has a ^3H content of 1.73 TU and a ^{14}C age of 1,550 RCYBP. Conflicting ^3H and ^{14}C data indicate that waters of different ages are mixing. When this occurs, each water dilutes the age signature of the other and neither method provides an accurate age. A combination of intermediate ^{14}C ages and low levels of ^3H can only be formed by combining water older than ~5,500 RCYBP with water recharged in the last 50 years.

Groundwater from springs near La Cienega is generally younger (higher ^3H content and higher ^{14}C activity) than groundwater sampled from wells. Spring samples average 0.19 TU, compared with 0.13 TU for wells; and average 60 pmC in ^{14}C activity, compared with 42 pmC in wells. These results indicate that spring discharge contains a larger portion of recent recharge than deeper well waters, which is consistent with the conceptual model of how groundwater from different aquifer zones mixes in a discharge area (Fig. 23).

Spatial differences in the age of groundwater east and west of the Cienega Creek valley replicate the differences observed in the water's ion and stable isotope content (discussed in previous sections, Figs. 32 and 34). Groundwater from springs and wells east of Cienega Creek is relatively younger, with ^{14}C ages between 2,480 and 5,720 RCYBP and tritium concentrations between 0.04 and 0.9 TU (Table 12 data from 2011 samples). Springs and wells west of Arroyo Hondo and Cienega Creek have notably older ^{14}C ages (4,860 to 10,780 RCYBP) and lower ^3H contents (0.01 to 0.13 TU). These spatial differences in age between east and west wetland zones result from mixing of deep and shallow water sources and different pathways of groundwater movement through the El Dorado and ancestral Santa Fe River buried valleys.

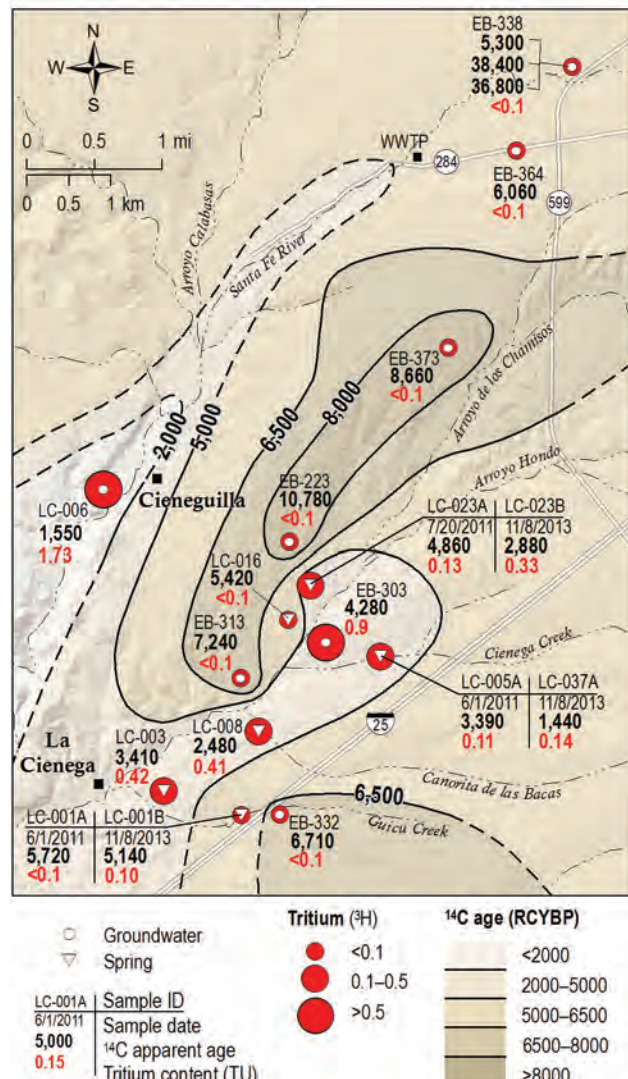


Figure 35. Contoured distribution of the apparent ^{14}C age of groundwater (RCYBP), shown with tritium (^3H) content (tritium units, TU), in La Cienega wells and springs. Three springs, resampled in November 2013 following heavy September storms, showed a slight increase in tritium content and a significant decrease in apparent ^{14}C age of discharging groundwater. Isotopic and age data are presented in Table 12.

Changes in groundwater isotopes and ages following the 2013 monsoon

Three springs sampled in June–July 2011, at the end of an eight-month drought, were resampled in November 2013 following the wettest summer monsoon in three years. Significant increases in spring and stream discharge were widely observed during and after large storms in September 2013, and water levels rose in local wells (Figs. 25 and 30). Well LC-025 recorded a water-table rise of nearly 6 feet within a 12-hour period on September 15, 2013 in direct response to a 2-inch rain event. The purpose of resampling was to

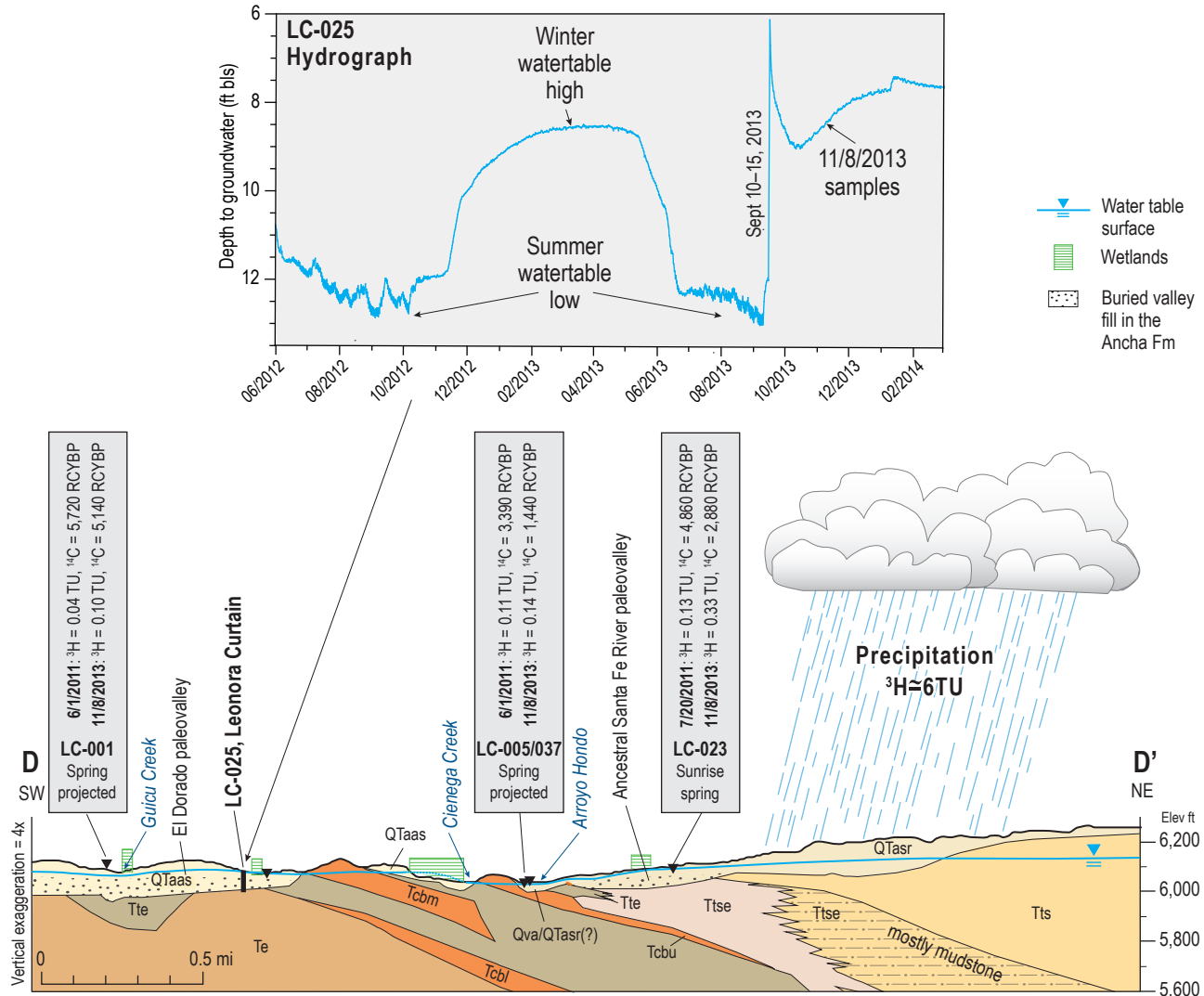


Figure 36. Age dating of wetland spring discharge shows that ${}^3\text{H}$ content increased and apparent ${}^{14}\text{C}$ ages decreased in samples (LC-001, LC-005/037, LC-023, Table 12) taken after large monsoon storms in September 2013, compared to samples from the preceding drought period in June-July 2011. The rapid water-table rise and decreasing groundwater ages demonstrate that storm recharge to high permeability aquifer zones occurs through quick infiltration, rapid mixing and discharge to springs and wetlands.

investigate whether and how isotopic and age characteristics of pre-monsoon groundwater might change in response to recent, local, storm-generated recharge. The sites resampled were: (1) Sunrise Spring (LC-023), which discharges groundwater from ancestral Santa Fe River channel deposits; and (2) small springs in Cienega Creek (LC-005/037) and Guicu Creek (LC-001), which are associated with the El Dorado buried valley. The samples were analyzed for stable isotopes of hydrogen ($\delta^{2}\text{H}$) and oxygen ($\delta^{18}\text{O}$), ${}^{14}\text{C}$ and ${}^3\text{H}$; data are included in Table 12. The hydrogeologic setting, the water-level hydrograph from 2013, and the chemical characteristics of

groundwater before and after the September 2013 storms are illustrated in Figure 36.

Results of the resampling demonstrate that the isotopic and age characteristics of spring discharge changed significantly between June 2011 and November 2013. Higher ${}^3\text{H}$ content and younger ${}^{14}\text{C}$ ages in all post-storm samples (Figs. 35 and 36, Table 12) confirm that a significant volume of storm-derived recharge was added to the wetland aquifer system. Stable isotope compositions for springs in Arroyo Hondo (23A and 23B) and Guicu Creek (1A and 1B) shifted between June-July 2011 and November 2013 from values showing

evaporation to values equivalent to local precipitation (Fig. 34). The comparison of groundwater chemistries before and after large September storms indicates that local precipitation infiltrated rapidly to raise groundwater levels and augment spring discharge. These interpretations assume that samples collected in June-July 2011 still represent the chemical conditions of local groundwater during the drought-affected summer of 2013.

Summary of Chemical and Isotopic Investigations

The chemistry and age characteristics of spring and shallow well waters illustrate aspects of wetland hydrology that are critical to the successful conservation of wetland resources.

1. Groundwater mixing

Shallow and deep groundwater zones in the SFG aquifer have distinctive chemical, isotopic and age characteristics. Groundwater samples from depth-specific piezometers located northeast of La Cienega, beyond the Rancho Viejo hinge zone, show that sodium, chloride, TDS and apparent age increase, and the ^2H and ^{18}O content becomes more depleted, with depth in the SFG aquifer. These chemical differences also distinguish waters in shallow and deep wells in the study area. Spring discharge exhibits ion and stable isotope chemistries, and young (^3H) and old (^{14}C) age markers, that demonstrate the wetland waters are a mixture of shallow and deep sources (Figs. 31–35).

2. Two wetland zones at Cienega Creek

Wetland spring zones have unique chemical, isotopic and age characteristics depending on their location east or west of Cienega Creek and relative to the Rancho Viejo hinge zone (Figs. 31–35). The eastern spring zone (Cienega Creek, Guicu Creek and Cañorita de las Bacas) is controlled by the El Dorado buried valley system and lies southwest of the hinge zone. The chemical signature of these springs indicates a larger portion of recent, local recharge. The western spring zone (Arroyo Hondo, Sunrise Springs, and

El Rancho de las Golondrinas) is controlled by the ancestral Santa Fe River buried valley northeast of the hinge zone. Eastern springs contain a higher portion of older deep groundwater from the Tesuque Formation. Spatial differences in chemistry between the two spring zones reflect the different mixtures and pathways of groundwater movement through the two buried valley systems. Exceptionally low chloride-to-bromide (Cl/Br) ratios in groundwater near Sunrise Spring (western spring zone) correspond to values reported for inland rain and snow and possibly link this discharge zone with old Santa Fe River recharge from the northeast (Fig. 33B).

3. Wastewater discharge

Wastewater discharge exhibits ion chemistry (sodium, calcium, and bicarbonate with high chloride) and a Cl/Br ratio (443) that is unique from all other well and spring water sampled in the study area. By using Cl content and Cl/Br ratios to reconstruct the movement of wastewater through the aquifer (Fig. 33), it is clear that there is no physical mixing of wastewater effluent and natural groundwater between the WWTP and La Cienega. The Piper diagram (Fig. 32) leads to the same conclusion. Well and spring waters in La Cienega are not chemically influenced by treated wastewater.

4. Storm-generated recharge

Large storms produced 3.7 inches of precipitation near La Cienega in mid-September 2013, increasing stream and spring discharge and raising water levels in wells (Fig. 36). Resampling Sunrise Spring (LC-023), a spring in Guicu Creek (LC-001), and the head of Cienega Creek (LC-037) following the storms showed that the isotopic and age characteristics of spring discharge changed significantly between June-July 2011 and November 2013. Higher ^3H content, younger ^{14}C ages, and a shift in stable isotope composition from evaporated water to that of local precipitation, was indicated in all post-storm samples. The results demonstrate rapid infiltration and enhanced local recharge, which are characteristic of the high hydraulic conductivity of coarse gravel-sand, buried-valley deposits.



One of the many ponds found along Cañorita de las Bacas in the Leonora Curtin Wetland Preserve.

VI. SUMMARY AND DISCUSSION

La Cienega's springs and wetlands are important hydrologic, ecologic and cultural resources. Wetlands provide many beneficial water-related functions that include integrating groundwater and surface water, flood and erosion control, protecting water quality, providing water for acequia irrigation and riparian habitats, and sustaining unique ecosystems. The wetlands discharge groundwater from regional and local aquifers that provide the sole water source for the southern Santa Fe region. We understand the wetland system by examining hydrologic interactions expressed in the water balance (Figs. 15 and 23). This investigation addresses all aspects of the wetland system, including:

1. The links between geology, groundwater flow, and wetland location (Figs. 6–14)
2. Groundwater conditions surrounding the wetlands (Figs. 21–22)
3. Chemical, isotopic and age indicators of water sources for the wetlands (Figs. 31–36)
4. The effects of climate variability on streamflow and groundwater levels (Figs. 16–20, 30)
5. Wetland evapotranspiration (Figs. 24A–25)
6. Groundwater depletion and water-level declines (Figs. 24B and 27–29)

In this report, the various data are integrated into a physical, conceptual model of wetland hydrogeology, which can support and enhance wetland conservation plans. To be successful in their objectives, hydrologic models and wetland management plans must incorporate the hydrogeologic features that create and maintain the wetlands.

Geology, Groundwater, and Wetlands

The groundwater that feeds springs and wetlands discharges from the Santa Fe Group aquifer, which is a regional system of thick deposits of sand, gravel, silt, and clay of the Tesuque Formation, overlain by shallow, thin, coarse deposits of the Ancha Formation. The wetlands at La Cienega are

located at the western edge of the basin, where the SFG aquifer thins and dissipates over older, low-permeability strata (Fig. 37). Thinning of the aquifer forces groundwater to the surface where it emerges from buried valleys in the Ancha Formation to maintain springs and seeps that create the wetlands. Groundwater stored in the Ancha Formation is the primary source of water for the wetlands. The accretion and storage of groundwater in the Ancha Formation depends on local recharge, upflow of deep groundwater from the Tesuque Formation, permeability contrasts between the Ancha and sub-Ancha formations (Figs. 10, 11 and 37), and the buried valleys at the base of the formation that direct groundwater flow and control wetland location (Fig. 12).

Buried-Valley aquifers in the Ancha Formation

Buried valleys in the Ancha Formation (Figs. 10, 12, 14) create coarse-grained, highly transmissive aquifers that take the form of long, narrow, ribbon-like channels scoured into less permeable underlying formations. Two large buried valleys are identified in the Ancha aquifer (Figs. 12 and 14). These buried valleys behave as drains that gather groundwater from the surrounding aquifer, concentrate flow, and direct discharge to the springs and wetlands (Spiegel, 1963; Johnson and Koning, 2012; Johnson et al., 2012). The El Dorado buried valley east of La Cienega directs water flow to wetlands at Las Lagunitas in Guicu Creek and at the Leonora Curtin Wetland Preserve in Cañorita de las Bacas. Wetlands in upper Cienega Creek are associated with a smaller channel parallel to the El Dorado buried valley.

Sunrise Springs and wetlands along the western slopes of the Arroyo Hondo valley are formed by the buried valley of the ancestral Santa Fe River. Buried-valley aquifers can be important sources of groundwater, but the coarse nature and relatively high hydraulic conductivity of the deposits increase the vulnerability of the aquifers to excessive drawdowns. Pumping from or adjacent to a buried valley leads to greater drawdown and more distant drawdown effects along the axis of the valley than in the adjacent

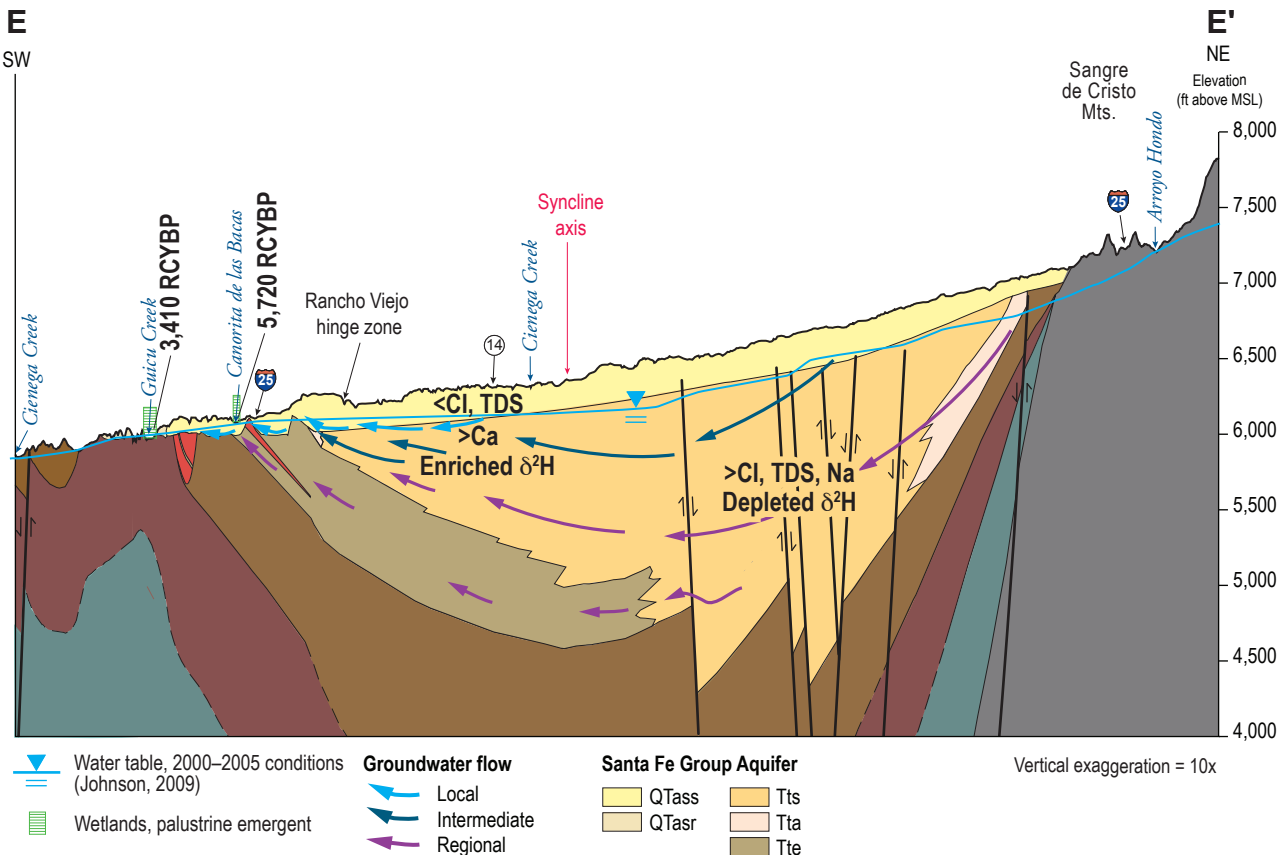


Figure 37. The regional hydrogeologic setting for groundwater-fed wetlands at La Cienega is illustrated in a west-to-east cross section located south of Santa Fe (see Fig. 5 for section location and Table 3 for geologic unit descriptions). Groundwater flows west across the basin and circulates to various depths within the Tesuque Formation, producing an age-stratified flow system. Groundwater from multiple flow paths collects in the Ancha Formation in the western third of the basin and discharges to wetlands along Guicu Creek, Canorita de las Bacas, and the eastern slopes of Cienega Creek.

finer-grained deposits (van der Kamp and Maathuis, 2012; Seifert et al., 2008; Weissmann and others, 2004).

Based on 2004 groundwater conditions, we estimate that the thickness of the Ancha saturation zone at the El Dorado buried valley ranged from about 30 feet at the edges to more than 100 feet near Las Lagunitas (Fig. 14). The smaller zone of saturation encompassing the ancestral Santa Fe River near Sunrise Springs was about 20 to 90 ft thick. We also estimate that the Ancha aquifer contained about 67,000 acre-ft of groundwater at the time.

Groundwater flow conditions surrounding the wetlands

Water-table maps of regional groundwater conditions in 2005 and local conditions in 2012 define groundwater flow paths and areas of recharge and discharge in the SFG aquifer near La Cienega (Figs. 21 and 22). The wetlands in Cienega Creek,

Arroyo Hondo, Guicu Creek, and Canorita de las Bacas receive groundwater from the SFG aquifer south of the Santa Fe River. A prominent recharge mound (water-table high) exists beneath the Santa Fe River between Agua Fria and approximately Arroyo Calabasas. Groundwater flows southwest from the water-table mound and diverges around finer-grained deposits in the Tesuque Formation located east of La Cieneguilla (Figs. 12 and 22) (Johnson and Koning, 2012). Some flow from Santa Fe River recharge upstream of NM-599 may contribute water to Sunrise Springs and the western slopes of Arroyo Hondo via the buried valley of the ancestral Santa Fe River. Groundwater discharge to the Cienega Creek wetlands originates from the SFG aquifer to the east via the El Dorado buried valley.

Sources of groundwater feeding the wetlands

As groundwater flows across the basin from the Sangre de Cristo Mountains it circulates to various

depths, creating an age-stratified aquifer (Fig. 37). Chemical, isotopic, and age (^{14}C and ^3H) data verify that wetland waters consist of a mixture of modern (post-1952) and older waters from shallow and deep aquifer zones, as well as recent storm recharge. These sources intermix at the edge of the basin, southwest of the Rancho Viejo hinge zone, where thickness of the SFG aquifer is less than 250 ft (Fig. 38).

The chemical and age characteristics of wetland waters are spatially distinctive depending on their buried-valley source, location east or west of Cienega Creek, and location relative to the Rancho Viejo hinge zone. The east wetland zone in upper Cienega Creek, Guicu Creek and Canorita de las Bacas discharges groundwater through the El Dorado buried valley and lies southwest of the hinge zone. The eastern springs exhibit relatively young ^{14}C ages (2,480 to 5,720 RCYBP uncorrected), small amounts of tritium (0.1 to 0.9 TU), and high concentrations

of calcium relative to sodium. These characteristics indicate a mixture of old groundwater and modern recharge derived from local storms. The west wetland zone at El Rancho de las Golondrinas and the western slopes of Arroyo Hondo (Sunrise Springs) is influenced by the buried valley of the ancestral Santa Fe River. The western springs are rich in sodium, have older ^{14}C ages (4,860 to 7,240 RCYBP uncorrected) and zero tritium, indicating a source dominated by older groundwater from the Tesuque Formation, north of the Rancho Viejo hinge zone. Stable isotope and ion chemistry show similar partitioning between east and west wetland zones and reinforce the conclusions drawn from groundwater age dating (Figs. 32 and 34).

Age dating of wetland spring discharge following the large monsoon storms in September 2013 shows that ^3H content increased and apparent ^{14}C ages decreased in samples taken after the storms compared with samples collected during the preceding drought

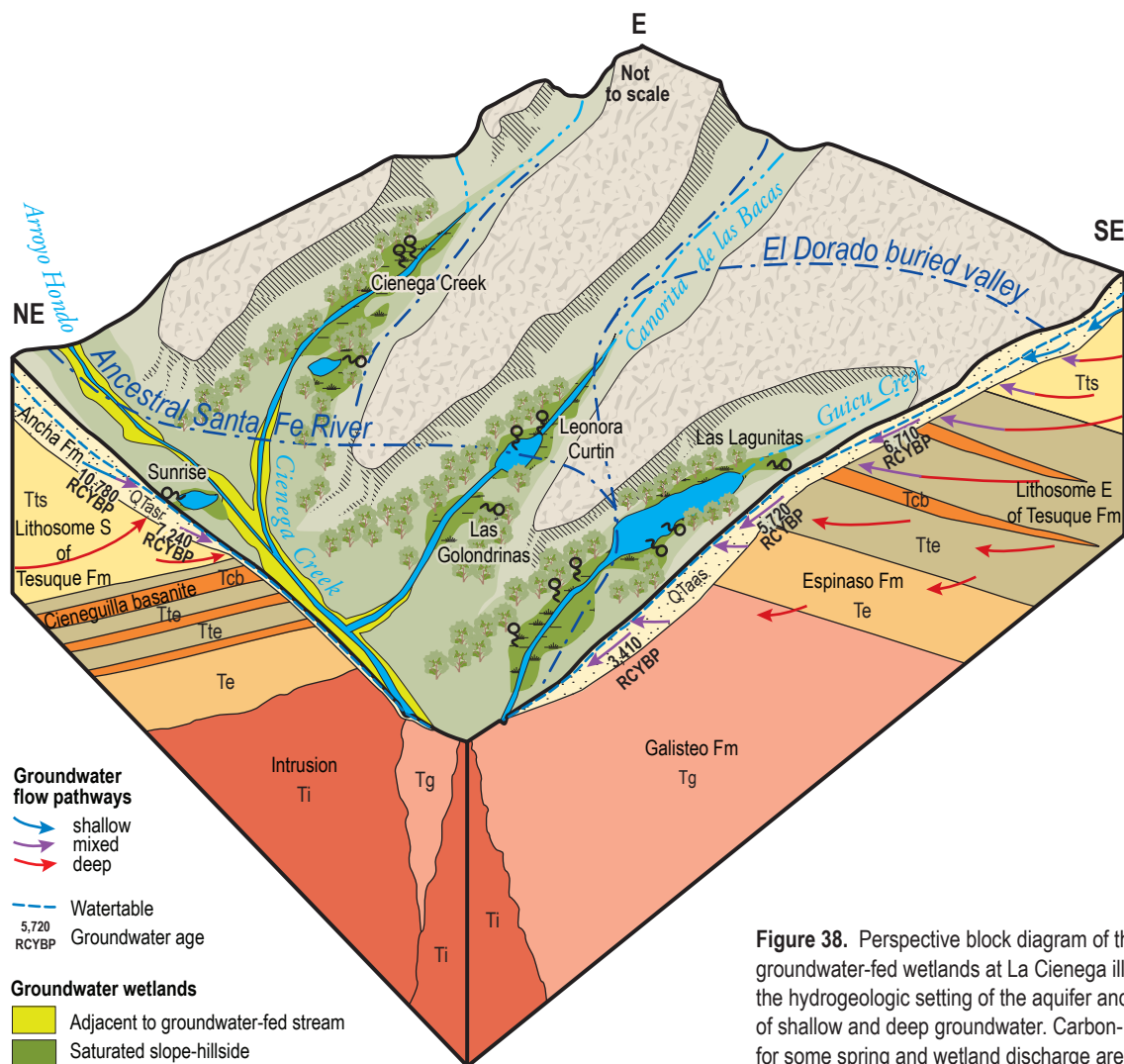


Figure 38. Perspective block diagram of the groundwater-fed wetlands at La Cienega illustrating the hydrogeologic setting of the aquifer and the mixing of shallow and deep groundwater. Carbon-14 ages for some spring and wetland discharge are listed.

period in June–July 2011. A rapid water-table rise coinciding with the storms, and decreasing spring-water ages following the storms, demonstrate rapid infiltration and enhanced local recharge, which are characteristic of the high hydraulic conductivity of coarse gravel-sand, buried-valley deposits. (Fig. 36).

Effluent discharge from the WWTP has a unique ion chemistry (sodium, calcium, and bicarbonate with high chloride) and chloride-bromide content relative to well and spring waters sampled in the study area. The Cl content, Cl/Br ratios and ion chemistry (Figs. 32 and 33) indicate that well and spring waters in La Cienega are not chemically influenced by treated wastewater.

Wetland Water Balance

The wetland water balance describes water inflows, outflows and changes in groundwater storage in the wetland (Fig. 15). Water inflow to the wetlands comes directly from groundwater and indirectly from precipitation transported to the wetlands through the groundwater and surface-water systems. Wetland outflows include evapotranspiration (ET), groundwater discharge to surface water, and groundwater withdrawals from wells, which became a significant anthropogenic impact to groundwater storage starting in the mid-20th century.

Groundwater storage and wetlands

Changes in groundwater storage reflect imbalances between recharge to and discharge from an aquifer. Storage changes manifest in fluctuations of the water-table surface and are documented by measuring groundwater levels over time. A long-term negative water balance (where discharge exceeds recharge) could result from prolonged drought, increased evaporation, well withdrawals and/or decreased recharge, and could lead to reductions or disruptions in groundwater discharge to springs, or elimination of springs and wetlands altogether. Drought, recharge, ET and groundwater depletion from pumping each generates a unique water-level variation, which is observable in groundwater hydrographs with high measurement frequencies. We examined how extreme wet and dry cycles, seasonal cycles, ET, and groundwater extraction affect wetland groundwater storage and surface-water discharge, by applying water-table fluctuation methods.

Climate variability and drought—Highly variable precipitation and streamflow, punctuated by periods of high runoff and drought, are characteristic of the upper Rio Grande in New Mexico. The Santa Fe area suffered severe to extreme drought conditions from April 2011 through July 2014 (<http://droughtmonitor.unl.edu/MapsAndData/MapArchive.aspx>), while the summer-monsoon months of 2013 were among the wettest on record (Fig. 17). Streamflow reconstructions for the upper Santa Fe River (Margolis et al., 2011) indicate that the 1950s and 2000s droughts were among the most extreme low-flow and drought events of the past seven centuries. Recent analysis of the region's climate variability (Gutzler and Robbins, 2011) indicates that droughts of the mid-20th century are likely to return with greater frequency as a result of climate change. Assessments of groundwater vulnerability to climate change have consistently projected that groundwater levels will be adversely affected by increasing the global mean temperature by 1.0°C, regardless of changes in rainfall (e.g., Rosenberg et al., 1999; Loáiciga et al., 2000). A warming climate is projected to increase evaporation and groundwater withdrawals, reduce recharge, and escalate groundwater depletion.

The groundwater-level response to climate events near La Cienega was revealed in a time-series comparison of local groundwater levels and monthly precipitation from extreme wet and dry periods. Wet-dry cycles were defined from the 90th and 10th percentile monthly precipitation values at the SFCMA weather station (Fig. 30, Table 10). The largest water-table spikes, about +1.2 feet, were seen in wells near the head of Cienega Creek following a record monsoon in 1991 and near the Santa Fe River following record snowmelt runoff in spring 2005. Small increases in the water table of +0.1 to +0.4 inches occurred when monthly precipitation exceeded 4 inches. Annual water-table cycles, with high water levels in fall following a summer monsoon and low levels in the spring, occur near the Santa Fe River (well EB-338) and in shallow Ancha wells east of the Cienega Creek wetlands (EB-607 and EB-220). The monsoon storm events in September 2013 coincided with rising groundwater levels in fall-winter 2014. Droughts lasting a year or more coincided with drops in the water table of 0.4 to 0.6 ft (well EB-220), but the drought-depressed water table was typically restored by post-drought rainfall.

Streamflow—Periodic measurements of streamflow in Cienega Creek have been taken since 1966 at the Cienega head gate (USGS station 08317150)

(Fig. 19A). Both the mean and median streamflow values equal 0.53 ft³/s as a consequence of the steady flows from groundwater discharge. Only four measurements ranging from 1.55 to 0.55 ft³/s were taken between 1966 and 1975. Measurements taken at more regular intervals beginning in 1986 indicate that post-1986 discharge was generally lower than pre-1986 flows, falling near or below the long-term mean. The variability of post-1986 data is small, with a standard deviation 0.09.

Streamflow at the Cienega head gate shows a strong seasonal variation where discharge is lowest during summer months and generally higher the rest of the year, despite a substantial increase in precipitation from the summer monsoon (Fig. 19A). The seasonal variation accounts for the small-scale variability in streamflow measurements and is associated with a summer water-table decline produced by higher ET (Figs. 24A and 25). Long-term streamflow variability relates to climate cycles and is most affected by multi-year drought. During the dry intervals of 2001–2004 and 2012, the average streamflow dropped to 0.48 and 0.38 ft³/s, respectively, and most measurements fell considerably below the long-term mean. Conversely, wet (1991) and average (1997) years of precipitation have an average streamflow (0.54 ft³/s) that closely matches the long-term mean.

Streamflow decline after 1966 cannot be attributed solely to drought. Comparisons of recent and historic measurements provide a means of estimating if, and how much, streamflow may have declined since the 1960s. Limited measurements prior to 1990 suggest that streamflow was generally higher during and before the mid-1970s than it has been since 1986. Streamflow in March 1966 (1.55 ft³/s) was exceptionally high for a dry year compared to measurements taken during the post-2001 droughts (March 1966 received 0.03 inches of precipitation). A comparison of the post-2001 mean non-summer streamflow (0.55 ft³/s) and the March 1966

measurement (1.55 ft³/s) implies that stream flow has declined at the Cienega head gate by roughly 1 ft³/s, or 64%, since 1966.

Evapotranspiration—Seasonal and daily fluctuations of the wetland water table at the Leonora Curtin Wetland Preserve relate to groundwater losses by ET. A seasonal variation with low summer water levels and high winter levels is common in wetland aquifers and documents a response to changes in ET between

growing and dormant vegetation stages (Carter, 1996; Vincke and Thiry, 2008). Paired measurements in summer-fall 2011 and winter 2012 show that groundwater levels in the Cienega Creek valley rose during winter months by +0.04 to +6.60 ft, while declining by -0.04 to -0.50 feet in areas outside of wetlands and valleys (Fig. 24A). Continuous monitoring at the Preserve shows that the spring water table drop closely follows leaf emergence and coincides with the start of a diurnal (12-hour) fluctuation. Diurnal fluctuations cease after killing frosts and just prior to the winter water-table rise. In 2012, the diurnal signal in well LC-025 at the Preserve began in early April, continued through the growing season, and ended in late October (Fig. 25). The diurnal cycle had a magnitude of about 0.1 to 0.2 ft. Large, summer water-level drops (-4.9 ft at LC-025 in 2012) indicate that ET produces a significant seasonal groundwater outflow from the wetlands. Managing invasive phreatophytes in the wetlands may reduce the magnitude of the summer water-level decline and increase groundwater discharge to wetlands, springs, and acequias when the agricultural demand is highest.

Groundwater depletion and declining water levels

Groundwater levels—Groundwater levels in the Ancha aquifer east of La Cienega have been dropping steadily since at least the early 1970s (Figs. 27 and 39). In one well monitoring the wetland aquifer (EB-220 near the racetrack), the water level has declined 7.5 ft since 1973, leaving a remaining saturated thickness of 31 ft (Figs. 27 and 28) (Johnson and Koning, 2012, Table 1).

Long-term groundwater depletion is driven largely by overexploitation, whereas shorter-term local trends in depletion are dominated by natural climate variability over months to years (Konikow, 2015). The long-term trends in declining groundwater levels documented near La Cienega cover periods of one to four decades, cross multiple precipitation cycles, and extend beyond the wetland area (Fig. 27). The groundwater declines are of the style discussed by Konikow (2015) and demonstrate an anthropogenic connection between groundwater depletion and unsustainable withdrawals from wells. The coarse nature and relatively high hydraulic conductivity of the buried-valley aquifers that maintain the wetlands enhances the drawdown response to pumping along the buried channels and aggravates groundwater depletion near the wetlands.

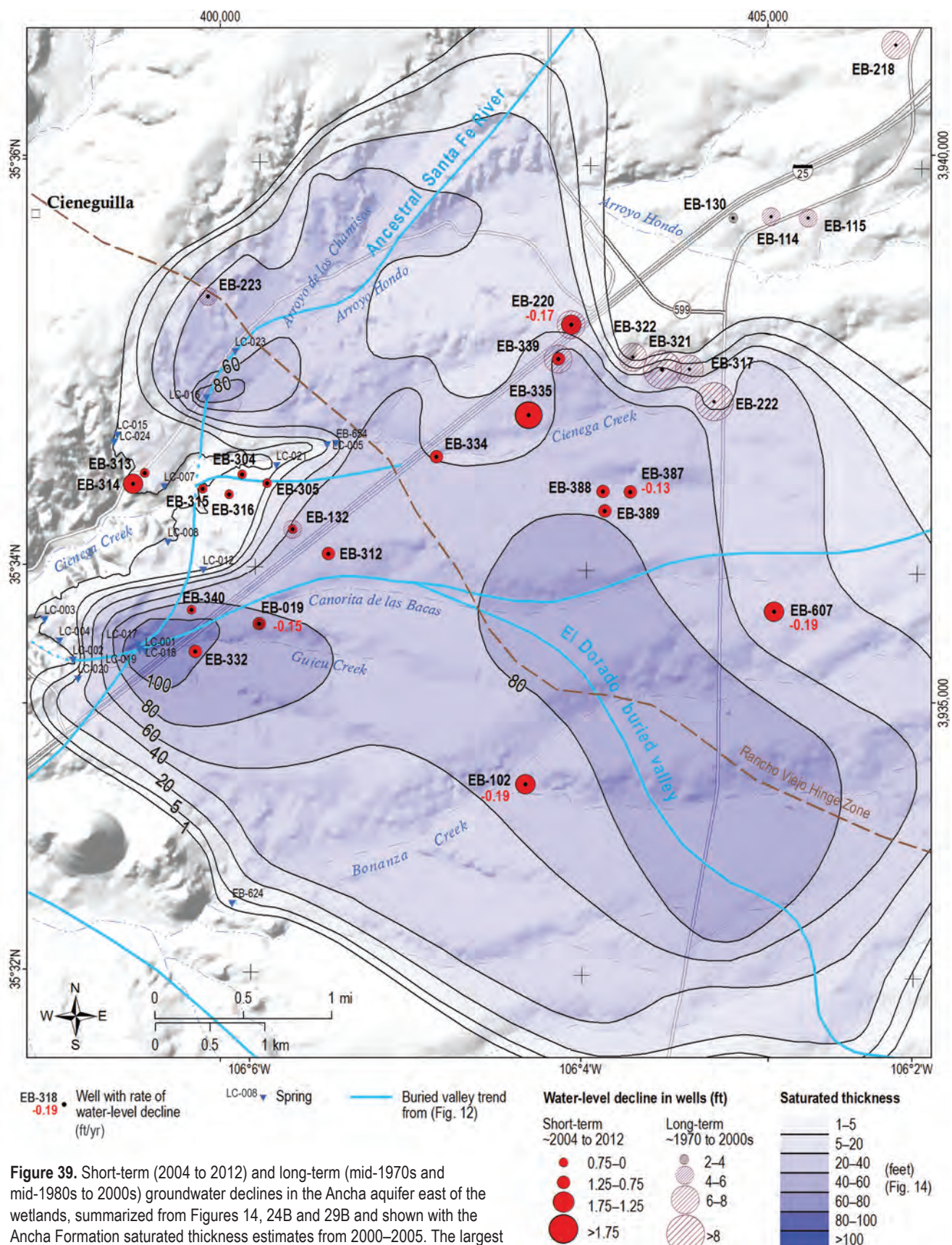


Figure 39. Short-term (2004 to 2012) and long-term (mid-1970s and mid-1980s to 2000s) groundwater declines in the Ancha aquifer east of the wetlands, summarized from Figures 14, 24B and 29B and shown with the Ancha Formation saturated thickness estimates from 2000–2005. The largest water-level declines are observed in the Valle Vista area east of Cienega Creek springs.

The largest declines in the Ancha aquifer occur immediately up-gradient (east) of the Cienega Creek valley (Fig. 29B). Water levels measured between 2004 and 2012 show an eight-year decline of as much as -1.9 ft (Figs. 24B and 39). Water-level measurements in the same wells over three to four decades show long-term declines of 7 to 9 ft (Figs. 29B and 39). The largest depletions and decline rates are observed in the Valle Vista and penitentiary areas, east and up-gradient of the La Cienega wetlands and along the margins of the Ancha zone of saturation.

Groundwater hydrographs with long records and high measurement frequencies near La Cienega show the cumulative effects of natural variations in precipitation and recharge superimposed on long-term declines (Fig. 30). The natural, short-term variations observed include: 1) seasonal groundwater fluctuations that manifest in high winter water levels and low summer water levels, and appear to be driven by monsoon-related recharge; and 2) recharge spikes such as occurred near the Santa Fe River from exceptionally high snowmelt runoff in spring 2005. Long-term declining trends in Ancha water levels are aggravated during drought, but time-series comparisons of groundwater levels and precipitation indicate that drought-depressed water tables are restored by large post-drought rainfall, while long-term declines continue. The unchanging, long-term declining trends in groundwater levels are a key indicator of human-caused groundwater depletions from wells (Konikow, 2015).

Building Hydrologic Resilience into the La Cienega Wetlands

The widespread, persistent depletion of groundwater in the Ancha aquifer, primarily associated with the unsustainable withdrawal of groundwater from wells, presents the greatest threat to springs and wetlands in La Cienega. Findings from this investigation of groundwater-fed springs and wetlands emphasize possible solutions towards hydrologic resilience and successful preservation of the important wetland resources at La Cienega. These solutions focus on reducing groundwater depletions in the Ancha Formation and supporting a positive wetland water balance. Possible remedies include:

- Eliminate groundwater withdrawals from areas near the ancestral Santa Fe River and El Dorado buried valleys;
- Manage the timing and location of groundwater withdrawals from the Ancha saturation zone to eliminate or reverse further losses to the Ancha aquifer near the wetlands;
- Utilize the natural recharge capabilities of buried-valley aquifers in the Ancha saturation zone and develop effective aquifer storage projects where opportunities exist; and
- Manage overgrowth of unwanted invasive vegetation in the wetland riparian zones to minimize summer losses to evapotranspiration.



High and dry on the bank of Arroyo Hondo.

PROJECT STAFF & ACKNOWLEDGMENTS

Peggy S. Johnson, Principal Hydrogeologist,
 peggy@nmbg.nmt.edu
*Principal Investigator, hydrology, geology,
 geochemistry, reporting*

Daniel J. Koning, Senior Field Geologist,
 dkoning@nmbg.nmt.edu
Geologic mapping, reporting

Stacy S. Timmons, Aquifer Mapping Program
 Manager,
 stacyt@nmbg.nmt.edu
*Field data collection and compilation, water-level
 measurement, geochemical sampling*

Brigitte Felix, GIS Specialist,
 Report Production Coordinator,
 bfk@nmbg.nmt.edu
*ARC GIS, cartography, illustrations, report
 design, layout and production*

Trevor Kludt, Hydrogeologic Lab Associate,
 tkludt@nmbg.nmt.edu
Field data collection, water-level measurement

Cathryn Pokorny, Hydrogeological Lab Technician,
 kittyp@nmbg.nmt.edu
Data base, field data collection

Bonnie Frey, Chemistry Lab Manager, Geochemist,
 bfrey@nmbg.nmt.edu
Geochemical sample analysis

The authors thank our collaborators in the La Cienega Geohydrology Group—Maryann McGraw (NMED SWQB), Jan-Willem Jansens (Ecotone), Jim Dick (USFWS), Laura Petronis and Jack Frost (NMOSE), and Karen Torres (Santa Fe County Public Works Department)—who pooled resources and expertise on wetland ecology and hydrology to produce the prototype for this study, *Exploring Springs and Wetlands and their Relationship with Surface Flows, Geology, and Groundwater in the La Cienega Area, Santa Fe County, New Mexico* (McGraw and Jansens, 2012). This project would not have been possible without the kind cooperation of the numerous individual residents and land owners at La Cienega and La Cieneguilla who allowed access to their lands and wells. The manuscript was improved significantly by the constructive reviews and insight of colleagues John Shomaker, Marianne Wasiolek, and Laura Petronis. This work was supported in part by funds from the Aquifer Mapping Program at New Mexico Bureau of Geology & Mineral Resources, New Mexico Tech, Healy Foundation, and the U.S. Environmental Protection Agency through a Wetlands Program Development Grant administered by the NMED SWQB.

REFERENCES

- Alley, W.M., Reilly, T.E., and Franke, O.L., 1999, Sustainability of ground-water resources: U.S. Geological Survey Circular 1186, Denver, 79 p.
- Anderholm, S.K., 1994, Ground-water recharge near Santa Fe, north-central New Mexico: U.S. Geological Survey Water-Resources Investigations Report 94-4078, 68 p.
- Biehler, S., Ferguson, J., Baldridge, W.S., Jiracek, G.R., Aldern, J.L., Martinez, M. Fernandez, R., Romo, J., Gilpin, B., Braile, L.W., Hersey, D.R., Luyendyk, B.P., and Aiken, C.L.V., 1991, A geophysical model of the Española Basin, Rio Grande rift, New Mexico: Geophysics, v. 56, p. 340–353, doi:10.1190/1.1443048.
- Brassington, R., 2007, Field Hydrogeology: West Sussex, John Wiley & Sons, Ltd., 264 p.
- Candelario, J., 1929, Noticias de Juan Candelario: New Mexico Historical Review, v. 4, p. 282–284.
- Carter, V., 1996, Wetland hydrology, water quality, and associated functions; in Fretwell, J.D., Williams, J.S., and Redman, P.J., eds., National Water Summary on Wetland Resources, Technical Aspects of Wetlands, U.S. Geological Survey Water-Supply Paper 2425, p. 35–48.
- Cavazza, W., 1986, Miocene sediment dispersal in the central Española Basin, Rio Grande rift, New Mexico, USA: Sedimentary Geology, v. 51, p. 119–135.
- Clark, I.D. and Fritz, P., 1997, Environmental Isotopes in Hydrogeology: Boca Raton, CRC Press, 328 p.
- Cowardin, L.M., Carter, V., Golet, F.C., and LaRoe, E.T., 1979, Classification of wetlands and deepwater habitats of the United States: Fish and Wildlife Service Report FWS/OBS-79/31, 131 p.
- Craig, H., 1961, Isotopic variations in meteoric waters: Science 133, p. 1702–1703.
- Daniel B. Stephens and Associates, 1994, Santa Fe County water resource inventory, Santa Fe, New Mexico: Daniel B. Stephens and Associates, Inc.
- Davis, S.N., Whittemore, D.O., and Fabryka-Martin, J., 1998, Uses of chloride/bromide ratios in studies of potable water: Ground Water, v. 36, no. 2, p. 338–350.
- Dick, J.A., 2012, Chapter 2, Wetlands Program Project Report, La Cienega area wetlands; in McGraw and Jansens (eds.), Exploring Springs and Wetlands and Their Relationships with Surface Flows, Geology, and Groundwater in the La Cienega Area, Santa Fe County, New Mexico: Wetlands Program Project Report, New Mexico Environment Department, Surface Water Quality Bureau, p. 11–35.
- Dolan, T.J., Hermann, A.J., Bayley, S.E., and Zoltek, Jr., J., 1984, Evapotranspiration of a Florida, USA, freshwater wetland: Journal of Hydrology, v. 74, p. 355–371.
- Finch, S.T., Jr., and Peery, R.L., 1995, Springs at La Cienega: American Water Resources Association, New Mexico Section Field Trip: Santa Fe Area Water Resource Issues—Bring the Regulators and Private Sector Together, October 12–13, 1995.
- Grauch, V.J.S., Phillips, J.D., Koning, D.J., Johnson, P.S., and Bankey, V., 2009, Geophysical interpretations of the Southern Española Basin, New Mexico, that contribute to understanding its hydrogeologic framework: U.S. Geological Survey Professional Paper 1761, 88 p.
- Gutzler, D.S., and Robbins, T.O., 2011, Climate variability and projected change in the western United States: regional downscaling and drought statistics: Climate Dynamics, v. 37, p. 835–849.
- Harrar, W.G., Sonnenborg, T.O., and Henriksen, H.J., 2003, Capture zone, travel time, and solute-transport predictions using inverse modeling and different geological models: Hydrogeology Journal, v. 11, no. 5, p. 536–548.
- Harriss, R.C., and Williams, H.H., 1969, Specific-ion electrode measurements on Br, Cl and F in atmospheric precipitation: Journal of Applied Meteorology, v. 8, p. 299–301.
- Hays, K.B., 2003, Water use by saltcedar (*Tamarix* sp.) and associated vegetation on the Canadian Colorado and Pecos Rivers in Texas, [M.S. Thesis]: College Station, Texas A&M University, 116 p.
- Healy, R., and Cook, P., 2002, Using underground levels to estimate recharge: Hydrogeology Journal, v. 10, p. 91–109.
- Heikurainen, L., 1963, On using ground-water table fluctuations for measuring evapotranspiration, Acta Forestalia Fennica, v. 76, p. 1–15.
- Helsel, D.R., and Hirsch, R.M., 1995 (3rd printing), Statistical Methods in Water Resources, Studies in Environmental Science 49: Amsterdam Elsevier Science B.V., 529 p.
- Hounslow, A.W., 1995, Water Quality Data Analysis and Interpretation: New York, CRC Lewis Publishers, 379 p.
- Hunt, R.J., Walker, J.F., and Krabbenhoft, D.P., 1999, Characterizing hydrology and the importance of ground-water discharge in natural and constructed wetlands: Wetlands, v. 19, no. 2, p. 458–472.
- HydroScience Associates, Inc., 2004, Evaluation of the Hydrogeology of the La Cienega area, Santa Fe County, New Mexico: Consultant's report prepared for the Acequia de la Cienega, 47 p. plus appendix.
- Jackson, J.A., 1997, Glossary of Geology: Alexandria, Virginia, American Geological Institute, 769 p.
- Johnson, P.S., 2009, Water-level contours and ground water flow conditions (2000 to 2005) for the Santa Fe area, southern Española Basin, New Mexico: New Mexico Bureau of Geology and Mineral Resources Open-File Report 520, 2 map plates.
- Johnson, P.S., and Koning, D.J., 2012, Geologic and hydrologic maps of the Ancha Formation, Santa Fe County, New Mexico: New Mexico Bureau of Geology and Mineral Resources Open-File Report 550, 11 p., 4 plates.

- Johnson, P.S., Koning D.J., Timmons, S.W., and Felix, B., 2008, Geochemical characterization of ground water in the southern Española Basin, Santa Fe, New Mexico: New Mexico Bureau of Geology and Mineral Resources Open-File Report 511, 65 p.
- Johnson, P., Koning, D., and Timmons, S., 2012, Chapter 4, Wetlands Program Project Report, Geology and hydrology of wetlands and springs, *in* McGraw, M.M. and Jansens, J.W. eds., Exploring Springs and Wetlands and Their Relationships with Surface Flows, Geology, and Groundwater in the La Cienega Area, Santa Fe County, New Mexico: New Mexico Environment Department, Surface Water Quality Bureau, p. 53–95.
- Johnson, P.S., Koning, D.J., and Partey, F.K., 2013, Shallow groundwater geochemistry in the Española Basin, Rio Grande rift, New Mexico: Evidence for structural control of a deep thermal source; *in* Hudson, M.R. and Grauch, V.J.S., eds., New Perspectives on Rio Grande Rift Basins: From Tectonics to Groundwater: Geological Society of America Special Paper 494, p. 261–301, doi:10.1130/2013.2464(11).
- Kehew, A.E., and Boettger, W.M., 1986, Depositional environments of the buried-valley aquifers in North Dakota: *Ground Water*, v. 24, no. 6, p. 728–734.
- Konikow, L.F., 2015, Long-term ground-water depletion in the United States: *Groundwater*, vol. 53, no. 1, p. 2–9.
- Koning, D.J., and Hallett, R.B., 2002, Geologic map of the Turquoise Hill quadrangle, Santa Fe County, New Mexico: New Mexico Bureau of Geology and Mineral Resources Open-File Geologic Map OF-GM-41, scale 1:24,000.
- Koning, D.J., and Johnson, P.S., 2004, The Ancha Formation: textural subdivisions, lower contact, and hydrogeologic implications, *in* Read, A.S., Koning, D.J., and Johnson, P.S., Preliminary geologic map of the Southern Española Basin: New Mexico Bureau of Geology and Mineral Resources Open-File Report 481, 21 p.
- Koning, D.J., and Johnson, P.S., 2006, Locations and textural contrasts of Tesuque Formation lithostratigraphic units in the southern Española Basin, NM, and hydrogeologic implications; *in* McKinney, K.C., ed., Proceedings, Española Basin Workshop, 5th, Santa Fe, March 2006: U.S. Geological Survey Open-File Report 2006-1134, p. 24.
- Koning, D.J., and Maldonado, F., 2002, Geologic map of the Horcado Ranch quadrangle, Santa Fe County, New Mexico: New Mexico Bureau of Geology and Mineral Resources Open-File Geologic Map OF-GM-44, scale 1:24,000.
- Koning, D.J., and Read, A.S., 2010, Geologic map of the southern Española Basin: New Mexico Bureau of Geology and Mineral Resources Open-File Report 531, scale 1:48,000.
- Koning, D.J., Connell, S.D., Pazzaglia, F.J., and McIntosh, W.C., 2002, Redefinition of the Ancha Formation and Pliocene-Pleistocene deposition in the Santa Fe embayment, north-central New Mexico: *New Mexico Geology*, v. 24, no. 3, p. 75–87.
- Koning, D.J., Read, A., and Borchert, C., 2003, Sedimentologic and structural framework of the southern and central Española Basin - Insights from recent STATEMAP and EDDMAP efforts [abstract]; *in* Hudson, M.R., ed., Geologic and Hydrogeologic Framework of the Española Basin – Proceedings, Española Basin Workshop, 2nd, Santa Fe, March 2003: U.S. Geological Survey Open-File Report 2003-369, p. 10.
- Koning, D.J., Smith, G., Lyman, J., and Paul, P., 2004, Lithosome S of the Tesuque Formation: Hydrostratigraphic and tectonic implications of a newly delineated lithosome in the southern Española Basin, New Mexico, *in* Hudson, M., ed., Proceedings, Española Basin Workshop, 3rd, Santa Fe, March 2004: U.S. Geological Survey Open-File Report 2004-1093, p. 17.
- Koning, D.J., Grauch, V.J.S., Connell, S.D., Ferguson, J., McIntosh, W., Slate, J.L., Wan, E., and Baldridge, W.S., 2013, Structure and tectonic evolution of the eastern Española Basin, Rio Grande rift, north-central New Mexico, *in* Hudson, M., and Grauch, V.J.S., eds., New Perspectives on the Rio Grande Rift: From Tectonics to Groundwater: Geological Society of America Special Paper 494, p. 185–219, doi:10.1130/2012.2494(11).
- Kuhle, A., and Smith, G.A., 2001, Alluvial-slope deposition of the Skull Ridge Member of the Tesuque Formation, Española Basin, New Mexico: *New Mexico Geology*, v. 23, no. 2, p. 30–37.
- Linsley, R.K., Franzini, J.B., Freyberg, D.L., Tchobanoglou, G., 1992, *Water-Resources Engineering* (4th edition): New York, McGraw-Hill, Inc. 841 p.
- Loáiciga, H.A., Maidment, D.R., and Valdes, J.B., 2000, Climate-change impacts in a regional karst aquifer, Texas, USA: *Journal of Hydrology*, vol. 227, p. 173–194.
- Loheide II, S., Butler Jr., J., Gorelick, S., 2005, Estimation of groundwater consumption by phreatophytes using diurnal water table fluctuations: a saturated-unsaturated flow assessment: *Water Resources Research*, v. 41, p. 1–14.
- Margolis, E.Q., Meko, D.M., and Touchan, R., 2011, A tree-ring reconstruction of streamflow in the Santa Fe River, New Mexico: *Journal of Hydrology*, v. 397, p. 118–127.
- McGraw, M.M., and Jansens, J.W., eds., 2012, Exploring Springs and Wetlands and Their Relationships with Surface Flows, Geology, and Groundwater in the La Cienega Area, Santa Fe County, New Mexico: Wetlands Program Project Report, New Mexico Environment Department, Surface Water Quality Bureau, 125 p.
- Manning, A.H., 2009, Ground-Water Temperature, Noble Gas, and Carbon Isotope Data from the Española Basin, New Mexico: U.S. Geological Survey Scientific Investigations Report 2008-5200, 69 p.
- Mazor, E., 2004, *Chemical and Isotopic Groundwater Hydrology* (3rd edition): New York, Marcel Dekker, Inc., 453 p.
- McAda, D.P., and Wasiolek, M., 1988, Simulation of the regional geohydrology of the Tesuque aquifer system near Santa Fe, New Mexico: U.S. Geological Survey Water-Resources Investigations Report 87-4056, 69 p.
- Minor, S.A., ed., 2006, The Cerrillos uplift, the La Bajada constriction, and hydrogeologic framework of the Santo Domingo Basin, Rio Grande rift, New Mexico: U.S. Geological Survey Professional Paper 1720, 189 p.
- Moore, S.J., 2007, Chapter F, Streamflow, infiltration, and recharge in Arroyo Hondo, New Mexico, *in* Stonestrom, D.A., Constantz, J., Ferré, T.P.A., and Leake, S.A. eds., *Ground-Water Recharge in the Arid and Semiarid Southwestern United States: U.S. Geological Survey Professional Paper 1703*, p. 137–155.
- Moreland, J., 1993, Drought: U.S. Geological Survey Open-File Report 93-642 (reprinted April 2001), 2 p.

- Mourant, W.A., 1980, Hydrologic maps and data for Santa Fe County, New Mexico: New Mexico State Engineer Basic Data Report, Santa Fe, 180 p.
- Myer, C., and Smith, G.A., 2006, Stratigraphic analysis of the Yates #2 La Mesa well and implications for southern Española Basin tectonic history: *New Mexico Geology*, v. 28, no. 3, p. 75–83.
- Nachabe, M., Shah, N., Ross, M., and Vomacka, J., 2005, Evapotranspiration of two vegetation covers in a shallow water table environment: *Soil Science Society of America Journal*, v. 69, p. 492–499.
- New Mexico Bureau of Geology and Mineral Resources, 2003, Geologic map of New Mexico: New Mexico Bureau of Geology and Mineral Resources, scale 1:500,000.
- New Mexico Bureau of Geology & Mineral Resources, 2008, Española Basin Well and Water Database: unpublished Access Database, December 2008.
- Newton, B.T., Rawling, G.C., Timmons, S.S., Land, L., Johnson, P.S., Kludt, T., and Timmons, J.M., 2012, Sacramento Mountains Hydrogeology Study: New Mexico Bureau of Geology and Mineral Resources Open-File Report 543, 77 p.
- NM Hydrologic, LLC and the New Mexico Office of the State Engineer, 2012a, Streamflow Measurement Study of the Lower Santa Fe River, Santa Fe County, NM: City of Santa Fe Wastewater Treatment Plant to the USGS Gage, Santa Fe River above Cochiti Lake, NM, report for the New Mexico Office of the State Engineer Hydrology Bureau, December 2012.
- NM Hydrologic, LLC and the New Mexico Office of the State Engineer, 2012b, Streamflow Measurement Study of the Cienega Creek and tributaries and the lower Santa Fe River, Santa Fe County, NM, report for the New Mexico Environment Department Surface Water Quality Bureau and the New Mexico Office of the State Engineer Hydrology Bureau, December 2012.
- Peery, R.L., Parker, J.S., Miller, S.A., and Graham, I.A., 2007, Hydrogeologic assessment for the Three Rivers Ranch, Santa Fe County, New Mexico: unpublished consultant's report, John Shomaker and Associates, Inc., for Cohiba Club, 10 p. plus illustrations.
- Petronis, L., Frost, J., and Veenhuis, J., 2012, Chapter 3, Wetlands Program Project Report, Summary of surface water data in the La Cienega area; in McGraw, M.M. and Jansens, J.W. eds., *Exploring Springs and Wetlands and Their Relationships with Surface Flows, Geology, and Groundwater in the La Cienega Area, Santa Fe County, New Mexico*: New Mexico Environment Department, Surface Water Quality Bureau, p. 37–52.
- Piper, A.M., 1944, A graphic procedure in the geochemical interpretation of water-analyses [abs.]: (*Transactions, American Geophysical Union*), v. 25, p. 914–923.
- Read, A.S., Koning, D.J., and Johnson, P.S., 2003, Geologic and hydrostratigraphic mapping of the Santa Fe region, New Mexico: Applications for assessing and managing groundwater resources: *Geological Society of America Abstracts with Programs*, November 2003, v. 35, no. 6, p. 71.
- Read, A.S., Koning, D.J., and Johnson, P.S., 2004, Preliminary geologic map of the southern Española Basin: New Mexico Bureau of Geology and Mineral Resources Open-File Report 481, scale 1:50,000.
- Rosenberg, N.J., Epstein, D.J., Wang, D., Vail, L., Srinivasan, R., and Arnold, J.G., 1999, Possible impacts of global warming on the hydrology of the Ogallala aquifer region: Climatic Change, v. 42, p. 677–692.
- Rosenberry, D., and Winter, T., 1997, Dynamics of water-table fluctuations in an upland between two prairie pothole wetlands in North Dakota: *Journal of Hydrology*, v. 191, p. 266–289.
- Sawyer, D.A., Shroba, R.R., Minor, S.A., and Thompson, R.A., 2002, Geologic map of the Tetilla Peak quadrangle, Santa Fe and Sandoval Counties, New Mexico: U. S. Geological Survey Miscellaneous Field Studies Map MF-2352, scale 1:24,000.
- Seifert, D., Sonnenborg, T.O., Scharling, P., and Hinsby, K., 2008, Use of alternative conceptual models to assess the impact of a buried valley on groundwater vulnerability: *Hydrogeology Journal*, v. 16, no. 4, p. 659–674.
- Shaver, R.B., and Pusc, S.W., 1992, Hydraulic barriers in Pleistocene buried-valley aquifers: *Ground Water*, v. 30, no. 1, p. 21–28.
- Sivinski, R., and Tonne, P., 2011 Survey and Assessment of Aridland Spring Cienegas in the Southwest Region, ESA Section 6 Report: New Mexico Energy, Minerals and Natural Resources Department, Santa Fe, and USFWS Region 2, Albuquerque, New Mexico, 139 p.
- Spiegel, Z., 1963, Water Resources, Part 3 in Spiegel, Z. and Baldwin, B., eds., 1963, *Geology and Water Resources of the Santa Fe Area, New Mexico*: U.S. Geological Survey Water-Supply Paper 1525, p. 91–143.
- Spiegel, Z., 1975, Preliminary Report on the Hydrology of the Cienega Area, Santa Fe County, New Mexico: Consultant's report prepared for Santa Fe Downs, Inc., 34 p. plus appendices.
- Spiegel, Z., and Baldwin, B., 1963, *Geology and Water Resources of the Santa Fe area, New Mexico*. U.S. Geological Survey Water-Supply Paper 1525, 258 p. plus plates.
- Springer, A.E., and Bair, E.S., 1992, Comparison of methods used to delineate capture zones of wells: 2. Stratified-drift buried-valley aquifer: *Ground Water*, v. 30, no. 6, p. 908–917.
- Stearns, C.E., 1953, Early Tertiary vulcanism in the Galisteo-Tonque area, north-central New Mexico: *American Journal of Science*, v. 251, p. 415–452.
- Stewart-Deaker, A.E., Stonestrom, D.A., and Moore, S.J., 2007, Streamflow, infiltration, and ground-water recharge at Abo Arroyo, New Mexico; in Stonestrom, D.A., Constantz, J., Ferré, T.P.A., and Leake, S.A., eds., *Ground-Water Recharge in the Arid and Semiarid Southwestern United States*: U.S. Geological Survey Professional Paper 1703-D, p. 83–105.
- Sun, M., and Baldwin, B., 1958, Volcanic rocks of the Cienega area, Santa Fe County, New Mexico: New Mexico Bureau of Geology and Mineral Resources, Bulletin 54, 80 p., map scale 1:15,840.
- Taylor, C.J., and Alley, W.M., 2001, Ground-water-level monitoring and the importance of long-term water-level data: U.S. Geological Survey Circular 1217, 68 p.
- Thomas, C.L., Stewart, A.E., and Constantz, J., 2000, Determination of infiltration and percolation rates along a reach of the Santa Fe River near La Bajada, New Mexico: U.S. Geological Survey Water-Resources Investigations Report 00-4141, 65 p.

- Thompson, R.A., Sawyer, D.A., Hudson, M.R., Grauch, V.J.S., and McIntosh, W.C., 2006, Cenozoic Volcanism of the La Bajada Constriction Area, New Mexico; in Minor, S.A., ed., The Cerrillos Uplift, the La Bajada Constriction, and Hydrogeologic Framework of the Santo Domingo Basin, Rio Grande Rift, New Mexico: U.S. Geological Survey Professional Paper 1720, p. 43-60.
- Timmons, S.W., Land, L., Newton, B.T., and Frey, B., 2013, Aquifer Mapping Program technical document: water sampling procedures, analysis and systematics: New Mexico Bureau of Geology and Mineral Resources Open-File Report 558, 9 p.
- Tiner, R.W., 1996, Wetland definitions and classifications in the United States; in Fretwell, J.D., Williams, J.S., and Redman, P.J., eds., National Water Summary on Wetland Resources, Technical Aspects of Wetlands, U.S. Geological Survey Water-Supply Paper 2425, p. 27-34.
- Todd, D.K., and Mays, L.W., 2005, Groundwater Hydrology (3rd edition): John Wiley & Sons, Inc., Hoboken, 636 p.
- van der Kamp, G. and Maathuis, H., 2012, The unusual and large drawdown response of buried-valley aquifers to pumping: *Groundwater*, v. 50, no. 2, p. 207-215.
- Vincke, C., and Thiry, Y., 2008, Water table is a relevant source for water uptake by a Scots pine (*Pinus sylvestris* L.) stand: Evidences from continuous evapotranspiration and water table monitoring: *Agricultural and Forest Meteorology*, v. 148, p. 1419-1432, Elsevier www.sciencedirect.com.
- Wasiolek, M., 1995, Subsurface recharge to the Tesuque aquifer system from selected drainage basins along the western side of the Sangre de Cristo Mountains near Santa Fe, New Mexico: U.S. Geological Survey Water-Resources Investigations Report 94-4072, 57 p.
- Weissman, G.S., Zhang, Y., Fogg, G.E., and Mount, J.F., 2004, Influence of incised-valley-fill deposits on hydrogeology of a stream-dominated alluvial fan: Society for Sedimentary Geology Special Publication No. 80, p. 15-28.
- White, W., 1932, A method for estimating ground-water supplies based on discharge by plants and evaporation from soil: U.S. Geological Survey Water Supply Paper 659-A, 105 p.
- White, W.D., and Kues, G.E., 1992, Inventory of springs in the State of New Mexico: U.S. Geological Survey Open-File Report 92-118, 253 p.
- Wilson, W.E., and Moore, J.E., 1998, Glossary of Hydrology: Alexandria, American Geological Institute, 248 p.
- Winter, T.C., 1976, Numerical simulation analysis of the interaction of lakes and ground water: U.S. Geological Survey Professional Paper 1001, 45 p.

APPENDICES

Supplementary data available in Data Repository:

<http://geoinfo.nmt.edu/repository/index.cfm?rid=20160001>

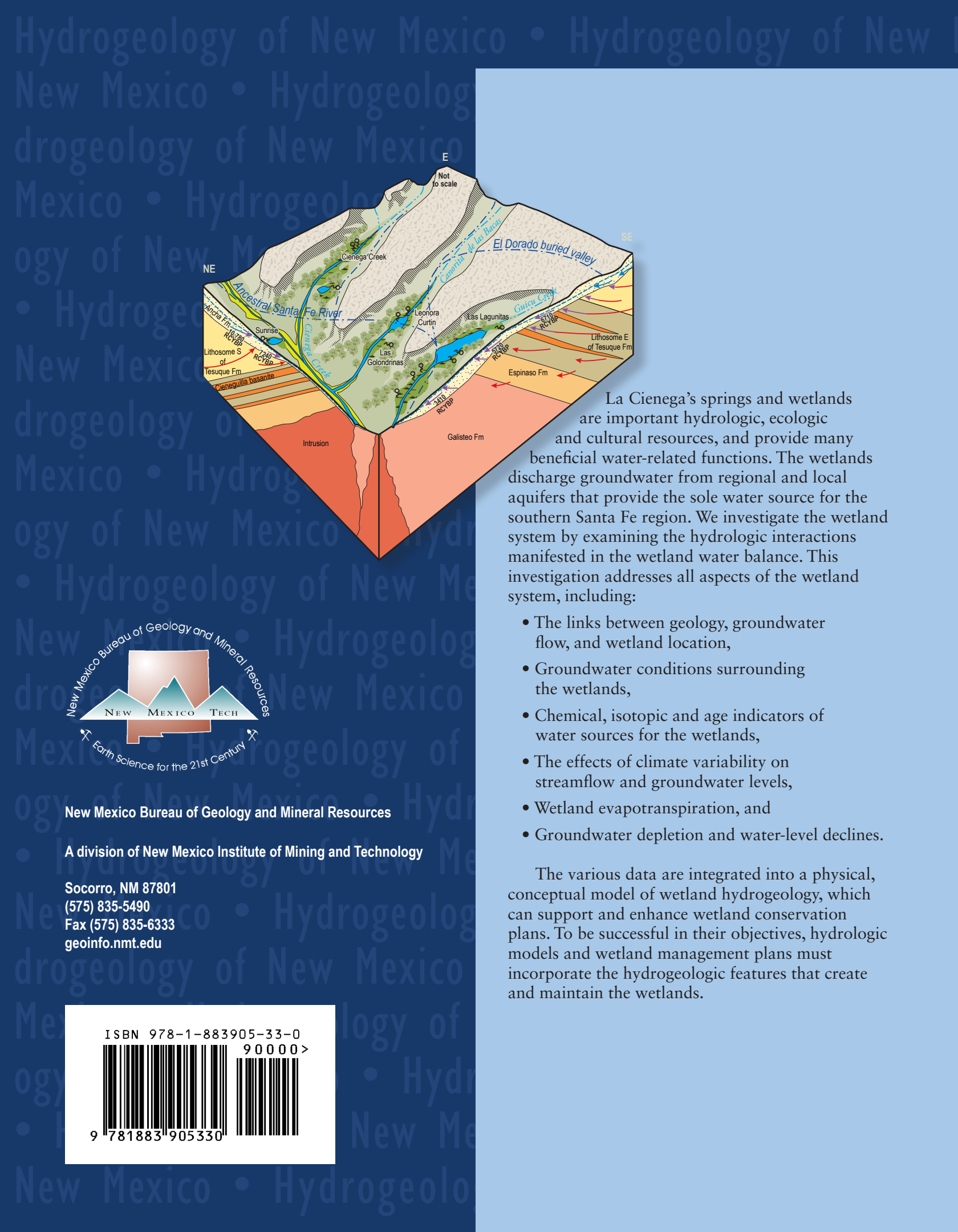
1. Groundwater data from continuous recorders
2. Groundwater data and hydrographs from periodic measurements
3. Chemistry data
4. Streamflow data



Acronyms

- asl—above sea level
bls—below land surface
CFC—chlorofluorocarbon
CFS—cubic feet per second, ft³/s
DEM—digital elevation model
DIC—dissolved inorganic carbon
DO—dissolved oxygen
GIS—geographic information system
GPS—global positioning system
LMWL—local meteoric water line
meq/L—milliequivalents per liter
MWL—meteoric water line
NAD83—North American datum of 1983
NMBGMR—New Mexico Bureau of Geology and
Mineral Resources
NMED SWQB—New Mexico Environment
Department Surface Water Quality Bureau
NMOSE—New Mexico Office of the State Engineer
NOAA NCDC—National Oceanic and Atmospheric
Administration, National Climatic Data Center
NWIS—National Water Information System
pmC—percent of modern carbon, unit for expressing
carbon-14 (¹⁴C) content
RCYBP—radio carbon years before present
RVHC—Rancho Viejo hinge zone
SC—specific conductance
SFCMA—Santa Fe County Municipal Airport
SFG—Santa Fe Group
TDS—total dissolved solids
TU—tritium units, unit for expressing tritium (³H)
content
USGS—United States Geological Survey
USF&WS—United States Fish and Wildlife Service
UTM—Universal Transverse Mercator coordinate
system
WWTP—wastewater treatment plant

This page intentionally left blank to avert any facing-page issues.



New Mexico Bureau of Geology and Mineral Resources

A division of New Mexico Institute of Mining and Technology

Socorro, NM 87801
(575) 835-5490
Fax (575) 835-6333
geoinfo.nmt.edu

ISBN 978-1-883905-33-0



9 0000 >

9 781883 905330

La Cienega's springs and wetlands are important hydrologic, ecologic and cultural resources, and provide many beneficial water-related functions. The wetlands discharge groundwater from regional and local aquifers that provide the sole water source for the southern Santa Fe region. We investigate the wetland system by examining the hydrologic interactions manifested in the wetland water balance. This investigation addresses all aspects of the wetland system, including:

- The links between geology, groundwater flow, and wetland location,
- Groundwater conditions surrounding the wetlands,
- Chemical, isotopic and age indicators of water sources for the wetlands,
- The effects of climate variability on streamflow and groundwater levels,
- Wetland evapotranspiration, and
- Groundwater depletion and water-level declines.

The various data are integrated into a physical, conceptual model of wetland hydrogeology, which can support and enhance wetland conservation plans. To be successful in their objectives, hydrologic models and wetland management plans must incorporate the hydrogeologic features that create and maintain the wetlands.